Electrochemical affinity sensors for biomedical, food and environmental applications

Anca Stefana Florea

N° d'ordre: 126-2015 Année 2015

THESE DE L'UNIVERSITE DE LYON

Délivrée par

L'UNIVERSITE CLAUDE BERNARD LYON 1

ECOLE DOCTORALE: Chimie

Spécialité: Chimie

DIPLOME DE DOCTORANT

(Arrêté du 7 août 2006)

Soutenue publiquement le 14 Septembre 2015

Par

Mlle FLOREA Anca Stefana

TITRE:

Electrochemical affinity sensors for biomedical, food and environmental applications

JURY:

Rapporteurs:	**Prof. Dr. Camelia Bala**
	Dr. Serge Cosnier
Examinateurs:	**Dr. Cecilia Cristea**
	Dr. Joelle Saulnier
Directeurs de these:	**Dr. Nicole Jaffrezic-Renault**
	Prof. Dr. Robert Săndulescu

"I am not young enough to know everything"

Oscar Wilde

Dedicated to my family

Acknowledgements

There are more people that I can count who helped making this work possible. I owe a huge debt of gratitude to my supervisors, my coworkers, my family and my friends.

I would like to express my deepest gratitude to my supervisors Prof. Dr. Robert Sãndulescu and Dr. Nicole Jaffrezic-Renault for the opportunity to work in their excellent research groups. Their constant support, valuable time, constructive advices and positive attitude and confidence towards me have been wholehearted and made me believe in myself as a researcher.

I owe a big debt of gratitude to Dr. Cecilia Cristea for her friendship, continuous support, confidence in me and precious advices in both my work and life.

I am greatly appreciative to prof. Dr. Giovanna Marrazza from Univeristy of Florence for her guidance and support and to dr. Andrea Ravalli for his valuable advices and help.

I also thank the comitee for the advices and help in improving my thesis.

I owe special thanks to all my collegues and friends from the Department of Analytical Chemistry Cluj, from ISA Lyon and "Ugo Shiff" Department Florence, who contributed not only to work but also to making it fun. There are countless people that have been helpful throughout time and with whom I shared great experiences, so I apologize in advance for forgetting naming some of them. Thanks to Bogdan, Andreea, Mihaela, Lumi, Bibi, Oana, whose advices, friendship and support was essential to my progress. I thank Coco, Rebecca and Diego for their friendship and cheerfulness and for making Florence home for me. I am greatly thankful to Mamis for the support, friendship and good spirit all along the way. I am grateful to fam. Lacroix for their hospitality during my staying in Lyon. I would like to thank to all doctorants in ISA Lyon, Elena, Sylvia, Nedjla, Mohamed, Vika, Katya etc, for the memorable experiences in and outside work in Lyon. To ZhenZhong, Huy and Madiha for their collaboration and help regarding MIP sensors. Special thanks to Alvaro for his friendship and encouragement. I also thank Eli for her friendship, cheerfulness and inspiration.

I would like to thank all my friends for their support and understanding.

Finnaly, I am deeply thankful to my parents, my brother, my sister-in-law and to my whole family for their endless love, encouragement and support. Words truly can not express how lucky I feel to have had them every step along the way.

TITRE en français: **Capteurs électrochimiques d'affinité applique dans l'analyse biomédicale, sécurité alimentaire et environnementale**

RESUME en français:

Les capteurs électrochimiques sont des outils pour la détection fiable, peu coûteux, avec une haute sensibilité et sélectivité, pour la détermination des composés biologiques et chimiques dans les domaines du diagnostic clinique, l'environnement et l'industrie alimentaire. Particulièrement, les Immunocapteurs, alliant une très grande spécificité. Également des nouveaux techniques produisent des résultats similaires, par exemple, les capteurs basés sur la technique des Polymères à empreinte moléculaire, la quelle produise des récepteurs artificiels. La technique devient très important dans les sciences bioanalytiques parce qu'il porte des avantages inhérents sur les récepteurs naturels: une grande stabilité dans des diffèrent environnement et conditions, également comptent avec une grande flexibilité dans la conception, une large gamme de molécules peuvent être utilisées.

L'objectif du travail présenté ici est de développer des capteurs électrochimiques avec une très grande affinité et spécificité pour une analyte. Les quelles comprennent des applications très divers comme dans la protection de l'environnement, la sécurité alimentaire et le domaine biomédical. La première partie de la thèse présent l'état actuel de la conception et techniques de fabrication des biocapteurs. Ensuite, les aspects généraux des immuno capteurs électrochimiques et capteurs base sur des aptamères sont présentés ici, ainsi que plusieurs exemples rapportés dans la littérature pour la détection de marqueurs biologiques du cancer. Les avantages de l'intégration nanomatériaux dans les dispositifs de détection sont présentés. Ensuite, plusieurs aspects sur la technique des Polymères à empreinte moléculaire sont introduits.

La partie personnelle de contribution est structuré en trois chapitres: en premier temps la méthodologie et les résultats obtenus pour le développement de deux essais biologiques pour la détection du marqueur tumoral Mucin1. Le premier chapitre est dédié sur un capteur à base de billes magnétiques, dans le deuxième chapitre une capteur aptamère base sur des nanoparticules d'or sans aucun marquage et finalement un capteur basée sur la technique des Polymères à empreinte moléculaire, cette protocole a été appliqué pour la détection d'explosifs, des médicaments, des hormones et les pesticides.

Mots-clés: capteur électrochimique, immunocapteur, aptamères, Polymères à empreinte moléculaire, biomarqueur du cancer, sécurité alimentaire, contrôle de l'environnement, analyses biomédicales.

TITRE en anglais: **Electrochemical affinity sensors for biomedical, food and environmental applications**

RESUME en anglais:

Electrochemical sensors provide reliable and inexpensive tools for the determination of biological and chemical compounds with high sensitivity and selectivity, in the fields of clinical diagnosis, environment protection and food industry. Immunosensors hold particular promise, combining the high specificity of immuno-reactions with the sensitivity of electrochemical methods. Artificial receptors based on molecularly imprinted technique attracted considerable attention in bioanalytical sciences due to inherent advantages over natural receptors, such as high stability in harsh conditions and freedom of molecular design towards a wide range of molecules.

The aim of the thesis presented here was to develop electrochemical affinity sensors based on various recognition receptors for environment monitoring, food safety and biomedical field.

The first part of the thesis reviews the current state of knowledge in these fields. General aspects of electrochemical immuno- and apta-sensors are presented herein, together with several examples reported in the literature for the detection of cancer biomarkers. The advantages of integrating nanomaterials in sensing devices are then presented. At last, several aspects of the molecularly imprinted polymers are introduced.

The personal contribution part is structured in three chapters, that include the methodology and results obtained for the development of biosensors for the detection of Mucin1 tumor marker, the first chapter being focused on bioassays based on magnetic beads and second chapter on a label-free aptasensor based on gold nanoparticles, and finally, a third chapter dedicated to the molecularly imprinted-based sensors for the detection of explosives, drugs, hormones and pesticides.

Keywords: electrochemical sensor, immunosensor, aptasensor, molecularly imprinted polymers, cancer biomarker, food safety, environmental control, biomedical analysis.

Résumé substantiel

Les techniques électrochimiques peuvent fournir un outil peu coûteux et sensible pour le développement de petits dispositifs portables qui sont capables de détecter rapidement des composés biologiques et chimiques avec de hautes sensibilité et spécificité. Les capteurs électrochimiques peuvent être appliqués dans différents domaines, y compris le diagnostic précoce des maladies, le control des médicaments et la détection rapide et précise des polluants de l'environnement et des contaminants alimentaires.

Un objectif de ce travail a été de développer des dispositifs de diagnostic électrochimiques pour la détection précoce du cancer. Le biomarqueur tumoral MUC1 a été choisi comme molécule modèle et des anticorps et des aptamères ont été utilisés comme éléments de bioreconnaissance. Les nanomatériaux ont été intégrés dans les capteurs proposés comme plates-formes d'immobilisation. Des particules magnétiques avec protéine G et des particules magnétiques avec streptavidine ont été utilisées pour une analyse de type sandwich d'anticorps et d'aptamère, respectivement. Les nanoparticules d'or ont été utilisées pour l'immobilisation des aptamères thiolés non marqués spécifiques pour MUC1.

La technique des polymères à empreinte moléculaire est une méthode versatile pour la synthèse de récepteurs artificiels, surmontant certains inconvénients lors de l'utilisation des anticorps ou des aptamères. Un autre objectif de ce travail a été le développement de capteurs électrochimiques à empreintes moléculaires pour la détection de médicaments, de polluants de l'environnement et de contaminants alimentaires. Nous avons cherché à développer un protocole générique qui pourrait être appliqué à une large gamme de molécules, y compris les composés non électroactifs, en utilisant comme médiateur redox le couple hexacyanoferrite / hexacyanoferrate. Les films imprimés ont été préparées par électropolymérisation par voltamétrie cyclique de nanoparticules fonctionnalisées avec *p*-aminothiophénol en présence de molécules de la substance modèle. L'extraction ultérieure de la substance modèle conduit à la formation de cavités capables de reconnaissance spécifique, qui sont capables de lier les analytes.

Nous avons investigué l'application pratique des capteurs proposés par l'analyse de matrices complexes qui contiennent l'analyte, comme l'eau du robinet et l'eau de la rivière, le miel, le sérum et les formulations de médicaments.

Le premier chapitre de la contribution personnelle présente un bio-essais optimisés pour la détection de la mucine1 dans des échantillons de sérum.

MUC1 est une glycoprotéine transmembranaire exprimée sur la surface apicale de différentes cellules épithéliales, qui est surexprimée dans le sang dans le cas des processus néoplasiques. Par conséquent, la MUC1 peut être utilisée comme marqueur tumoral potetiel pour établir le diagnostic et le pronostic dans plusieurs types de cancer.

Cette étude présente deux approches différentes pour la détection du marqueur tumoral MUC1 dans un format sandwich en utilisant des particules magnétiques comme support solide et des anticorps ou des aptamères comme molécules de bioreconnaissance. Les aptamères utilisés dans ce travail ont été sélectionnés d'une bibliothèque d'aptamères, conçu par SELEX, qui ont la capacité de reconnaître la protéine MUC1.

La molécule cible est capturée entre l'anticorps primaire ou l'aptamère immobilisé sur des particules magnétiques et un anticorps ou aptamère secondaire. La réaction d'affinité est marquée avec la phosphatase alcaline dans des différentes configurations d'essai. Toutes les variables concernant les bio-essais ont été optimisées. La multidétection électrochimique est réalisée par voltamétrie pulse différentielle (DPV), en utilisant huit cellules imprimées sérigraphiques, par l'addition du substrat enzymatique (1-naphtyle phosphate) et sa conversion ultérieure en 1-naphtol, un composé électroactif. Tout d'abord, nous avons optimisé plusieurs paramètres expérimentaux qui influencent la performance des bio-essais. Ensuite, les performances analytiques obtenues dans des conditions optimisées des deux capteurs développés ont été comparées en termes de sensibilité et de sélectivité afin de choisir la meilleure méthode pour analyser les échantillons de sérum de cancer. Le dosage à base d'aptamère envisagée du a montré une meilleure sensibilité et sélectivité pour la détection de biomarqueur pour cancer MUC1 par rapport au dosage à base d'anticorps. Dans des conditions optimisées, une courbe d'étalonnage linéaire pour des solutions tampon de MUC1 a été obtenue dans un intervalle de 0 à 10 ng/mL avec une limite de détection (LD = $3S_{blank}$/pente) de 1,4 ng/mL (correspondant à l'intervalle de 0 à 0,28 nM, LOD de 0,037 nM), bien en dessous des limites de détection rapportées pour d'autres aptasensors présents dans la littérature. Afin d'évaluer l'applicabilité de l'aptasensor développé et d'évaluer l'influence de l'effet de la matrice, des échantillons de sérum non pathologiques dopés avec différentes concentrations connues de la protéine MUC1 ont été aussi analysés. Une limite de détection de 3,0 ng / mL et une limite de quantification (LQ = 10 S_{blank} / pete) de 10,0 ng / mL ont été obtenus. De plus, nous avons déterminé une corrélation semi-quantitative entre la concentration de MUC1 trouvée dans des échantillons de sérums de patients avec cancer et du stade de malignité obtenu par le diagnostic immunohistochimique, démontrant les applications potentielles pour le dépistage du cancer.

Le deuxième chapitre présente un aptasensor sans marquage basé sur l'électrodéposition de nanoparticules d'or sur des électrodes imprimées sérigraphiquement pour la détection du marqueur tumoral MUC1. Dans la première étape, la surface des électrodes en graphite est modifiée par électrodéposition avec des nanoparticules d'or. Ensuite, les aptamères spécifiques pour l'antigène MUC1 ont été auto-assemblés sur la surface d'or. L'interaction entre l'aptamère et la protéine MUC1 a été étudiée par la technique de spectroscopie électrochimique d'impédance par la variation de la résistance de transfert de charge. Une augmentation de la résistance de transfert de charge a été observée après l'immobilisation des aptamères et des protéines à la surface du capteur. Les résultats démontrent que la méthode électrochimique utilisant une sonde d'aptamères est simple et commode, et permet la détection quantitative de la protéine MUC1 humaine. La courbe d'étalonnage pour la détermination de la protéine MUC1 a été obtenue dans des conditions optimisées. La limite de détection estimée de la protéine MUC1 a été de 3,6 ng/mL dans l'intervalle linéaire de 2.5-15 ng/mL.

Enfin, le dernier chapitre présente le développement de MIP-capteurs électrochimiques pour la détection sensible et sélective de différents analytes cibles. Nous avons cherché à développer un protocole générique sur la base d'une membrane hybride de polymère à empreintes moléculaires/ AuNPs qui peut être appliquée à une large gamme de molécules électroactives et non électroactives. TNT, la gemcitabine, la tétracycline, l'estradiol et le glyphosate ont été étudiés comme molécules modèles. Tout d'abord, une monocouche d'auto-assemblage de PATP est formée à la surface de l'électrode d'or par des liaisons Au-S. Ensuite, le film MIP a été déposé sur l'électrode par électropolymérisation du groupement aniline de PATP greffés sur des électrodes d'or et sur AuNPs. Afin d'obtenir des films imprimés, le processus d'électropolymérisation a été réalisé en présence de molécules modèles, l'élimination subséquente du modèle laissant des cavités qui servent de sites de reconnaissance sélective. Combinant les avantages de l'impression moléculaire et de l'électrodéposition avec ceux conférés par AuNPs, les capteurs développés présentent une bonne sensibilité et une grande sélectivité. Plusieurs paramètres qui influencent les performances des capteurs ont été optimisés et les matériaux de détection ont été appliquées avec succès pour l'analyse des échantillons réels.

LIST OF PUBLICATIONS

1. **A. Florea**, Z. Taleat, C. Cristea, M. Mazloum-Ardakani, R. Săndulescu, Label free MUC1 aptasensors based on electrodeposition of gold nanoparticles on screen printed electrodes, Electrochemistry Communications, 33 (2013) 127-130, **ISI Impact Factor 4.287**
2. **A. Florea,** C. Cristea, R. Săndulescu, MUC1 tumor marker for the detection of ovarian cancer. A minireview, Farmacia LXII, 1 (2014) 1-13, **ISI Impact Factor 0.971**
3. Z.Z. Guo, **A. Florea**, C. Cristea, F. Bessueille, F. Vocanson, F. Goutaland, A.D. Zhang, R. Săndulescu, F. Lagarde, N. Jaffrezic-Renault, 1,3,5-Trinitrotoluene detection by a molecularly imprinted polymer sensor based on electropolymerization of a microporous-metal-organic framework, Sensors and Actuators B 207 (2015) 960-966, **ISI Impact Factor 3.840**
4. **A. Florea**, Z.Z. Guo, C. Cristea, F. Bessueille, F. Vocanson, F. Goutaland, S. Dzyadevych, R. Săndulescu, N. Jaffrezic-Renault, Anticancer drug detection using a highly sensitive molecularly imprinted electrochemical sensor based on an electropolymerized microporous metal organic framework, Talanta. 138 (2015) 71-76. **ISI Impact Factor 3.511**
5. **A. Florea**, A. Ravalli, C. Cristea, R. Săndulescu, G. Marrazza, An optimized bioassay for Mucin1 detection in serum samples, Electroanalysis. 27 (2015) 1594-1601. **ISI Impact Factor 2.502**
6. C. Cristea, **A. Florea**, R. Săndulescu, M. Tertis. Biosensors, Chapter XII, Immunosensors. Ed. Intech (2015) *in press*
7. **A. Florea**, C. Cristea, F. Vocanson, R. Săndulescu, N. Jaffrezic-Renault. Electrochemical sensor for the detection of estradiol based on electropolymerized molecularly imprinted polythioaniline film and gold nanoparticles amplification. Electrochemistry Communications. 59 (2015) 36-39. **ISI Impact Factor 4.287**
8. M. Bougrini, **A. Florea**, C. Cristea, R. Sandulescu, F. Vocanson,A.Errachid, B. Bouchikhi ,N. El Bari, N. Jaffrezic-Renault. Detection of tetracycline in honey using a molecularly imprinted sensor. Food Control. 59 (2016) 424-429. **ISI Impact Factor 2.819**

Table of Contents

ABBREVIATIONS

Ab	Antibody
Ag	Antigen
Apt	Aptamer
AP	Alkaline phosphatase
$A_{(n)}$	Adenine nucleotide
BSA	Bovin serum albumin
CE	Counter electrode
cDNA	Complementary deoxyribonucleic acid
CDR	Complementary determining region
CNT	Carbon nanotubes
CV	Cyclic voltammetry
DEA	Diethyleneamine
DNA	Deoxyribonucleic acid
DNT	Dinitrotoluene
DPV	Differential pulse voltammetry
DPSV	Differential pulse stripping voltammetry
dT	Deoxytymine
E2	Estradiol
EDTA	Ehylenediaminetetraacetic acid
EIS	Electrochemical impedance spectroscopy
ELISA	Enzyme-linked immunosorbent assay
GC	Gas Chromatography
GC/MS	Gas chromatography mass spectrometry
GCE	Glassy carbon electrode
Gly	Glyphosate
GMT	Gemcitabine
HPLC	High Performance Liquid Chromatography
Ig	Immunoglobulin
LBL	Layer by layer
LOD	Limit of detection
LOQ	Limit of quantification
LSV	Linear sweep voltammetry

LR	Linear range
mAb	Monoclonal antibody
MUC1	Mucin 1
MUC4	Mucin 4
MUC16	Mucin 16
MIP	Moleclularly imprinted polymer
MMOF	Microporous metal-organic framework
mRNA	Micro-ribonucleic acid
MW	Molecular weight
NIP	Non-imprinted polymer
ODN	Oligodeoxy nucleotide
pAb	Polyclonal antibody
PATP	*Para*-aminothiophenol
PCR	Polymerase chain reaction
rAb	Recombinant antibody
RE	Reference electrode
RNA	Ribonucleic acid
SAMs	Self-assembled monolayers
SCE	Saturated calomel electrode
SEM	Scanning electron microscopy
SPE	Screen-printed electrode
SPCs	Screen-printed cells
SPR	Surface plasmon resonance
SWV	Square wave voltammetry
TC	Tetracycline
TNT	Trinitrotoluene
TRIS	*Tris*(hydroxymethyl)aminomethane
WE	Working electrode
WHO	World heath organization
QD	Quantum dots
QCM	Quartz crystal microbalance

INTRODUCTION

The increasing concern worldwide for environment pollution, contamination of foodstuff, drug safety and security issues creates an urge for the development of fast, sensitive and reliable methods for the detection of biological and chemical compounds.

Electrochemical techniques can provide an inexpensive and sensitive tool for the development of small, portable devices that are able to rapidly detect such analytes with high sensitivity and specificity. Electrochemical sensors are expected to have an essential impact on multiple fields, including early disease diagnosis with better outcome for patients, drug monitoring and fast and accurate detection of environment pollutants and food contaminants.

Despite the attempts to progress research in the oncology field, cancer remains one of the leading causes of death worldwide, mainly due to its late diagnosis. Thus, there is an increasing demand for the development of rapid and sensitive detection methods for cancer biomarkers that are abberantly expressed in human serum in early stages of cancer. Electrochemical immunosensors are attractive candidates for the development of diagnostic tools, as they combine the specificity of antibody-antigen reaction with the sensitivity of electrochemical techniques. Recently, aptamers have been widely used as alternatives to antibodies, due to their versatile synthesis and ability to discriminate between similar molecules. Highly specific aptasensors were thus obtained.

Molecularly imprinting technique is a versatile method for the synthesis of artificial receptors, overcoming some of the drawbacks of using antibodies or aptamers. Inexpensive materials with special recognition abilities towards a wide range of molecules can be obtained, which exhibit high stability in harsh environmental condition.

This research was directed towards the development of various electrochemical affinity sensors using different receptors (antibodies, aptamers and molecularly imprinted films) for the detection of different target analytes of environmental, food safety, biomedical and biopharmaceutical interest.

One objective of this work was to develop electrochemical diagnostic devices for early detection of cancer. MUC1 tumor biomarker was chosen as a model molecule and antibodies and aptamers were employed as biorecognition elements. Nanomaterials

were integrated in the proposed sensors as immobilization platforms. Protein G-magnetic beads and streptavidin-magnetic beads were employed for an antibody sandwich assay and an aptamer sandwich assay, respectively. Gold nanoparticles were used for the immobilization of thiolated aptamers specific for MUC1 in a label free configuration.

Another objective of the present work was the development of molecularly imprinted electrochemical sensors for the detection of drugs, environment pollutants and food contaminants. We aimed to develop a generic protocol that could be applied to a broad range of molecules, including non-electroactive compounds, using hexacyanoferrite/ hexacyanoferrate redox mediator. Imprinted films were prepared by electropolymerization *via* cyclic voltammetry of *p*-aminothiophenol functionalized nanoparticles in the presence of template molecules. The subsequent extraction of the template from the polymer matrix results in the formation of specific recognition cavities that are able to bind the analytes.

We aimed also to investigate the practical applicability of the proposed sensors by analyzing complex matrices that contain the analyte, such as tap and river water, honey, serum and drug formulations.

STATE OF THE ART

1. General aspects of affinity sensors

The field of sensor development has broadened considerably in recent years, with a vast pool of applications in basically every analytical task from biomedical analysis to food safety and environmental analysis. Among sensing systems, affinity sensors represent a large group of the chemical and biological sensors that gained increased attention in the past 20 years.

Sensors are devices that detect a physical, chemical or biological change and convert it into a measurable signal[1].

A biosensor is an analytical device that incorporates a biological molecular recognition element at the surface of a transducer which outputs an electric or optical signal that is directly related to the concentration of the target analyte. The biological molecule confers the selectivity of the sensor[2-4]. Various biological elements may be employed as bioelements, such as enzymes, antibodies, aptamers, DNA/RNA, cells, tissues, vitamins, which enable recognition and binding interactions of the target analyte with high selectivity. The transduction of the recognition event to an electronic signal can be achieved by electrochemical, optical, piezoelectric and thermal methods. The general scheme of a biosensor is illustrated in Fig. 1.

An affinity sensor can be defined as an analytical device that incorporates a biological receptor immobilized at the surface of a transducer that can reversibly detect a receptor-ligand interaction with high selectivity and in a non-destructive way[3]. Affinity sensors are based on molecular recognition and selective binding of biomolecules (antibodies, nucleic acids, receptors) with the analyte of interest, event that is determined by complementarity in size and shape of the binding site to the analyte of interest[5]. Due to the high affinity and specificity of this interaction, affinity sensors exhibit high sensitivity and selectivity.

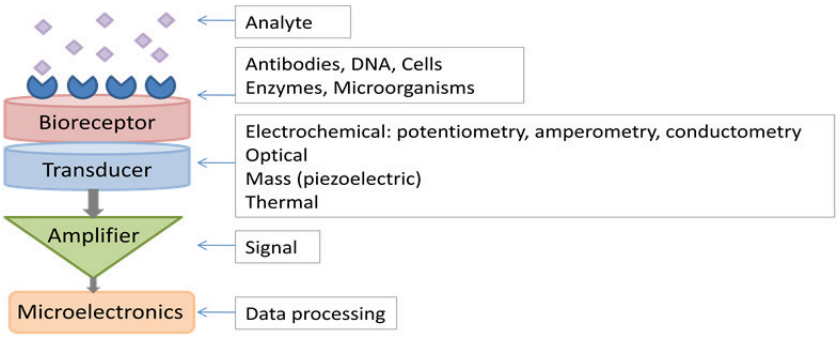

Fig. 1. Schematic representation of a biosensor

1.2. General classification

Various classifications for sensors can be found in the literature:

- According to the transduction principles:
  - *Optical*: based on the conversion of light rays into electronic signals (fluorescence, absorbtion, reflection); they have the advantage of high sensitivity, wide dynamic range and multiplexing capabilities;
  - *Thermal*: uses thermal effects to measure physical parameters and involves a transduction in two steps: first the input signal is transduced in a thermal signal, which is then transduced in an electrical signal;
  - *Mass (piezoelectric)*: based on the measurement of the vibrational frequency of the quartz crystal, which in air depends on the mass of the crystal and the immobilized analyte[6].
  - *Electrochemical*: are the most widely used and can be categorized in:
    - *Potentiometric* – based on determination of the potential difference between two electrodes - one reference electrode and one sensitive electrode which can be specific (e.g pH electrodes, ionic electrodes); they have a wider range of detection, but lower sensitivity, than other electrochemical techniques;
    - *Conductimetric* - based on altering the conductivity of the sample solution; they have the drawbacks of low selectivity and interference in real samples;
    - *Amperometric* – based upon the measurement of the current generated by the oxidation or reduction of electroactive species at a constant potential.
- According to the interaction mode between the medium and the sensor (surface or volume interaction)[2]
- According to the nature of the biological recognition process:
  - *Biocatalytic sensors*: incorporate enzymes, microorganisms, cells, tissues and biomimetic catalysts to recognize the analyte of interest and produce electroactive species or other detectable outcome.
  - *Affinity sensors*: based on a selective binding interaction between the analyte and a bioelement such as antibody, nucleic acid, receptor proteins or synthetic receptors[5,6].

- According to its use: control of air and water pollution, health, defense and security, food and process control, biomedical field etc[2].

1.3. Voltamperometric sensors

Electrochemical biosensors currently dominate the sensing devices field, due to their simplicity, low cost and high sensitivity. The growth in the field of electrochemical biosensors has been remarkable since the development of the first biosensor by Clark in 1962[7].

There are mainly three categories of measurement for electrochemical methods: current, potential and impedance. The most commonly used technique in sensors' development is the former class. In voltammetric and amperometric methods a potential is applied and the current resulted by the electrochemical oxidation or reduction is measured. In voltammetric techniques the potential is scanned over a set of potential range, while in amperometry the potential is maintained constant. Amperometric detection is commonly used with biocatalytic and affinity sensors because of its simplicity and low detection limit[5].

Depending on the analytic principle involved, amperometric sensors can be classified in three main categories:

- *Analysis by pre-concentration*, requires the presence at the surface of the electrode of a complexing agent or molecular recognition elements that selectively preconcentrate a given analyte. This leads to the increase of the local concentration of the analyte at the the electrode surface, prior to detection itself, in order to perform the detection in very diluted media.
- *Direct electrocatalytic detection*, which uses electron transfer accelerating agents (chemical mediators or electrode material acting as solid state catalyzer), that increases the sensitivity of detection.
- *Indirect amperometric detection*, for species that are not electroactive, but which perturb the electrochemical proprieties of an electrode[2].

Perhaps the most important advantage of electrochemical biosensors is that they ensure in one device both the sensitivity towards the measured quantity and the transduction into an electric signal, which is easily and directly adaptable, in most cases, to a measuring instrument[2]. Electrochemical biosensors have the advantage of high specificity due to the incorporated bioelement, short response time (in general shorter than 1 min), low cost, ease of use, as well as the possibility of miniaturization and automation. Moreover they give rapid and specific detection of analytes in complex media such as blood, plasma, urine, river waters, food matrices etc, eliminating the need for sample preparation which makes them suitable for

application in a wide range of fields. The biggest portion of the developed electrochemical sensors is for healthcare and disease diagnosis; other fields include food industry, pharmaceutical analysis, sport, national defense and domestic safety, environmental analysis[2,3,5]. Some of the drawbacks include the problematic stability of the bioelement, which is sensitive and can be altered under environmental conditions such as pH or temperature, as well as the heterogeneity of the immobilized receptor at the surface of the transducers.

1.4. Impedimetric sensors

Electrochemical impedance spectroscopy (EIS) is an effective and sensitive surface characterization technique widely used in chemical sensors and biosensors having the main advange of label-free detection[8]. It can be employed for the detection of analytes in low concentrations[9] and for the study of electrode/electrolyte interface and electrode surface kinetics[10]. EIS is based on the measurement of resistive and capacitive properties of materials. An AC potential is applied to an electrochemical cell and the resulted AC current signal is measured. The fundamental of a spectrum is frequency: an impedance spectrum is obtained by varying the frequency over a wide range[5]. According to Ohm's law, resistance can be defined as the ratio between potential, E, and current, I; thus the impedance of a system can be calculated using the following equation:

$$Z = \frac{E_t}{I_t} = \frac{E0\ \sin(\omega t)}{I0\ \sin(\omega t + \Phi)} = Z0\ \frac{\sin(\omega t)}{\sin(\omega t + \Phi)}$$

Where Z is impedance, E_t potential at time t, I_t current at time t, E_0 and I_0 signal amplitudes, ω frequency and Φ phase shift between Et and It[5]. Impedance is thus expressed in terms of magnitude Z_0 and phase shift Φ.

EIS can be performed in two ways:

- *faradaic impedance* – when electrochemical redox reactions occur that generate electrons, which are transferred through the electrode surface; these electrons confront a resistance against their transfer towards the surface of the electrode, which is called faradaic impedance.
- *non-faradaic impedance* – is a DC form of impedance, its electrical properties being generated by double layer capacitance[8].

The diagram of the EIS measurement is represented by the Nyquist plot which includes the imaginary part of impedance, -Z, on Y axis and the real part, Z, on X axis.

For proper data calculation an impedimetric model circuit must be designed (Randless cell circuit), which include as elements electrolyte solution resistance (Rs), electron transfer resistance (Ret), Warburg impedance, (W) and capacitance (C). Thus, this circuit model represents the electron transfer ability of the layer on electrode surface (Ret), mass transfer (W) and electrode surface capacitance (Cdl)[8]. EIS is widely used for the construction of label-free affinity sensors, with the advantages of ease of detection, low cost, no sample pretreatment, insensitivity to most environmental disturbances and the suitability for the detection of any types of molecules that exhibit interactions between a recognition receptor and analyte[5,8]. The method became particularly attractive in the immunosensors field, where the formation of antibody-antigen can be directly monitored without the need of further labeling, by simply monitoring the change in the electron transfer resitance when the analyte binds. Some limitations of the method include the difficulty in surface regeneration, especially for antibodies with high affinity constants, and in minimizing nonspecific adsorption[5].

1.5. Single use sensors

Screen printed electrodes (SPEs) are disposable minielectrodes patterned with working, reference and counter electrodes (Fig. 2) and have gained increased popularity in electrochemical biosensors due to their low cost and ease of mass production using thick film technology[11]. They are fabricated using the screen printing technique which involves a sequential deposition of thick films on a solid substrate which permits to obtain all-solid-state, flat and mechanically robust sensors. The methods consist in the deposition of a graphitic ink to the solid substrate through a mask covering its surface; different inks and masks can be used to obtain various patterns and configurations. A thermal treatment is then applied to remove the solvent and an insulating layer can also be applied in order to delimitate the surface of the electrodes maintaining electrical contacts on the one side[2]. The main advantages of these kind of electrodes include: the elimination of surface fouling, as they can be used one time and replaced with other electrodes from the same batch; contamination is avoided when used for the analysis of biological liquids being discarded after one use; they are suitable for use in flow analysis and for portable device for *in situ* monitoring; use of low volumes of samples due to their small dimensions[12]. A limitation of SPE is the use of organic solvents which might lead to the dissolution of the ink.

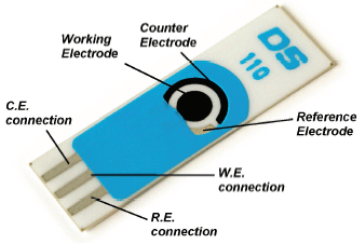

Fig. 2. Screen-printed electrode

1.6. Immobilization of the bioelements

A crucial step in the elaboration of sensors relies in the appropriate immobilization of the bioreceptor at the surface of the transducer, which affects the sensitivity of the sensor. The immobilization method should ensure the stability of the bioreceptor, preserving its activity, assuring at the same time a facile accessibility at the biomolecule. A low nonspecific adsorption of biomolecules is also desirable. These problems limit in fact the commercialization of biosensors. Several immobilization techniques can be employed:

- *Adsorption* – the receptor is adsorbed either *directly* on the surface of the transductor or after a *modification* of the surface that increases the affinity between the two parties - tranducer and receptor. Weak bonds are involved - Van der Waals forces, hydrophobic forces, hydrogen bonds, ionic forces - therefore the main disadvantage of the method is the low stability of the formed films due to desorption phenomena[2]. An example is the Langmuir-Blodgett technique in which a solid surface is introduced vertically in a solution of amphifilic molecules and then withdrawn, leading to the formation of a monolayer of amphiphilic molecules on the solid support at the water/air interface.
- *Reticulation* - involves the formation of imino bondings through polyfunctional agents such as glutaraldehyde. The aldehyde groups react with the amino groups of the proteins linking them together.
- *Inclusion (entrapping)* – based on the formation of an encapsulation matrix around the bioreceptor. The method has the drawback of steric hindrance and possibly hard accesibility to the receptor. It can be done by:
    - depositing a mixture of receptor molecules and matrix components (in generally preformed polymers or clays) onto the surface of the transducer by dip-coating, drop-coating or spin-coating.
    - including the receptor along with the matrix formation by electropolymerization of monomer molecules directly on the surface

of an electrode, having the advantage of a more uniform coverage and control over the film thickness

- *Covalent grafting* – the bioreceptor is linked to the transducer by strong, irreversible covalent bondings, leading to stable films. Most transducers do not permit direct grafting, therefore the surfaces are often modified with compounds that exhibit functional groups that allow grafting (COOH, OH, SH, CN etc), such as polymers or by silanization[2]. A widely used technique is the self-assembled monolayers (SAMs) technique, which involves irreversible chemisorption of thiols on gold surfaces, with the formation of highly ordered, packed layers.
- *Bioaffinity attachment* - among the biochemical interactions used to bind proteins on solid supports in an oriented and uniform way, the biotin-(strept)avidin interaction is the most widely used, having the advantage of high stability, specificity and efficiency[13]. Other affinity immobilization reactions include recombinant proteins with engineered histidine-tag systems and Protein A/Protein G based systems that interact with Fc regions of antibodies[14].

2. Immunosensors and aptasensors

Among the large class of biosensors, immunosensors attracted considerable attention, due to their enormous potential for the highly specific detection of biochemical targets of medical[15-17], environmental[18,19] and food safety interest[20,21].

The conventional enzyme linked immunosorbent assay (ELISA) has been widely used for clinical diagnosis and in biochemical field. However the long analysis time and the sometimes inadequate sensitivities, make immunosensors attractive alternatives for the detection of various targets. Besides the high specificity, immunosensors also have the advantages of low detection limits, small sample volumes and reduced use of chemical which leads to lower cost, little sample preparation, ease of miniaturization and automation, and the elusion of mass transfer limitations when flow systems are used[5, 22].

2.1. Definitions

Immunosensors are affinity ligand-based biosensor solid state devices in which immunochemical reactions are coupled with a transducer[23]. The general working principle of the immunosensors is based on the fact that the specific immunochemical recognition of antibodies (or antigens), immobilized on a transducer, to antigens (or antibodies), in the sample media, generates analytical signal that vary with the concentrations of the analytes of interest. Therefore the main advantage of immunosensors is their high specificity, preserved even in complex matrix samples, due to the formation of specific immunocomplexes between antibodies and their antigens.

An immunoassay is a solid state system based on the reaction between an antibody and an antigen in which the detection of the recognition process takes place elsewhere. For immunosensors the formation of the immunocomplex and the detection takes place on the same device[24].

Aptasensors are analytical devices that are using aptamers as recognition elements. They are characterized by even higher specificity, due to the capability of aptamers to differentiate between targets with similar structures.

2.2. General classification

As a subclass of biosensors, immunosensors can be as well classified according to their transduction mode in electrochemical (potentiometric, conductometric, impedance, amperometric), optical (fluorescence, luminescence, refractive index) and piezoelectric devices[23,25,26].

- *Amperometric immunosensors* are the most popular types of immunosensors and are based on the measurement of the electrochemical oxidation and reduction of species. Only few applications of direct amperometric immunosensors are available, because most antibodies and antigens are not electroactive. The majority of amperometric immunosensors use electroactive labels or mediators for the detection.
- *Potentiometric immunosensors* are based on the change in potential that occurs when the antibody-antigen complex is formed. They have low sensitivities due to the relatively small change in the potential that occurs during the immunoaffinity reaction and the high influence of interferences[24].
- *Impedimetric immunosensors* have been widely applied for the detection of various target molecules, as they permit a simple, label-free detection. Their detection principle is based on the change in interfacial properties when the immunorecognition event occurs[26].
- *Optical immunosensors* have also gained popularity lately as an alternative to traditional immunoassays. As optical transduction techniques the most commonly used are surface-plasmon resonance (SPR), which offers a direct, real-time detection of immunological targets, and fluorescence-based immunosensors that use fluorescence labeled antigens or antibodies.
- *Piezoelectric immunosensors* offer simple, direct and real-time detection of immunological analytes based on the changes in mass loading and interfacial properties of the sensing surface upon the immunocomplex formation[24, 25].

Another classification of immunosensors can be made depending on the operation mode:

- *Direct (label-free) immunosensors* – based on direct detection of the physical or chemical effects arrising from the antigen-antibody complex formation. They do not require labels and can be used for fast, real-time analysis. A major drawback is the significant influence of non-specific adsorption on their performance[25,27].

- *Indirect immunosensors* – are based on the signal obtained from one or more labeled species offering more sensitive and versatile detection. Labels or redox mediators are often used for electrochemical immunosensors, since antigens and antibodies are not intrinsecally electroactive. Although it has the advantage of higher sensitivity and lower interference from non-specific adsorption,

indirect detection is more time consuming, requiring several washing and separation steps[25]; moreover the use of labeling reagents can affect the antigen-antibody binding[28]. A variety of labels can be used such as enzymes, e.g. horseradish peroxidase[29], alkaline phosphatase[30], catalase and glucose oxidase[31], electroactive compounds such as ferrocene[32] and nanomaterials, that also amplify the signal, such as gold nanoparticles (AuNPs)[33] or various quantum dots (QD)[34].

2.3. Types of format

The functional principle of immunosensors is based on monitoring the binding event between an antibody and an antigen. This can be assessed by directly evaluating the occupied binding sites or indirectly, on measuring the unoccupied sites, leading to two types of possible immunosensor formats: competitive format and non-competitive format[27].

2.3.1. Competitive immunosensors

They are used for small antigens with only one epitope and are referred to as "limited reagent assay" because of the limited amount of antibodies used[5]. They are based on the competition between the sample analyte and a labeled analyte for a fixed number of binding sites: the antibody is immobilized on the transducer and a mixture solution containing a known amount of labeled antigens and the unknown sample is added to compete for the limited binding sites. The signal of the labeled analyte is inversely proportional to the amount of sample analyte, thus the higher the amount of bound sample antigen, the lower the obtained signal.

Competitive immunoassays can be run in homogenous or heterogenous formats. A homogenous assay quantifies the amount of labeled, unbound antigen, without the need for separation steps, while in the heterogenous assay the labeled unbound antigen is eliminated in a washing/separation step and the remained labeled bound antigen is measured. The homogenous format is faster, but exhibits lower sensitivity, due to the susceptibility to non-specific adsorption. The heterogenous format is more time-consuming, but exhibits higher sensitivity.

Despite their simplicity, competitive immunosensors have the drawback of possibly reduced binding affinity, especially if the labeling takes place at a site that is closely associated with an epitope[25]. The working principle of competitive immunosensors is illustrated in Fig. 3A.

2.3.2. Non-competitive immunosensors

Non-competitive immunosensors are applicable for large antigens with at least two epitopes and are also called "excess reagent assay" because an excess of antibodies

is used[5]. They are usually performed in a "two-site", "sandwich" format, although a "one-site" format is also possible. In a "two-site" assay the analyte is sandwiched between two antibodies: a capture antibody immobilized on the surface of the transducer that captures the antigen from the bulk sample and a signal antibody which binds on the existing antigen-antibody complex. A washing step is performed after each incubation step to separate unbound reagents. (Fig. 3B)

The signal antibody is tagged with an enzyme or a redox label which exhibits a signal directly proportional to the concentration of bound antigen. However, labeling an antibody specific for each antigen can be cost- and time-consuming, therefore a third indifferent labeled antibody (IgG) is used that binds to the second antibody.

Although, normally, no signal should be obtained in the absence of the antigen-analyte, because the labeled antibody has no site to bind to, a small signal always occurs due to the non-specific binding of the labeled antibody on other constituents of the immunosensor. Non-specific adsorption offently occurs when serum samples are analyzed, when other proteins present in the serum can bind to antibodies or other materials of the immunosensor[35]. This increases the background signal and seriously affects the limit of detection. Thus, an effective blocking agent should be used, such as surfactants (Tween 20, polyethylene glycol)[5], bovine serum albumin (BSA)[36,37], casein[38] or thiolic compounds in the case of gold surfaces[39]. Fouling of the electrode surface can occur if the blocking agent adsorbes directly on it and should be avoided[5].

A one-site assay is based on the immunoaffinity reaction between the immobilized antigen and a labeled antibody. The unbound labeled antibody is washed and the signal given by the bound antibody is measured.

The non-competitive sandwich format has the advantage over competitive assays of higher sensitivity, specificity and greater dynamic range, but it is not suitable for the detection of monovalent small molecules (molecular weight < 1000 Da)[40].

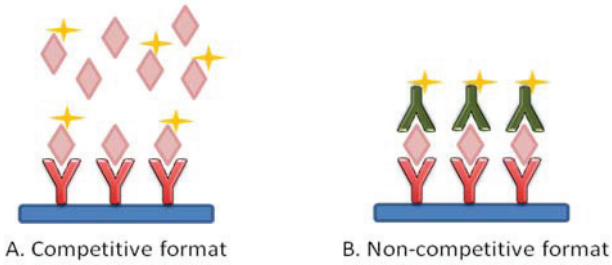

Fig. 3. Working principle of immunosensors in competitive (A) and non-competitive (B) format

2.4. Types of biorecognition element

The proper selection and immobilization of the biorecognition element is of paramount importance for the successful development of an immunosensor. Depending on the biorecognition element, affinity sensors can be classified in immunosensors (using antibodies, antibody fragments or antigens as recognition elements), aptasensors (based on aptamers), DNA sensors (based on hybridization of DNA), peptide nucleic acid sensors (peptasensors, using peptides as bioelements), whole cell biosensors and molecularly imprinted polymer based sensors (including a biomimetic recognition element)[41].

2.4.1. Antibodies

Antibodies (Abs) are glycoproteins produced by specialized B lymphocyte cells of the host, as response of the immune system to the presence of foreign species called antigen (Ag). They are also known as immunoglobulins. There are five classes of immunoglobulins (IgG, IgA, IgM, IgD, IgE), IgG being the most widely spread in nature and commonly used in the fabrication immunosensors[24].

The structure of Ab is illustrated in Fig. 4. IgGs are "Y"-shaped molecules constituted of two identical light chains (MW about 25000 Da) and two identical heavy chains (MW about 50000 Da), bound together by disulfide bonds and noncovalent interactions (hydrogen bonds). Both light and heavy chains have constant and variable domains: one variable domain for both light and heavy chains, V_L and V_C, and one constant domain for light chains, C_L, and three for heavy chains, C_{H1}, C_{H2}, and C_{H3}. The variable regions, V_L and V_H, are the most important for the antigen-antibody reaction, and are different among different antibodies, giving the specificity of the binding, depending on the amino acid sequences. They are the complementarity-determining regions (CDRs) and present hypervariable loops that represent the binding site to the antigen[5,24]. The high diversity of CDRs permits to produce high specifity Ab towards many kinds of Ag[24].

IgG can be divided in an antigen binding fragment (Fab) and a non-antigen binding fragment (Fc). Abs are bivalent and can bind two Ag, the Fab region exhibiting two identical binding sites for the antigen. The antigen-binding region is called "paratope" and the complementary site on the antigen is called "epitope", their complementarity being based on size, shape and chemical compatibility[5]. The interaction of antibodies with their antigens is based on hydrogen bonds, ionic bonds, hydrophobic interactions and van der Waals forces, but a close fit determined by a high degree of complementarity between Ab and Ag is necessary for the non-covalent interactions to take place. In some cases the binding event is accompanied by conformational changes in Ab, Ag or both, which brings them in a closer fit but may also affect the binding affinity[5].

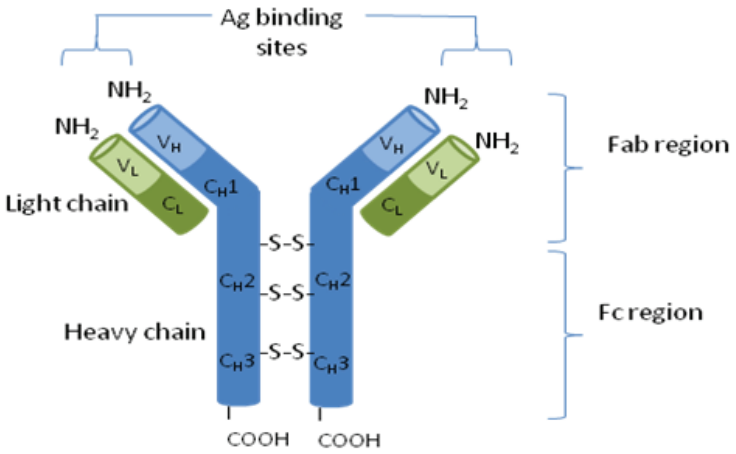

Fig. 4. The structure of an antibody

The strength of the binding of an Ab to its Ag is described by the equation[24]:

$$K=\frac{[Ab-Ag]}{[Ab][Ag]}$$

where K is the equilibrium constant of the interaction (affinity constant) and Ab-Ag is the resulted immunocomplex; the values of K can vary from 10^6 to 10^{12}, with low cross-reactivities when $K>10^8$.

Although the Ab-Ag reaction is highly sensitive, cross-reactivity can sometimes occur in the case of antigens that present identical or similar epitopes. Ab can bind to these similar Ag leading to false positives or interference for the immunosensor[5].

Antibodies can be produced by immunization of host animal, when a sub-lethal dose of Ab is injected to trigger the immune response. However, these procedures are complicated and time-consuming[5,42]. The production of recombinant Ab (rAb) is shorter and allows to obtain a high diversity of Ab. It is based on the isolation of mRNA from the B-lymphocytes from the spleen of animals followed by cDNA synthesis and amplification of the variable regions by PCR. The amplified regions are then cloned in a plasmid vector. After the transformation of the host (*Escherichia coli*), different heavy and light chains can be randomly combined to obtain a DNA library with high diversity[42]. Monoclonal antibodies (mAb) are produced by identical immune cells (clones of a sigle parent cell). They have affinity for a single epitope, which offers high specifity towards an Ag, being offently used as a primary Ab in the construction of immunosensors. Polyclonal antibodies (pAb) are produced by several different

immune cells as a mixture of immunoglobulins against an Ag, each of them binding a different epitope. They are in general used as secondary antibodies in immunoassays[5].

Ab fragments can also be used in immunoassay, since Ab can be fragmented in their Fc and Fab regions using proteolytic enzyme digestion (pepsin, papain)[43].

2.4.2. Aptamers

Aptamers are short single stranded DNA or RNA oligonucleotides that specifically bind a wide range of target molecules with high affinity and specificity[42]. They can selectively bind to small molecules, such as organic dyes, drugs, nucleotides, amino acids or to small parts of macromolecules, such as protein, polypeptides, polysaccharides[5,44,45]. Aptamers towards membrane bound receptors, cell surface epitopes, whole cells and even whole organisms[46] or difficult haptens such as toxins or prions[44] were also synthesized. In the binding of the aptamer to its target, hydrogen bonds, hydrophobic interactions, stacking interactions and electrostatic interactions are commonly involved[46]. Their affinity is given by their folding characteristic, aptamers being able to fold into a binding pocket upon the binding of small molecules by hydrogen bonds, or integrate in the structures of macromolecules, by complementarities driven by noncovalent interactions[44-46]. Aptamers have dissociation constants in the pico- to micro-molar range[44,46] with affinity and specificity equal or superior to mAb[47]. Therefore they successfully substitute Ab as recognition elements in immunoassays and immunosensors, being more stable and able to discriminate between closely related targets. They also have the advantage of avoiding the use of animals for their production since they are synthesized *in vitro* by Systematic Evolution of Ligands by Exponential Enrichment (SELEX). The method, introduced in 1990[48,49], starts with the synthesis of a single-stranded oligonucleotide library which contains a very large number of individual species (around 10^{15}) that increases the probability to obtain aptamers that are highly specific for a target. By PCR amplification a double stranded oligonucleotide pool is obtained, which is transcribed (for RNA) or strand separated (for DNA). The obtained oligonucleotides are incubated with the target and the aptamers that bind the target are partitioned (by filtering or by affinity chromatography), eluted and amplified by PCR to provide an enriched pool of nucleic acid. Several cycles of the SELEX process are required to obtain only a few aptamers that exhibit high specificity towards a target[44,46].

The synthetic preparation offers them other advantages such as: stability to heat and wide range of pH and salt concentrations, affinity towards a wide range of target molecules, reduced batch-to-batch variations, they are more resistant to denaturation which makes them suitable for reusable applications and can be chemically modified to increase the stability, affinity and specificity[44,47]. A drawback of aptamers use is their

sensitivity to nucleases, but this problem was overcome by chemical modifications of 2'-position on ribose ring[44].

Due to their inherent advantages aptamers have been widely used in a diverse range of fields such as drug delivery[50,51], therapy[52,53] , diagnostics[54], and for various analytical applications such as immunoassay and immunosensors[55-57], chromatography[58], electrophoresis[59] or mass spectrometry[60].

2.5. Immobilization of antibodies/aptamers

Since the working principle of immunosensors is based on the measurement of the signal obtained through the specific immunoreactions between immobilized bioelements and analytes, the choice of a proper immobilization technique is pivotal for the performance of the sensor[25]. The immobilization method must firstly preserve the biological activity of the bioreceptors. Secondly, it must allow a proper orientation (binding sites exposed towards the sample), as well as an adequate density (a too high density can bring steric hindrance in binding the analyte)[5,23]. The recognition layer can be immobilized on the surface of the transducer by various procedures.

2.5.1. Physical adsorption

The physical adsorption is based on non-covalent interactions between the antibody/antigen and the surface of the transducer, involving electrostatic interactions, van der Waals forces, hydrophobic interaction and hydrogen bonding[61]. A common example is the immobilization of antibodies on ELISA microtiter plate[43]. A more efficient example of bio-functionalization of immunosensing surfaces is layer-by-layer (LBL) self-assembly, which is used to prepare multilayers based on inter-layer electrostatic attractions[41] that serve for the immobilization of antibodies via electrostatic adsorption[62]. Despite its simplicity, direct physiosorption of biomolecules on the solid support leads to a random orientation of antibodies and possible desorption due to the weak bonds involved leading to low sensitivity and reproducibility[63]. Moreover it may lead to conformational changes and decreased bioactivities with time[41].

2.5.2. Entrapment

This procedure is based on the encapsulation of antibodies and antigens in polymer matrices. Although it offers a more stable attachment than physiosorption, the availability of the binding sites is quite low, leading to decreased sensitivity. Among the entrapment immobilization methods, sol-gel-based immobilization gained attention due to its simplicity, possibility to entrap molecules at low temperature, optical

transparency, tunable porosity, mechanical rigidity and low chemical reactivity[25,43, 63, 64].

2.5.3. Covalent Binding

The covalent binding method is the most commonly used procedure for the immobilization of bioreceptors and is based on covalent interactions between the functional groups of antibodies (-NH_2, -COOH) or aptamers and the modified surface of the transducers[63]. In general, the surface of the transducers does not exhibit sites for covalent binding, thus, most of the times, it is necessary to pre-coat the sensing surfaces with thin films that exhibit groups that bind the amino groups of antibodies for instance. Such functional reagents are glutaraldehyde, *N*-hydroxysuccinimide, carbodiimide succinimide ester, maleinimide or periodate[25,61]. Glutaraldehyde is a bi-functional cross-linking agent that has two aldehyde groups which can interact with amines to form peptide bonds. Glutaraldehyde is recommended for smaller sized molecules, while for higher sized molecules (>20 nm) *N,N'*-carbonyldiimidazole is preferred[43]. A promising and widely used technique to obtain functionalized films for the immobilization of antibodies, antigens or aptamers is the self-assembled monolayer technique. It involves the semi-covalent binding of disulfides, sulfides and thiols on noble metal surfaces, such as Au, Ag or Pt, to form highly organized SAMs. Long-chained *N*-alkylthiols (> C_{12}) are generally used that have derivatized functional organic groups that crosslink bioreceptors[23]. Thiol modified antibodies or aptamers can be directly bound on Au surfaces[43]. Mixed SAMs of long-chain thiols with carboxylic and hydroxyl group can be used as well to obtain stable affinity interfaces, which further bind the functional groups of bioelements [65]. Another common monolayer is based on oligo-ethylene glycol thiol, which exhibits regular structure, minimal desorption and high biocompatibility[66]. Thin layers are desirable, that would reduce the diffusion time of the analytes and improve the speed of the sensors response. Moreover because most of the reagents used in these systems are organic molecules, the thinner the layer, the less the insulating effect will be[66]. The use of alkyl silanes with amine, thiol, aldehyde or carboxylic groups is another popular functionalization strategy for cross-linking[67]. The covalent binding procedure has the advantage of a more stable and better oriented immobilization.

2.5.4. Oriented Binding

In order to obtain a high capture efficiency and a better performance of the sensor, an oriented immobilization (recognition sites are exposed to the sample, with higher accessibility for antigen binding) of the biorecognition elements is important.

The antibody can bind to a surface in four different ways: ***end-on*** (the Fc region is attached to the transducer), ***head-on*** (the Fab region is attached to the transducer), ***sideways-on*** (one Fc and one Fab region is bound onto the trasducer),

and ***flat-on*** (all three regions are bound to the surface). Since the recognitions sites are on the Fab fragment the desired orientation is ***end-on***. This can be achieved by two types of strategies: *site-oriented immobilization* and *bioaffinity immobilization*[63].

For the *site oriented immobilization*, the cross-linking techniques mentioned above are widely used. 1-Ethyl-3-(3-dimethylaminopropyl)-carbodiimide (EDC) - N-Hydroxysuccinimide (NHS), based coupling method is commonly used to immobilize antibodies. The linkers bind to amine group of antibodies forming a highly reactive NHS ester intermediate that forms peptide bond with amine or glutaraldehyde modified surfaces[43]. Chemically modified aptamers (e.g amino groups) can covalently bind chemical groups (carboxyl, hydroxyl etc) on the modified surfaces of the transducers. SAM is another technique that allows the oriented end-up binding of antibodies and is also widely used to immobilize thiolated aptamers and DNA probes on gold transducers. Aptamer SAMs involve the direct binding of 3' or 5' thiolated aptamers onto gold surfaces such as gold electrodes, gold nanoparticles, gold nanorods, surface plasmon resonance (SPR) chips or quartz crystal microbalance (QCM) chips [47].

The *bioaffinity immobilization* technique is based on Protein A or G, (strept)avidin-biotin interactions, lectin-sugar, His-Tag systems or DNA-directed immobilization[63].

Protein A or G are bacterial proteins that specifically bind the Fc regions of antibodies with high affinity, allowing the Fab sites to be oriented away from the solid support[24]. This leads to a higher binding efficiency, sensitivity and stability[43]. Protein A was originally isolated from *Staphylococcus aureus* and presents five Fc binding domains located near the $-NH_2$ terminal. It only binds human IgG 1, 2 and 4 subclasses, weakly binds mouse IgG and does not bind goat and rat IgG[24]. Protein G is a cell surface protein isolated from *Streptococcus* group C and G, which presents three Fc binding domains near the –C-terminal and can bind antibodies from various subclasses and species[24].

(Strept)avidin-biotin is another widely used oriented immobilization technique and it is based on biotinylated capture bioreceptors (antibodies, aptamers) that are bound to avidin or streptavidin functionalized surfaces. Avidin and streptavidin are proteins found in egg whites, or produced by *Streptomyces* species respectively, that contain four identical units, each subunit being able to bind one biotin molecule. Therefore, each streptavidin can bind four biotinylated bioreceptors leading to an increased amount of immobilized receptors[47]. Biotin-(strept)avidin is one of the strongest non-covalent interaction, presenting dissociations constants of 10^{-15} mol/L; they are stable at high temperatures, pH variations and exposure to chemicals (e.g protein denaturants)[24].

2.6. Applications of electrochemical immunosensors for cancer biomarkers detection

Despite the efforts made in cancer research field, cancer still remains one of the leading causes of death in developed and developing countries, mainly due to late diagnosis and treatment failure. Although the rates of new cancer cases decreased with 0.7% each year in the past 10 years, according to the data from 2009-2011, 40.4% of men and women will develop cancer at some point during their lifetime. The estimated new cases in 2014 were 1665540 and the estimated deaths 585720[68]. The most common types of cancer in US, UK and Europe are breast, prostate, lung and colorectal cancer [68,69,70]. Biomarkers are defined as "a characteristic that is objectively measured and evaluated as an indicator of normal biological processes, pathogenic processes, or pharmacological responses to a therapeutic intervention"[71]. Cancer biomarkers are abberantly expressed during malignant processes, even from early stages, and can therefore represent a promising tool for early diagnosis and improvement of patient survival rate. The ideal cancer biomarker would be a protein or protein fragment, which can be easily detected in patient's biological fluids (e.g blood, urine), but not detected, in healthy patient[72]. Most of the proteins are present in the body in physiological conditions and are overexpressed in case of neoplasms. Cancer biomarkers are not tumor-specific, more than one marker is overexpressed in a particular type of cancer, therefore the simultaneous detection of a panel of cancer markers is usually required, in order to avoid false-postives. They can serve for diagnosis, prognostic, staging and therapy follow up. Thus, the development of new screening devices that are able to detect cancer biomarkers in biological fluids, in early stages, is of interest. An optimal screening assay should be non- or minimally-invasive, use small amount of sample, be site-specific and able operate at the level of differential diagnosis and to be specific enough to produce an acceptable limit of false-positive results[72]. The currently used methods for the detection of cancer include immunohistochemistry, ELISA, Western Blot, radioimmunoassay, immunofluorescence etc, but they have limitations in analysis time, cost, sensitivity for biomarkers whose normal range is in the low pg/mL, relatively large sample size, the need for qualified personnel and difficulty in measuring collections of proteins[73,74]. Electrochemical immunosensors have attracted considerable interest in recent years because of their rapidity, ease-of-use, low cost, high sensitivity and specificity, possibility of miniaturization, automation and in field analysis, and applicability for multianalyte detection of tumor markers[74].

Many electrochemical immunosensors have been reported in the literature in the past years for the detection of cancer biomarkers. Some exemples of electrochemical immunosensors for the detection of the most common cancer markers are presented in Table I.

Table I. Electrochemical immunosensor for the detection of various cancer markers

Biomarker and type of cancer	Method	Sensor performance	Ref.
Prostate specific antigen (PSA) In: Prostate cancer	Label-free sensor based on crumpled graphene-Au decorated composite modified electrode	LOD:0.59 ng/mL LR:0-10 ng/mL	75
	Label-free sensor using polypyrrole Au nanowire array as immobilization platform	LOD:0.3 fg/mL LR: 10 fg/mL -10 ng/mL	76
	Electrochemical immunosensor with integrated microfluidic system based on CNTs immobilization platform for primary antbodies and HRP labeled secondary antibodies	LOD:0.08 μg/L LR:0-60 μg/L	77
	Electrochemical immunosensor based on gold nanoparticles-polyamidoamine dendrimer-MWCNTs-ionic liquid-chitosan nanocomposite as immobilization platform for primary antibody and thionine and HRP labeled secondary antibody	LOD:1 pg/mL LR:0-80 ng/mL	78
Carcinogenic antigen 125 (CA125) In: Ovarian cancer, endometrial, lung, breast, gastrointestinal cancer	Sensitive electrochemical immunosensor was proposed for detection of CA125 based on ferrocenecarboxylic acid, HCl-doped polyaniline and chitosan hydrochloride	LOD:0.25 pg/mL LR:0.001-25 ng/mL	79
	3D microfluidic origami device combined with electrochemiluminescence (ECL) using AuNPs as immobilization platform and luminol-AuNPs as labels for secondary antibody	LOD:0.0074 U/mL LR:0.01-100 U/mL	80
Carcinoembryonic antigen (CEA)	Electrochemical immunosensor based on MoS_2 nanosheets-Au	LOD:0.27 pg/mL LR: 1 pg/mL	

In: Colorectal carcinoma, gastric, pancreatic,lung, breast, medullary thyroid cancer	nanocomposite as immobilization platform and Ag nanospheres-glucose oxidase as label	– 50 ng/mL	81
	Electrochemical immunosensor based on thionine functionalized CNTs-AuNPs composite as immobilization platform and HRP labeled signal antibody	LOD:0.008 ng/mL LR:0.02-80.0 ng/mL	82
Alpha-fetoprotein In: Hepatocelular and testicular carcinoma	Label-free electrochemical immunosensor based on gold nanoparticles–polydopamine–thionine–graphene oxide compsite immobilization platform	LOD:0.03 ng/mL LR:0.1-150 ng/mL	83
	Electrochemical immunosensor based on microfluidic microbeads-based multienzyme-nanoparticle amplification strategy	LOD:0.2 pg/mL LR:0.5-30 pg/mL	84
Carcinogenic antigen 19-9 In: Pancreatic, colorectal, gastric and hepatic carcinomas	Electrochemical immunosensor based on Au nanoparticles functionalized porous graphene as sensing platform and Au@Pd core/shell bimetallic graphene for immobilization of redox probe-thionine, HRP, and secondary antibodies	LOD:0.06 U/mL LR:0.015-150 U/mL	85
Tumor necrosis factor-alpha In: Cervical, ovarian, prostate, colon cancer	Label free electrochemical immunosensor based on ferricyanide-chitosan-glutaraldehyde composite as sensing layer, covered by chitosan as immobilization layer for primary antibodies	LOD:10 pg/mL LR:0.02–34 ng/mL	86
Squamous cell carcinoma antigen (SCCA) In: Cervical squamous cell carcinoma	Electrochemical immunosensor based on Au NPs decorated mercapto-functionalized graphene sheets as immobilization platforms and Au/Ag/Au core/double shell nanoparticles as enzyme-mimetic labels	LOD:0.18 pg/mL LR: 0.5 pg/mL - 40 ng/mL	87

Mucin 1 (MUC1, also known as episialin, PEM, H23Ag, EMA, CA15-3, CA19-9, MCA) is a potential tumor marker in ovarian[88], breast[89], lung[90], pancreatic[91], liver[92] or colon cancer[93].

It is a transmembrane glycoprotein from the Mucins family, that is expressed on the apical plasma membrane of most secretory epithelia. The core protein has a weight of 120–225 kDa and the mature glycosylated form's weight is 250–500 kDa. It consits of 2 subunits, an $-NH_2$ terminal large extracelular region and a –COOH terminal intracelular cytoplasmatic tail. The extracellular domain of MUC1 can be released into to the extracellular matrix by an enzymatic cleavage, and thus found into the serum, serving as tumor marker[74]. MUC1 is involved in the processes of proliferation, inflamation, invasion and metastasis, angiogenesis, chemoresitance and resitance to apoptosis[94].

Several sensing devices have been reported on its detection as seen in Table II.

Table II. Sensing devices for the detection of MUC1 [74]

Sensing mechanism	Sensor performance	Ref.
1) ferrocene-labeled aptamer-complementary DNA was used 2) complementary DNA immobilized on the electrode surface has the ability to hybridize both MUC1 and VEGF165 aptamers increasing the distance between ferrocene used to label aptamers and the electrode surface.	LOD: 0.33 nM LR: 1-20 nM	95
A gold interdigitated capacitor transducer was modified using magnetic beads for simultaneous detection of multiple tumor markers	LOD: 50 U/mL LR:1-200 U/mL	96
1) N-doped graphene sheets modified electrode was used 2) Detection of MUC1 in saliva	LOD:0.012 U/mL LR:0.1-20	97

	U/mL	
MUC1-binding aptamer is used to recognize MCF-7 human breast cancer cells, in a sandwich aptamer-cell-aptamer approach with an enzymatic label	LOD: 100 cells LR:100-10^{-7} cells	98
Thiolated MUC1 aptamers tethered with methylene blue are immobilized on gold electrodes	LOD: 50 nM LR: 0-1.5 μM	99
Ferrocene carboxylic-doped silica nanoparticles was used as an immobilized affinity support	LOD:0.64 U/mL LR:2-240 U/mL	100
Sandwich antibody-protein-aptamer assay based on electropolymerized *o*-aminobenzoic acid immobilization platform and methylene blue redox indicator	LOD: 0.62 ppb LR: 1-12 ppb	101
Sandwich aptamer-aptamer sensor combining a dual signal amplification strategy of poly(*o*-phenylenediamine)–Au nanoparticles hybrid film as carrier and AuNPs functionalized silica/multiwalled carbon nanotubes core–shell nanocomposites as tracing tag	LOD: 1 pM LR: 1-100 nM	102

3. Nanomaterials for the design of amperometric sensors

Nanomaterials, such as nanotubes, nanowires, nanofibers, nanorods, nanoparticles, nanocomposites and other nano-structured materials, have been widely used for the development of chemosensors and biosensors, due to their unique

physical and chemical properties, such as large surface area/volume ratio, good conductivity, excellent electrocatalytic activity and high mechanical strength [103]. Magnetic beads (MBs) and gold nanoparticles (AuNPs) have been widely applied for the development of immunosensors due to their excellent biocompatibility.

3.1. Magnetic beads

Magnetic nanoparticles have gained increased attention in recent years for the development of biosensors, being used as labels or as immobilization platforms, either integrated in the transducers materials or dispersed in the sample followed by their capture onto the sensing surface by an external magnetic field[104]. The magnetic character implies that they respond to a magnet, making sampling and collection easier and faster, but their magnetization disappears once the magnetic field is removed[105]. Among these particles, metal oxides are often preferred over pure metals (Fe, Co, Ni) because they are more stable to oxidation[106]. The properties of magnetic nanoparticles depend on their size. Their best performance is presented at sizes of 10–20 nm due to supermagnetism. They have large surface area and high mass transference, offering many advantages in the fabrication of sensors such as enhanced sensitivity, low limit of detection, high signal-to-noise ratio, shorter analysis time[104] and amenability to automation and miniaturization[105]. Among the magnetic nanomaterials Fe_3O_4 is most commonly used in biosensors, due to its superparamagnetic property, biocompatibility with antibodies and enzymes and ease of preparation. However, it has the drawback of possible aggregation in clusters in the presence of biological solution due to Fe_3O_4 magnetic dipolar attraction and its large ratio of surface to volume[104], thus surface functionalization with biological molecules or polymers is required in order to improve their stability and biocompatibility[104,106,107]. Several strategies of surface functionalization of MBs for immunosensing are presented in Fig 5. MBs can be coated with streptavidin for capturing biotinylated molecules (e.g single stranded (ss) or double stranded (ds) nucleic acids, aptamers, peptides, oligodeoxynucleotides (ODN), proteins), covalently attached oligo$(dT)_{25}$ chains (oligonucleotides of 25 deoxytymine bases) can bind nucleic acid involving adenine nucleotide, (A)*n,* stretches, including natural eukaryotic mRNAs tagged with (A)*n* adaptors, metal-affinity cobalt chelate for binding histidine tagged recombinant proteins, protein A or G can capture antibodies[107].

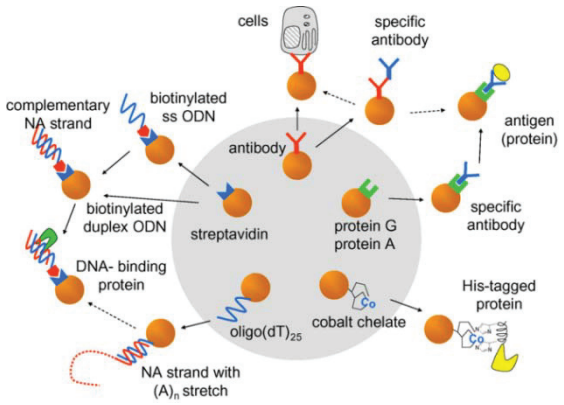

Fig. 5. MBs functionalized with various biorecognition elements with bioaffinity for different biomolecules[107] (Commercially available MBs are shown on they gray background)

3.2. Gold nanoparticles

Gold nanoparticles (AuNPs) (gold nanospheres, gold nanoshells, gold nanorods, gold nanocages [108]) are versatile platforms for the fabrication of biosensors with improved sensitivity, selectivity and stability, due to their unique physical and chemical properties, such as: straightforward synthesis that offers them high stability, unique optical and electronic properties, high surface-to-volume ratio that allows a higher load of biomolecules, excellent biocompatibility, possibility of tuning by varying their shape, size and the surrounding chemical environment, possibility of multifunctionalization with a wide range of organic and biological ligands that can selectively bind to small molecules or biological analytes[109].

Gold nanoparticles of different size, shape, and functionality can be synthesized in various ways, several methods being presented below:

- *Citrate method* – pioneered by Turkevich in 1951[110] is based on the reaction of hot $HAuCl_4$ and sodium citrate, which acts as both reducing and stabilizing agent. It leads to monodispersed spherical gold nanoparticles in water with diameter of about 20 nm;
- *Brust-Shiffrin method* – developed in 1994[111], is a two-phase synthesis of thiol-protected AuNPs with improved stability, based on the reduction of gold salts by sodium borohydride ($NaBH_4$). $HAuCl_4$ (or its salts) is transferred from aqueous solution to an organic solvent that is not miscible with water (e.g toluene) using

tetraoctylammonium bromide as surfactant, followed by reduction with $NaBH_4$ in the presence of thiol ligand;

- *Place exchange method* – based on the substitution of thiol ligands that are initially bound on AuNPs by free thiol ligands leading to mixed monolayer AuNPs for synergistic applications;
- *Polymer stabilized AuNPs* – synthesis of AuNPs covered with different polymers (e.g poly(*N*-vinylpyrrolidone), polyethyleneglycol, polyethyleneimine) using different techniques such as physisorption,"grafting from", "grafting to" or "post-modification of preformed AuNPs"[109];
- *Electrodeposition* – based on electrochemical methods: a potential is applied for the reduction of $HAuCl_4$.

4. Molecularly imprinted polymers

4.1. Definition and general principle

The molecularly imprinted technique in organic polymers was pioneered by Wulff and his group in 1972, using covalent reversible bonds between functional polymers and template molecules[118]. In 1981, Mosbach et al synthesized biomimetic receptors based on noncovalent interactions between the template and functional monomers[119].

Molecular imprinting is a technique used to fabricate biomimetic receptors: molecular recognition sites complementary in size, shape and chemical functionality with a target molecule (template) are created in a synthetic polymer. The preparation method is quite simple and it involves the use of functional monomers, template, cross-linkers and solvents[120]. The steps involved in the preparation of MIPs are depicted in Fig. 6 and consist of (1) the formation of a non-covalent adduct or covalent complex between the template molecules and functional monomers by assembly of the monomer in an orderly fashion around the template, (2) polymerization of the monomer in the presence of the template, resulting in a polymer matrix with embedded template molecules and (3) removal of the template from the polymer matrix, thus leaving specific cavities that exhibit high binding capacity and selectivity towards the template molecule[121].

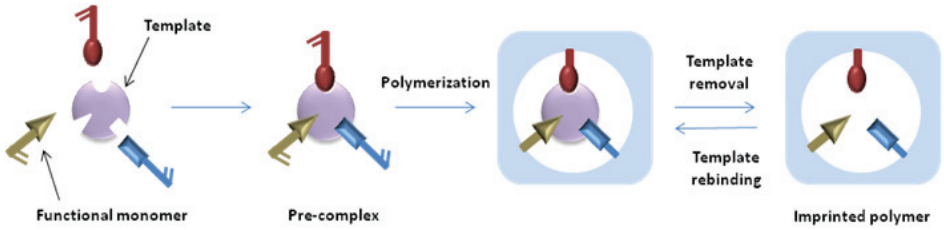

Fig. 6. Preparation of molecularly imprinted polymers

The molecular imprinting technique is simple, cheap and easy to perform in a tailor made fashion, without the need of complex organic synthesis[120]. Moreover MIPs are highly stable in a wide range of pH, pressure and temperature, they could be prepared for practically any target analyte, can work also in organic media (unlike natural biomolecules that perform mostly in aqueous media), are fully compatible with micromachining technology[122] and can be stored in dry state at room temperature for long time periods[123]. Their properties can be easily tuned due to the wide range of available monomers (over 4000 molecules) and, unlike antibodies, MIPs can be synthesized for small molecules, highly toxic compounds or immunosuppressants[124].

Numerous MIPs have been reported with recognision ability for drugs[125], pollutants[126], food contaminants[127], warfare agents[128] and used in various fields such as chromatography, electrophoresis, chemical sensing, catalysis, drug delivery and discovery, crystallization or cell culturing[124].

4.2. Classification

MIPs can be prepared by two approaches depending on the type of interactions between the template and functional monomers; a hybridization of the two approaches can also be made (e.g. formation of adducts my covalent bonds and rebinding of guest by non-covalent interactions):

- *Non-covalent*: In the first step adducts between template and monomers are formed via non-covalent interactions, such as hydrogen bonds, ionic interactions, van der Waals forces or hydrophobic effects. The adducts are then “frozen” in a three dimensional polymeric network by polymerization. The template is removed by extraction with solvents and the rebinding takes place via noncovalent interactions. It has the advantage of ease of preparation, fast template binding and release kinetics and easy removal of the template under mild conditions. However the polymerization conditions are restricted and they should be carefully chosen to maximize the formation of imprinting sites;

moreover the selectivity can be decreased due to the high amount of functional monomer that exists in excess[120].

- *Covalent:* In the first step, the monomer and the template are linked together via covalent bonds. Then the covalent conjugate is polymerized in conditions that keep the covalent bond intact. The template is then removed by breaking the covalent bonds. The uptake of the template in cavities takes place by the formation of the same covalent bonds. The conjugate formed between the template and the monomer is stable, which allows the use of a wide range of polymerization conditions and relatively clear-cut imprinting processes. Some of the drawback of the covalent approach are: rather harsh conditions are required to break the covalent bonds for the release of the template making the process more difficult and lowering the imprinting effect; the number of reversible covalent linkages available is limited; slow kinetics for the removal and rebinding of the template, because they involve formation and breakdown of covalent bonds[120].

4.3. Preparation of molecularly imprinted polymers

MIPs can be prepared using various strategies, starting from templates, functional monomers, solvents and cross-linking agents. A factor of paramount importance is the choice of the monomer. This has to possess functional groups that interact with the template, but must not react with it; it also has to be cross-linked enough so that the cavities remain intact after template removal[124]. The most common preparation method is based on the use of monomers with acrylate or vinyl groups, which are widely used due to the vast choice of possible functional monomers[123]. They can serve as both functional and cross-linking agents and by photopolymerization bulk MIP blocks are obtained. Bulk MIPs are not suitable for chemosensors applications therefore MIP particles have been synthesized that are more readily integrated with transducers[129]. The most commonly used polymers for sensors and chromatography applications are polyacrylate, polymethacrylate, polymethylmethacrylate, polyacrylamide, polyurethane, siloxanes, and solgels[124].

The polymerization mixture also contains, beside template and monomer, an inert solvent that has the role to dissolve all ingredients and provide a porous matrix that allows easy removal and rebinding of the analyte[123]. If the MIP is prepared by the non-covalent approach it is preferable to use for extraction an organic solvent, better the same solvent used for imprinting in order to obtain the same swelling effect. Since MIPs are usually hydrophobic a non-ionic surfactant or a miscible organic solvent (e.g. ethanol) may be used to reduce the surface tension and minimize hydrophobic interactions[130].

MIPs can be prepared by several imprinting techniques as shown in Fig 7: bulk imprinting (the template is added to the prepolymer and the obtained cavities are distributed all over the bulk), surface imprinting with stamps for large molecules, substructure imprinting (a small part of the molecule is imprinted), imprinting with substructural analogues, with antibody replica (antibodies for the target molecule are imprinted in the polymer) or with sacrifice layer (when the polymer reacts with the template an intermediate layer of molecules is used to cover the template; these molecule interact with the polymer to for the binding cavity)[124].

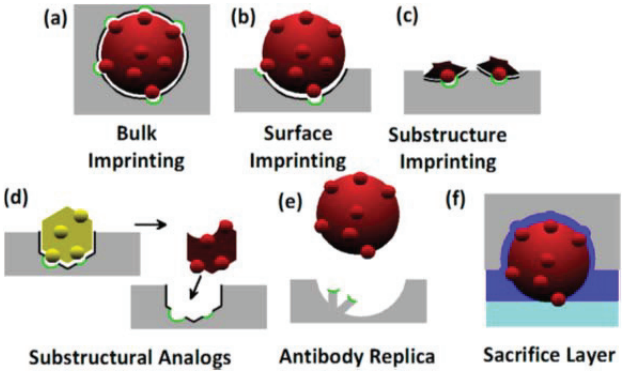

Fig. 7. Imprinting strategies for the fabrication of MIPs[124]

4.4. Molecularly imprinted polymers in sensors

The high specificity and stability of MIPs makes them promising alternatives to the biological receptors used in the development of sensors. However, there are limitations associated with the development of MIP sensors, such as absence of a general procedure for MIP preparation, difficulty in integrating them with transducer, difficulty in transforming the binding event into an electric signal, and generally poor performance of MIPs in aqueous solution[122].

The most common type of MIP sensors are affinity sensors, which can be classified in: immunosensor type sensors (based on the measurement of the concentration of the analyte bound by the MIP deposited at the surface of an optical, electrochemical or piezoelectric transducer) and receptor type sensors (based on conformational changes of the MIP upon binding of analytes which leads to a change in a measurable property e.g conductivity, permeability)[122].

If the target analyte has a measurable property such as fluorescence or electrochemical activity, this can be used to develop optical or electrochemical MIP based sensors; however a difficulty in this case is that small amounts of the analyte can remain entrapped in the polymer matrix leading to background currents and

decreased sensitivity. MIP sensors in competitive format can also be developed if the analyte does not have a measurable property. In this case a labeled analyte derivative may be used, which will compete with the analyte for the binding sites of MIP. The signal can also be obtained from the polymer itself (e.g. fluorescent polymer)[123].

Acrylic functional monomers and conducting polymers are the most widely used for the fabrication of sensors (Fig. 8).

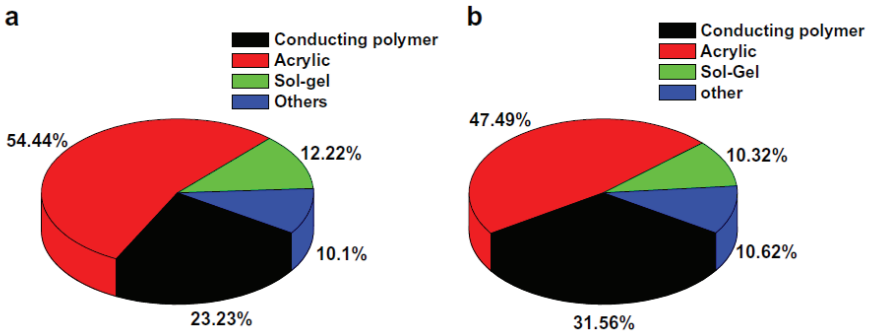

Fig. 8. Commonly used functional monomers for the fabrication of chemosensors (a) and electrochemical sensors (b) reported in literature between 2010-2014[129]

An essential aspect in the fabrication of MIP based sensors is the integration of MIPs in the detecting system (transducer), which can by employed in several manners. The most direct way is electropolymerization on the surface of the transducer, with the advantages of: control over film thickness and deposition density by changing the expeimental conditions, e.g. applied voltage; deposition at a precise spot at the surface of the transducer; possibility to obtain a homogenous film at the surface of an electrode with complex geometry[122]. Poly-*o*-phenylenediamine[131], poly-*p*-aminothiophenol[132], polypyrrole[133] with specific recognition abilities have been succesfully integrated in sensors. Drop or spin coating are also employed, using different materials: a solution of pre-prepared polymer; a composite of MIP particles, conductive materials (e.g CNTs) and a binder (e.g. PVC); a complex of functional monomer and template, which is then chemically polymerized[129]. Nanometer size MIP particles can also be entrapped in gels at the surface of transducers[123]. Another integration technique is the formation of self-assembled imprinted monolayers (MIMs) at the surface of the transducers[134]. Despite the ease of preparation, fast release and binding kinetics and the possibility to be applied for larger templates such as proteins, these 2D systems are less stable then 3D MIPs. Other methods of preparing MIP films on the surface of transducers (including inert materials) are chemical grafting, exposure to UV or thermoinitiated polymerization[122].

A few examples of sensor based on MIPs reported in recent years in the literature are presented in Table III.

Table III. Electrochemical sensing devices based on MIP

Target analyte	MIP fabrication	Detection method	LOD	Ref
Urea and creatinine	Solvent evaporation of poly(ethylene-co-vinyl alcohol)	EIS	$0.2x10^{-12}$ M $8.8x10^{-9}$ M	135
Trimethoprim	Electropolymerization of pyrrole	CV	$1.3x10^{-7}$ M	136
Cholesterol	Electropolymerization of p-aminothiophenol self-assembled on AuNPs (electrodeposited) /MWCNTs/GCE	DPV	$3.3x10^{-14}$ M	137
Dopamine	Electropolymerization of pyrrole-phenylboronic acid	DPV	$3.3x10^{-8}$ M	138
Estradiol	One step electrodeposition of AuNPs-poly(p-aminothiophenol)	DPV	$1.28x10^{-12}$ mg/mL	139
Paracetamol	MIP micelle formed via self-assembly of an amphiphilic photo-crosslinkable copolymer in an aqueous solution of paracetamol were electrodeposited on gold electrodes followed by photo-crosslinking	DPSV	$3.3x10^{-7}$ M	140
2-nonylphenol	Drop-coating with a MWCNTs-nafion film followed by electrodeposition of a sol-gel film by CV	DPV	0.06 µM	141
Chloramphenicol	MIP was chemically synthesized on the surface of MWCNTs using 3-hexadecyl-1-	DPV	$1x10^{-10}$ M	142

	vinylimidazolium chloride. The suspension was drop coated on electrodes that were previously modified with reduced graphene oxide and mesoporous carbon.			
Lorazepam	One step electrdeposition of polypyrrole, sol-gel and AuNPs and pencil graphite electrode	SWV	0.09 nM	143
Methidathion	Drop coating of a sol-gel/MIP particles suspension. MIP particles were obtained by theraml polymeraziation using N;N-methylene bis acrylamide as monomer, crosslinker ethylene glycol dimethacrylate, initiator 1,1 azobisisobutyronitrile.	EIS	5.14 µg/L	144
Norepinephrine	MIP-coated PdNPs were synthesized by sol-gel method using PdNPs as support, phenyltrimethoxysilane as monomer and tetramehoxysilane as crosslinker and were droped on GCE	DPV	0.1 µM	145

Despite the advances made in the fabrication of MIP-based sensors, the commercial availability of such devices remains low mainly due to limitations caused by the poor performance of MIPs in water and their integration in transducers [122].

PERSONAL CONTRIBUTIONS

Chapitre 1

Contexte

L'objectif de ce chapitre été de développer des immunocapteurs sensibles pour la détection du marqueur tumoral MUC1 dans des échantillons de sérum.

Le chapitre présente deux approches différentes pour la détection du marqueur tumoral MUC1 dans un format de type sandwich en utilisant des particules magnétiques comme support solide et des anticorps ou des aptamères comme molécules de bioreconnaissance.

La molécule cible MUC1 est capturée entre l'anticorps primaire ou l'aptamère immobilisé sur des particules magnétiques et un anticorps ou un aptamère secondaire. La réaction d'affinité est marquée avec la phosphatase alcaline dans différents configurations d'essai. La multi-détection électrochimique est réalisée par voltamétrie pulse différentielle (DPV), en utilisant huit cellules imprimées sérigraphiées, par l'addition du substrat enzymatique (1-naphtyle phosphate) et sa conversion ultérieure au 1-naphtol, un composé actif électrochimique.

Dans la première approche une paire d'anticorps a été utilisée pour capturer l'antigène et le protocole est présenté dans la section 1.2.2. Ensuite, les anticorps ont été remplacés par des aptamères, afin d'améliorer la sélectivité de la méthode d'analyse. Le protocole est présenté dans la section 1.2.3. Tous les paramètres qui influencent les performances des capteurs ont été optimisés comme présenté dans la section 1.3.1 et 1.3.2. La section 1.3.3. présente les courbes d'étalonnage obtenues pour l'analyse de MUC1 dans des solutions-tampon en utilisant l'apta-capteur développé. La sélectivité des deux capteurs a été évaluée et comparée avec l'affinité pour des protéines non spécifiques, MUC4 et MUC16, et les résultats sont présentés dans la section 1.3.4. Enfin, la section 1.3.5 présente l'applicabilité pratique de l'apta-capteur pour l'analyse des échantillons de sérums pathologiques et non-pathologiques.

1. Optimized bioassays for Mucin1 detection in serum samples

1.1. Introduction

The development of affinity sensors for biomedical, food-safety and environmental applications gained increasing attention in recent years[146-148].

A pivotal step in the fabrication of affinity biosensors is represented by the selection of an appropriate biorecognition element that binds the target molecule. Antibodies have been widely used as recognition elements [149, 150]. The performance of the designed immunosensor depends on the affinity and selectivity of the selected antibody to its antigen, as well as on the proper immobilization of the antibody, with an optimum density and adjusted orientation for the antigen binding [151, 152].

In order to improve the stability, selectivity and sensitivity of affinity biosensors, synthetic molecules such as peptides and nucleic aptamers have been recently explored [153].

Over the past decade, aptamers have been studied intensively due to their inherent advantages over antibodies such as ease of synthesis, ease of labelling, good stability and resistance to denaturation, high specificity for target molecules and the possibility to distinguish between targets with very similar structure [154].

Various affinity sensors have been designed, which improved the analytical performance in real samples. The use of micro- and nano-particles either as immobilization platforms [155-156] or as labels [157, 158] has attracted major attention lately. The use of magnetic nanoparticles as a solid support for the immobilization of the recognition element has many advantages such as fast and specific immobilization of a large amount of bioelements due to the large binding surface conferred by their geometry and small size, leading therefore to an improved sensitivity, easy separation after the washing and reaction steps, easy manipulation, reduction of the analysis time and of reagents consumption. Moreover, magnetic beads can be readily applied for the analysis of biological samples without the requirement of any purification steps. They also reduce the matrix effect due to the improved washing steps [159-160]. The proposed approaches use disposable screen-printed arrays as transducers and a simple target capturing step by aptamers or antibodies functionalized magnetic beads. Screen-printed cells (SPCs) are widely used as electrochemical transducers due to their simple, rapid and inexpensive manufacturing process, the possibility of mass production and the ability to print the electrochemical system on one solid support to

obtain disposable devices. SPCs arrays have many advantages, such as simultaneous analysis of different samples, which results in a shorter analysis time. Several disposable immunosensors have been developed on SPCs arrays in the field of clinical or food analysis [161-166].

Given the fact that immunosensors for tumor markers detection attracted considerable interest lately, MUC1 tumor marker was selected for this study. MUC1 is a trans-membrane glycoprotein expressed on the apical surface of various epithelial cells. Current methods used in clinical laboratories, performed by immunohistochemical analysis of breast and ovarian carcinomas tissue[167], demonstrate an overexpression of MUC1 protein in neoplastic processes. Therefore MUC1 can be used as potential tumor marker for establishing the diagnosis and the prognosis in different types of cancer such as ovarian [168], breast [169], lung [170] or pancreatic [171] cancer. Clinical cut-off level for MUC1 in serum was reported at 30 U/mL [172].

Several aptamer based sensors have been recently reported in the literature. For example, an interesting approach was reported recently by Wen *et al.* The group used an insertion approach together with an exonuclease-assisted amplification strategy. A thiolated capture probe was self-assembled on gold electrodes followed by hybridization at terminal ends with methylene blue tagged aptamer. The proximity of methylene blue near the electrode surface exhibited a high current response, which decreased as the target molecule was added, since the aptamers were bound around the protein. Aptamers were then digested by the addition of exonuclease. A low limit of detection of 4 pM was obtained [173].

The study herein presents two different approaches for the detection of MUC1 tumor marker in a sandwich format using magnetic beads as solid support and antibodies or aptamers as biorecognition molecules. The aptamers used in this work were selected from a library of aptamers, designed by SELEX, which were shown to have the ability to recognize MUC1 protein [174].

The target molecule is captured between the primary antibody or aptamer immobilized on the magnetic beads and a secondary antibody or aptamer. The affinity reaction is labelled with Alkaline Phosphatase (AP) in different assay configurations. All variables concerning the bioassays were optimized. The electrochemical multidetection is achieved by differential pulse voltammetry (DPV), using eight screen-printed cells, through the addition of the enzymatic substrate (1-naphthyl phosphate) and its subsequent conversion to 1-naphthol, an electrochemical active compound.

The analytical performances of aptamer-based assay were compared with antibody-based assay. Several analytical parameters, such as selectivity and limit of detection were considered in order to find the best conditions for the analysis of the

serum samples obtained from cancer patients. The proposed aptamer-based assay showed better sensitivity and higher selectivity for detection of MUC1 cancer biomarker respect to antibody-based assay. Under optimized conditions, a linear calibration curve of MUC1 buffered solutions was obtained in a range from 0 to 10 ng/mL with detection limit (LOD = $3S_{blank}$/Slope) of 1.4 ng/mL (corresponding to the range from 0 to 0.28 nM, LOD 0.037 nM), well below the detection limits reported by other aptasensors present in literature [175, 176].

In order to assess the suitability of the developed aptasensor and to evaluate the influence of the matrix effect, non-pathological serum samples spiked with different known concentration of MUC1 protein were also analysed. A detection limit of 3.0 ng/mL and a limit of quantification (LOQ = 10 S_{blank}/Slope) of 10.0 ng/mL were obtained. Moreover, a semi-quantitative correlation between MUC1 concentration found in cancer patient serum samples and malignancy stage obtained by immunohistochemical diagnosis was achieved, demonstrating the potential applications for cancer screening.

1.2. Materials and Methods

1.2.1. Chemicals and instrumentation

Dynabeads Protein G-coated magnetic beads and Streptavidin-coated magnetic beads were purchased from Invitrogen (Milan, Italy). MUC1 protein (M.W. 37.4 kDa), MUC1 monoclonal mouse antibody (Ab1), MUC1 polyclonal rabbit antibody (Ab2), MUC4 protein, MUC16 protein, polyclonal antibody anti-rabbit IgG (rIg) labelled with alkaline phosphatase (Ab3-AP) were provided by Novus Biological (Cambridge, UK).

Two different aptamers were used in this work, having the sequences:

(Apt1) 5'-GCAGTTGATCCTTTGGATACCCTGGTTTTTTTTTTTTTTT-3` - Biotin

(Apt2) 5`-GAAGTGAAAATGACAGAACACAACATTTTTTTTTTTTTTT-3` - Biotin

The aptamers were purchased from AlphaDNA (Canada) and Eurofins (Germany).

1-naphthyl phosphate, diethanolamine, sodium chloride, potassium chloride, magnesium chloride, polyoxyethylene sorbitan monolaureate (Tween 20), biotin, bovine serum albumin, streptavidin-alkaline phosphatase were purchased from Sigma-Aldrich (Milan, Italy).

Tris(hydroxymethyl)amino-methane (TRIS) and ethylene-diamine-tetra-acetic acid (EDTA) were purchased from Merck (Milan, Italy).

The sample mixer was purchased from Dynal Biotech (Milan, Italy).

All solutions were prepared using water from Milli-Q Water Purification System (Millipore, UK). The following buffers were used in the experiments:

Buffer A: PBS 0.1 M, pH 7.4, 0.005% w/w Tween 20

Buffer B: TRIS Buffer 50 mM, NaCl 10 mM, pH 8.0, 0.005% w/w Tween 20

Buffer C: TRIS 10 mM, EDTA 1 mM, NaCl 2 M, pH 7.5, 0.005% w/w Tween 20

Buffer D: TRIS 10 mM, NaCl 100 mM, KCl 100 mM, $MgCl_2$ 5 mM, pH 7.2, 0.005% w/w Tween 20

Buffer E: DEA Buffer DEA 0.1 M, KCl 0.1 M, $MgCl_2$ 1 mM, pH 9.6, 0.005% w/w Tween 20

Eight screen-printed cells were used in the experiments. Each cell is based on graphite working electrode (2.0 mm in diameter), a graphite counter electrode and a silver reference electrode. The arrays were screen-printed in-house using a DEK 248 screen-printing machine (DEK, Weymouth, UK). Silver based (Electrodag PF-410) and graphite-based (Electrodag 423 SS) polymeric inks were obtained from Acheson (Milan, Italy); the insulating ink (Vinylfast 36–100) was purchased from Argon (Lodi, Italy). A polyester flexible film (Autostat CT5), obtained from Autotype (Milan, Italy) was used as printing substrate. An 8-holes methacrylate box is fixed onto the strip by using a double layer adhesive. Each hole is 8 mm diameter and it is positioned exactly in correspondence of each cell.

Electrochemical measurements were performed with μAutolab type II PGSTAT (Methrom, The Netherlands) with General Purpose Electrochemical System (GPES) 4.9 software and PalmSens handheld potentiostat (PalmSens BV, The Netherlands).

Differential pulse voltammetry (DPV) was employed as electrochemical technique using the following parameters: potential range from 0 to + 0.5 V; pulse amplitude 0.070 V; scan rate 0.033 V/s. The measurements were carried out at room temperature.

1.2.2. Protocol of antibody-based bioassay

The scheme of antibody-based bioassay is illustrated in Fig. 9.

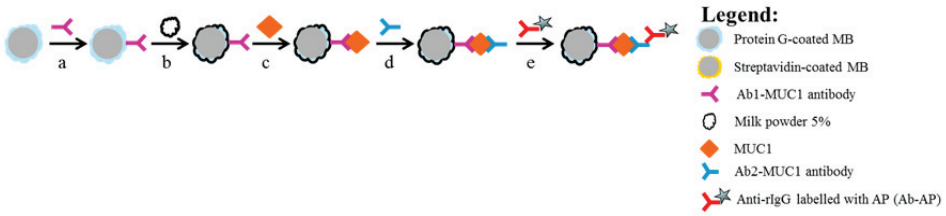

Fig. 9. Scheme of antibody-based bioassay: a) incubation of protein G-modified magnetic beads with primary anti-MUC1 antibody (Ab1); b) blocking step with milk powder; c) affinity reaction with MUC1 protein; d) incubation with secondary anti-MUC1 antibody (Ab2); e) incubation with alkaline phosphatase (AP)-labelled anti-rabbit IgG tertiary antibody (Ab3-AP). Differential pulse voltammetry (DPV) measurements were carried out in accordance with paragraph 2.2.5.

1.2.2.1. Immobilization of primary antibody

For the functionalization of the magnetic beads, 100 µl of the beads suspension were taken from the stock solution of Protein G-coated magnetic beads (30 mg/mL), added in a vial and washed with buffer A for three times. For the washing step the beads were re-suspended in 500 µl buffer and mixing by vortex. Then the tube was placed in a magnetic separation stand to capture the magnetic beads on the bottom of the tube, allowing the removal of the supernatant. After the washing steps 200 µl of Ab1 solution 50 µg/mL prepared in buffer A was added to the beads and incubated for 120 minutes in the rotating stand at room temperature.

1.2.2.2. Blocking of free binding-sites

In order to reduce the non-specific adsorption of the reagents used in the following steps of the immunoassay, the free binding-sites of the beads were blocked using the milk powder as a blocking agent. For the blocking step the functionalized beads were firstly washed for three times with 500 µl buffer A. Afterwards 1 mL milk powder solution 5% prepared in buffer A was added and incubated for 120 minutes in the rotating stand at room temperature. The beads were washed and reconstituted in 1 mL buffer A. The functionalized beads suspension was stored at 4ºC temperature for up to one week for further experiments.

1.2.2.3. Capturing the MUC1 protein

To obtain a calibration curve, 50 µl of the functionalized magnetic beads suspension were placed in a vial, in magnetic stand separator and, after removing the supernatant, 500 µl of MUC1 protein solution in buffer B was added in the

concentration range of 0 – 10 ng/mL. The samples were incubated for 60 minutes in the rotating stand at room temperature and then washed with buffer A.

1.2.2.4. Binding of secondary antibody and third antibody labelled with alkaline phosphatase

200 µl of Ab2 solution 5 µg/mL prepared in buffer A were added to the beads and incubated for 60 minutes in the rotating stand at room temperature. The beads were then washed three times with buffer E. Then, 200 µl of a solution containing Ab3-AP (0.5 µg/mL) prepared in Buffer E with 10 mg/mL BSA were added to the beads and incubated for 10 minutes. After a washing step, the beads were reconstituted in 50 µl buffer E, proceeding with the electrochemical measurements as reported in materials and methods section.

1.2.3. Protocol of aptamer-based bioassay

Fig. 10 depicts the steps for the development of the aptamer-based bioassay.

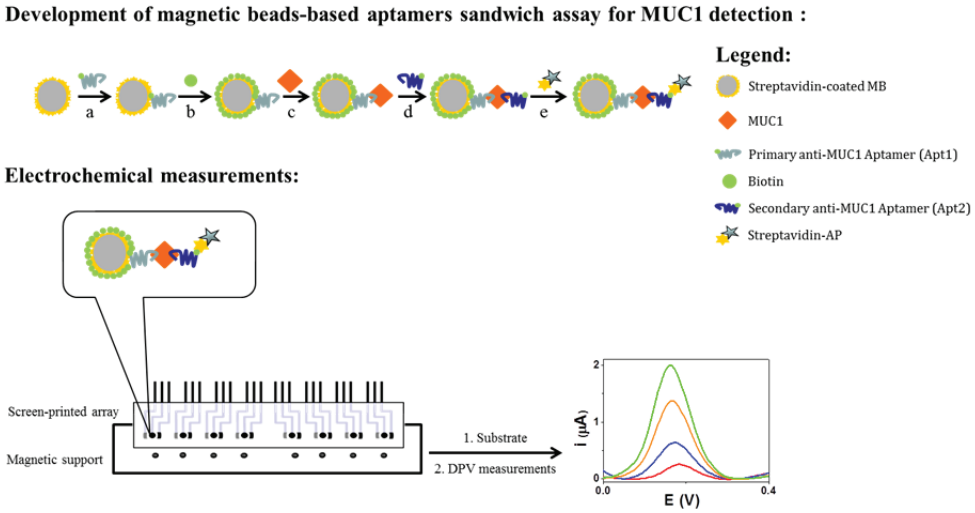

Fig. 10. Scheme of aptamer-based bioassay for MUC1 detection: a) incubation of streptavidin-modified magnetic beads with biotinylated primary aptamer (Apt1); b) blocking step with biotin; c) incubation with MUC1 protein; d) incubation with secondary biotinylated aptamer (Apt2); e) incubation with streptavidin-alkaline phosphatase. Electrochemical measurements: screen-printed arrays were placed on a magnetic support and modified-magnetic beads were deposited on the surface of each working electrode of the array. Differential pulse voltammetry (DPV) measurements were carried out in accordance with paragraph 1.2.5.

1.2.3.1. Immobilization of the primary aptamer

A thermal treatment was firstly applied to the aptamer in order to unfold the aptamer strand, before the immobilization on magnetic beads. For this purpose the biotinylated aptamer solution was heated at 90 ºC and then gradually cooled at 25 ºC followed by fast cooling in freezer to keep the folded structure of the aptamer. 100 µl streptavidin – magnetic beads suspension were taken from the stock solution (10 mg/mL) and placed in a vial. Using a magnetic separation stand the beads were washed three times with buffer C. The beads were then re-suspended in 200 µl buffer C and 200 µl solution of biotinylated aptamer (Apt1) in water was added, to reach the final concentration of aptamer of 5 µM and left to incubate for 30 minutes in the rotating stand at room temperature. The aptamer-functionalized beads were then washed with buffer A.

1.2.3.2. Blocking of free binding-sites

Apt1 functionalized-beads were incubated for 30 minutes with 500 µl biotin solution 1 mM prepared in buffer A in the rotating stand in order to block the remaining active sites. The beads were washed three times with buffer C and reconstituted in 1 mL buffer C.

1.2.3.3. Capturing the MUC1 protein

For the determination of MUC1, 50 µl of the functionalized magnetic beads suspension were incubated with 500 µl of MUC1 protein solutions in buffer D with various concentrations, in the range of 0 – 10 ng/mL, for 45 minutes in under stirrer, followed by washing three times with buffer D.

1.2.3.4. Binding of secondary aptamer and labelling with streptavidin-alkaline phosphatase

Apt1/MUC1-modified beads were then incubated with 200 µl secondary biotinylated aptamer (Apt2) solution 1 µM prepared in buffer D, for 10 min under stirrer. Then, the beads were washed with buffer E and incubated with 200 µl streptavidin-alkaline phosphatase solution in buffer D for 15 minutes. At last, after washing, the beads were suspended in 50 µl buffer D.

1.2.4. Analysis of human serum samples by the aptamer based bioassay

For the analysis of serum samples, the serum was firstly filtered (Filtropur S, diameter of filter pores 0.2 μM) and then diluted 1:200 with the buffer D. The prepared samples were then spiked with MUC1 solution. 50 μl beads suspension, functionalized with aptamer (Apt1), was incubated with 500 μl of the solutions above carrying out the experiments as previously described. Spiked samples of commercial normal human serum as well as pathological serum samples were analyzed with the proposed aptasensor. Standard addition method was carried out for each pathological serum sample in order to quantify the amount of antigen. MUC1 concentration was calculated by the intercept value on x-axis.

1.2.5. Electrochemical measurements with screen-printed arrays

10 μl of beads suspension were deposited onto the surface of each working electrode of the array, and kept in its position through the magnet holding block. Each well of the array was filled with 60 μl of a solution containing 1 mg/mL of 1-naphthyl phosphate prepared in buffer E. After 6 min of incubation time, DPV measurements were started. DPV was carried out simultaneously for each cell.

The entire procedure was repeated at least 10 times using different screen-printed cells and biochemicals (proteins and antibodies) batches. RSDs were calculated as measure of inter-assay reproducibility.

1.3. Results and discussion

1.3.1. Optimization of experimental parameters of aptamer-based bioassay

Several experimental parameters were investigated for the best performance of the bioassay, in accordance with other immuno- and aptasensors reported in literature [160, 178].

The effect of concentration and the incubation time of the primary aptamer (Apt1), incubation time of antigen, incubation time and concentration of secondary aptamer (Apt2), blocking agent, was investigated. The appropriate experimental parameters were chosen taking in consideration the current ratio between 5 ng/mL MUC1 and the blank (I_{MUC1}/I_{blank}) and the obtained RSD%.

The immobilization of the primary aptamer on the surface of the magnetic beads with an appropriate orientation and flexibility is of paramount importance for the performance of the aptasensor. Thus, the concentration and incubation time with the primary aptamer was firstly optimized. A solution of Apt1 1 μM and 5 μM was incubated for 30 min and overnight with the streptavidin beads, followed by a blocking step and the reaction with protein, Apt2 and streptavidin-AP. The assay showed better response for a higher concentration of aptamer (5 μM) and a lower incubation time (30 min), these conditions assuring a proper conformation of the aptamer for capturing the protein (Table IV, a).

To block the remaining active sites of the beads, biotin was chosen as blocking agent given the fact that streptavidin modified magnetic beads were employed. Solutions of 100 μM and 1 mM biotin were tested during different incubation times. An optimum blocking effect was obtained for 1 mM biotin solution incubated for 30 minutes (Table IV, b).

The best conditions for binding the protein to the immobilized aptamer were then investigated. Incubation times of 30, 45 and 60 minutes were tested. The incubation time of 30 min was not sufficient, whereas a higher signal to blank ratio being obtained after 45 and 60 minutes (Table IV, c). However the increase was not substantial when the incubation time increased from 45 to 60 minutes, thus, an incubation time of 45 minutes was selected.

The experimental conditions regarding the binding of secondary aptamers were also investigated. Apt1/MUC1-modified beads were thus incubated with various concentrations of Apt2 solution for 10, 15 and 30 minutes. The signal/blank ratio increased from 2.3 to 5.5 as the concentration of the secondary aptamer increased from 0.5 to 1 μM. A lower incubation time of 10 min seemed to be sufficient for the complete formation of the Apt1-MUC1-Apt2 complex (Table IV, d).

The incubation step with the enzymatic conjugate had to be optimized as well. The modified beads were incubated with streptavidin-AP solution for 10 and 15 min. A higher signal/blank ratio was obtained for 15 minutes incubation time (Table IV, e).

Table IV. Experimental parameters optimization for aptamer-based bioassay. $I_{MUC}1/I_{blank}$ represents the ratio between the current obtained using respectively 5 ng/ml and 0 ng/ml (blank) MUC1 buffered solutions. The letters of assay step column are in accordance to Fig 10. Average RSD% was calculated as reported in section 1.2.5.

Assay	Parameters	Current ratio	Average

step			(I_{MUC1}/I_{blank})	RSD%
a	Apt1 concentration (30 min)	1 μM	1.2	9
		5 μM	3.9	11
	Apt1 incubation time (5 μM)	30 min	3.9	13
		overnight	1.3	12
b	Biotin concentration (30 min)	100 μM	0.7	14
		1 mM	5.4	8
	Biotin incubation time (1mM)	30 min	5.4	9
		overnight	5.2	7
c	MUC1 incubation time	30 min	2.0	7
		45 min	5.0	8
		60 min	5.4	9
d	Apt2 concentration (15 min)	0.5 μM	2.3	6
		1.0 μM	5.5	9
	Ap2 incubation time (1 μM)	10 min	5.5	9
		15 min	4.9	12
		30 min	4.5	9
e	Streptavidin-AP incubation time	10 min	3.3	9
		15 min	5.5	9

1.3.2. Optimization of experimental parameters for antibody-based bioassay

The results obtained for the optimization of experimental parameters of the antibody based bioassay are summarized in Table V. The concentration and incubation time with the primary antibody were firstly optimized. The magnetic beads were incubated with 50 and 100 μg/ml Ab1 solution and the assay was carried out as previously described. The increase of the concentration of Ab1 did not result in an increase of the ratio I_{MUC1}/I_{blank} (1.6 for 50 μg/ml and 1.3 for 100 μg/ml), thus 50 μg/ml Ab1 solution was considered optimal.

The effect of different blocking agents in reducing the non-specific adsorption was investigated. The results are also shown in Table V. A PBS solution of milk powder 5% and a PBS solution of bovine IgG 10 μg/ml, were assayed as blocking agents after the functionalization of protein G beads with the primary antibody. To observe the effectiveness of using bovine IgG as blocking agent the beads were incubated, after the functionalization with primary antibody, with 1 ml 10 μg/ml bovine IgG solution in buffer A, for 120 minutes and overnight at 4ºC and the experiments were carried out as previously described. The incubation time with milk powder 5% was also optimized, incubating the functionalized beads with milk powder solution 5% in buffer A, for 120 minutes and overnight. For rabbit IgG in different incubation times and milk powder 5% overnight the signals obtained for the blank and one concentration MUC1 (5 ng/ml) were not improved, the best results being obtained in case of 120 minutes incubation time with milk powder 5% (I_{MUC1}/I_{blank} = 1.4).

For further optimization of the incubation time with the antigen, the beads were incubated with a solution of 5 ng/ml MUC1 for 60 and 90 minutes. A signal/blank ratio of 1.7 and 1.3 respectively, was obtained, indicating that for 60 minutes a steady-state is achieved.

The concentration and incubation time with secondary antibody was also optimized. Solutions of Ab2 of 2 μg/ml, 5 μg/ml and 10 μg/ml and incubation times of 30, 60 and 90 minutes were investigated. The concentration of 2 μg/ml and the incubation time of 30 minutes were insufficient for binding the whole amount of protein in the sample to form an immunocomplex. For a higher concentration (10 μg/ml) and a longer incubation time (90 minutes) the secondary antibody binds probably directly on the beads that were not completely covered by the primary antibody and blocking agent, leading to increased nonspecific adsorption of the following reagents added and a lower current signal/blank ratio. Thus, the intermediate concentration of 5 μg/ml and incubation time of 60 min were chosen for further experiments (I_{MUC1}/I_{blank} = 1.7).

Table V. Experimental parameters optimization for antibody-based bioassay. I_{MUC1}/I_{blank} represent the ratio between the current obtained using respectively 5 ng/ml and 0 ng/ml (blank) MUC1 buffered solution. Letters of assay step column are in accordance of Fig 9. Average RSD% was calculated as reported in section 1.2.5.

Assay step	Parameters		Current ratio (I_{MUC1}/I_{blank})	Average RSD%
a	Ab1 concentration	50 μg/ml	1.6	13
		100 μg/ml	1.3	12

b	Milk powder 5% incubation time	120 min	1.4	14
		overnight	0.9	10
	rIgG (10 µg/ml)	120 min	0.8	11
		overnight	0.9	12
c	MUC1 incubation time	60 min	1.7	13
		90 min	1.3	11
d	Ab 2 concentration (60 min)	2 µg/ml	0.9	10
		5 µg/ml	1.7	9
		10 µg/ml	1.0	11
	Ab2 incubation time (5 µg/ml)	30 min	0.9	14
		60 min	1.7	10
		90 min	1.0	11

1.3.3. Detection of MUC1 in buffered solutions

For each biosensor, a calibration curve was obtained under optimized conditions in MUC1 buffered solution and the results are shown in Fig. 11. A linear response was obtained in the range of 0 - 10 ng/mL, with detection limit (LOD= $3S_{blank}$/Slope) of 3.5 ng/mL and 1.4 ng/mL respectively for antibody- and aptamer-based assay. At least 10 determinations on different screen-printed cells were performed for each concentration in order to asses the reproducibility and the average RSD% was calculated. A better reproducibility and a lower detection limit was obtained for the aptamer-based (RSD 6%) respect to antibody-based assay (RSD 9%).

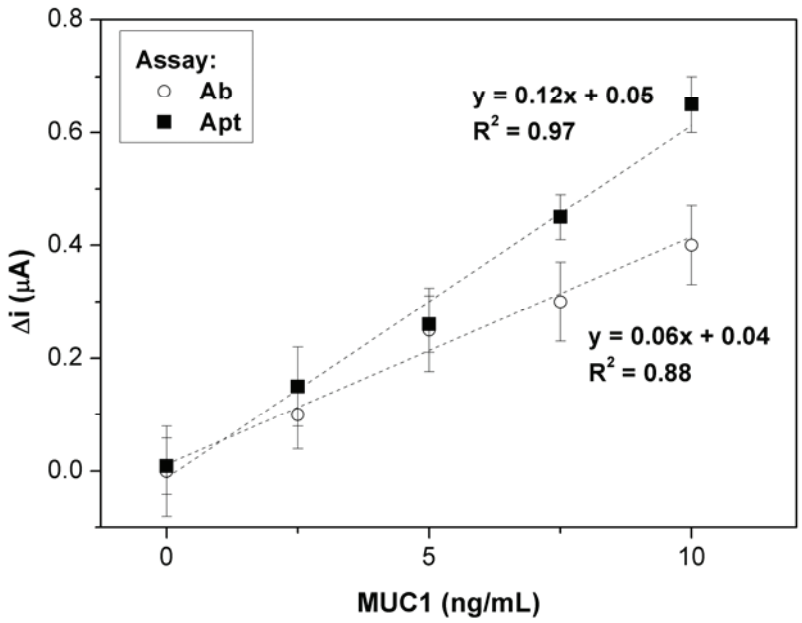

Fig. 11. Calibration curves obtained under optimized conditions for antibody– (Ab, ○) and aptamer–based assay (Apt, ■) in MUC1 standard solutions. The error bars represent +/- standard deviation. Blank signal was subtracted from each measurement. Electrochemical measurements were performed in accordance with section 1.2.5.

1.3.4. Selectivity studies of the bioassay

Selective determination of target analytes is important for the analysis of real samples. To evaluate the selectivity of the two immunosensors, MUC4 and MUC16 were tested with the developed sensors. Mucins exhibit an aberrant expression in different types of carcinomas and therefore they can be used as diagnosis, prognosis and therapeutic targets. In particular MUC4 and MUC16 overexpression were found in ovarian carcinoma [179], thus the selectivity of the developed affinity assays was investigated using these proteins at the same concentration similar to the value of the MUC1 concentration found in diluted non-pathological serum samples (8 ng/mL). MUC16 concentration was selected respect to the clinical approved cut-off level by the U.S. Food and Drug Administration [180].

Comparable signals to MUC1 were obtained for both MUC4 and MUC16 proteins showing that the antibody-based assay is not specific for MUC1 (Fig. 12), owing to the fact that the antibodies are not able to discriminate between similar structures of the three mucins. On the contrary the aptasensor displayed high specificity for MUC1, the signal obtained for MUC4 and MUC6 was approximately the same as the signal of the blank.

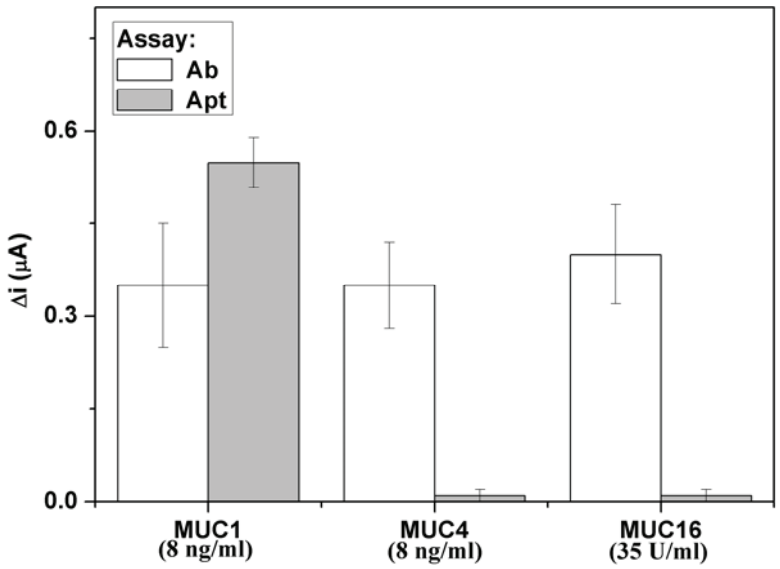

Fig. 12. Selectivity studies of the developed bioassays performed in MUC1 (8 ng/mL), MUC4 (8 ng/mL) and MUC16 (35 U/mL) buffered solutions. Blank signal was subtracted from each measurement.

1.3.5. Serum samples analysis

After the analysis of MUC1 in standard solutions, preliminary experiments using normal human serum samples were carried out to evaluate the clinical applicability of the aptasensor.

Batches of non-pathologic serum samples were spiked with MUC1 to reach final concentrations in the range from 0 to 10 ng/mL, after filtration and dilution 1:200. The current increased for the spiked samples compared to serum alone. Moreover, a linear increase in the current was observed with the concentration of MUC1 (Fig. 13). The concentration of MUC1 in non-pathological serum samples, calculated by standard addition method, was found to be 1.6 ± 0.2 μg/mL.

In spite of the high complexity of serum, the aptasensor allowed the discrimination between the different MUC1 spiked serum samples, thus proving to be highly selective. Moreover, good reproducibility RSD% (10%), a detection limit (LOD= $3S_{blank}$/Slope) of 3.0 ng/mL and a limit of quantification (LOQ = 10 S_{blank}/Slope) of 10.0 ng/mL were obtained.

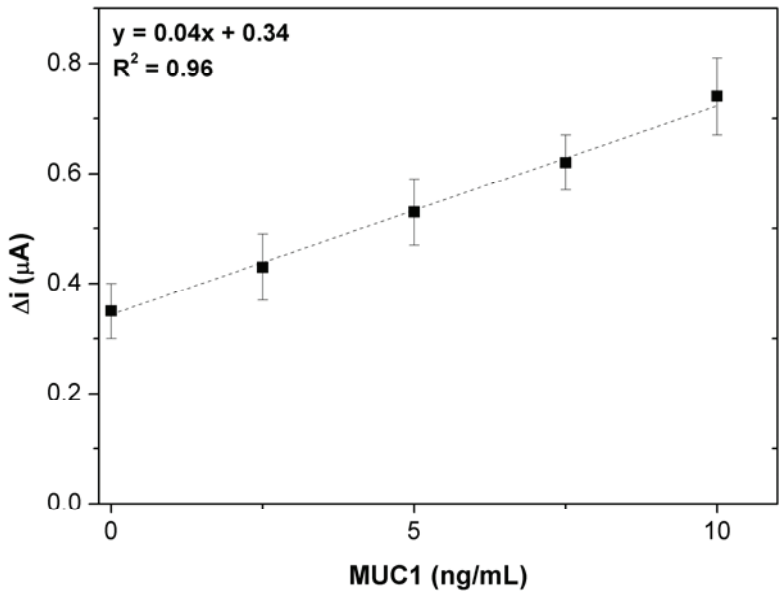

Fig. 13. MUC1 calibration curve with 1:200 diluted non-pathological human serum samples spiked with MUC1 at different concentrations using aptamer-based assay. Blank signal was subtracted from each measurement. Electrochemical measurements were performed in accordance with section 1.2.2.5.

Pathological serum samples of patients with cancer were also analyzed with the developed sensor. The samples were obtained from hospital women patients suffering from breast and ovarian cancer. Standard addition method was employed on diluted serum samples and MUC1 concentrations in real samples were calculated by the intercept value on x-axis. The applied standard addition method of diluted sample 4 (see Table V) in the Fig. 14 is reported as exemplary results. The blank signal was subtracted from each measurement.

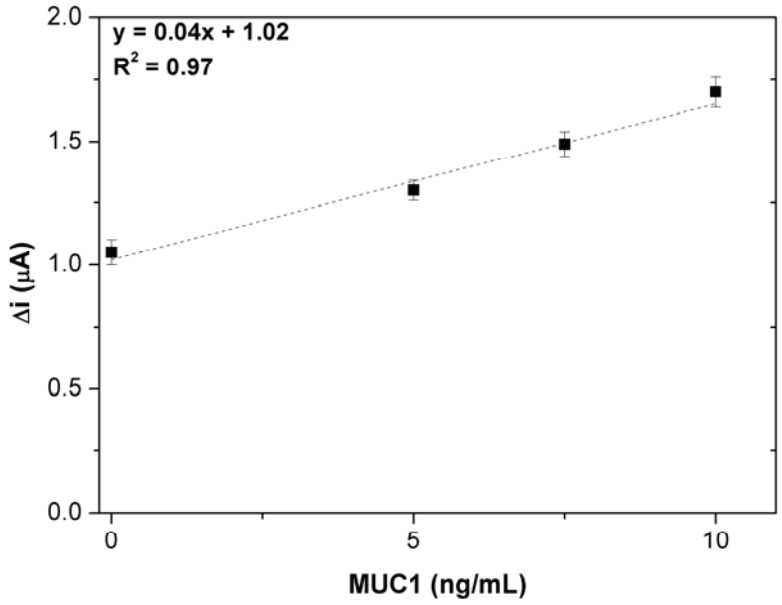

Fig. 14. The applied standard addition method of diluted cancer serum sample 4 (see Table V) in according with section 1.2.4. Electrochemical measurements were performed in accordance with section 1.2.5.

The results of the standard addition method applied for the analysis of pathological serum samples with the aptasensor are reported in Table V; MUC1 concentrations were referred to the undiluted cancer serum samples.

A semi-quantitative correlation between MUC1 concentration and malignancy stage obtained by histological diagnosis can be done.

Table V. MUC1 determination in cancer serum samples from cancer patients performed with aptamer-based bioassay in accordance with section 1.2.4. Results were referred to undiluted cancer serum samples.

Serum numbers	Histological Diagnosis	MUC1 concentration (μg/mL)	NPI
1	Left ovarian carcinoma	34±3	
2	Right ovarian tumor	55±3	
3	Bilateral ovarian carcinoma	100±7	

4	Right ovarian cyst	5.2±0.3	
5	Invasive ductal breast carcinoma	24±1	2
6	Invasive ductal breast carcinoma	128±5	3
7	Invasive ductal breast carcinoma	21±1	2
8	Invasive ductal breast carcinoma	47±2	3
9	Invasive ductal breast carcinoma	40±2	3
10	Non pathological serum	1.60±0.08	

The serum samples from 1 to 4 correspond to different ovarian pathological conditions. A higher MUC1 concentration in sample 3 respect to others was detected. This could be due to the fact that both ovaries are affected by the tumor. The lower concentration of MUC1 detected in sample 4 is related to the presence of a non-malignant pathology.

The serum samples from 5 to 9 are obtained from patients affected by invasive ductal breast carcinoma. These samples were characterized by the Nottingham Prognostic Index (NPI), which is used to determine the prognosis following surgery for breast cancer and is calculated using three criteria: the size of the lesion, the number of involved lymph nodes and the grade of tumor. A 93% 5-year survival rate is associated with score 2, whereas for score 3 the 5-year survival rate is 85%.

Comparable MUC1 concentrations were obtained in samples 5 and 7 corresponding to a NPI of 2. A higher MUC1 concentration was detected in samples 6, 8 and 9, which were characterized by a NPI value of 3. Thus a correlation between the detected concentration of MUC1 and NPI value can be established. An increase of RSD values, resulting in lower reproducibility, respect to standard MUC1 solutions assay, was found. This fact can be owing to the variability of the matrix due to the other physiological or pathological patients conditions that can influence MUC1 serum overexpression [181].

To further confirm the ability of the assay to discriminate between normal and pathological samples, MUC1-negative serum samples were also analysed (sample 10). MUC1 concentration was found to be at least 10 times lower than the MUC1 concentration found in the presence of ovarian and breast carcinomas and 3 times lower in the case of the presence of benign tumor (sample 4).

1.4. Conclusions

In the work presented herein, two simple and sensitive electrochemical approaches for the detection of Mucin1 tumor marker using magnetic beads coupling screen-printed arrays were developed.

In the first approach antibodies were used for capturing the target molecule in a sandwich assay. However, eventhough in this case a high sensitivity was obtained (3.5 ng/mL) the assay demonstrated low selectivity when tested in the presence of similar target molecules MUC4 and MUC16.

In order to increase the specificity for MUC1 protein the antibodies were replaced with aptamers, which are able to discriminate between closely related targets. The designed aptasensor demonstrated good analytical performance with good selectivity and sensitivity, with limits of detection 1.4 ng/mL in the linear range of 0 - 10 ng/mL (or LOD 0.037 nM in the linear range from 0 to 0.28 nM) in buffered solutions.

Moreover, the clinical applicability of the proposed aptasensor was demonstrated. The aptamer based bioassay was tested in non-pathological serum samples, as well as in pathological women serum samples for the detection of MUC1 protein. Good results were obtained demonstrating the potential practical applications in biological samples and offering a promising tool in biomedical applications.

Chapitre 2

Contexte

L'objectif de ce chapitre a été de développer un apta-capteur simple et sans marquage pour la détection du marqueur tumoral MUC1. Les nanoparticules d'or sont d'abord électrodéposées sur des électrodes de graphite imprimées sérigraphiées comme plate-formes d'immobilisation pour les aptamères thiolés. Les aptamères sont auto-assemblés sur la surface d'or. La technique EIS est utilisée pour la caractérisation du capteur développé. Dans les analyses d'impédance, une augmentation de la résistance de transfert de charge est observée après immobilisation d'aptamères et de protéines à la surface du capteur.

Section 2.2. présente le protocole pour l'électrodéposition de nanoparticules d'or, suivi par l'immobilisation d'aptamères et l'interaction avec les protéines. Une représentation schématique des étapes de la fabrication du capteur est présentée dans la section 2.3.1. Plusieurs paramètres ont été optimisés afin d'obtenir les meilleures performances du capteur et les résultats sont inclus dans la section 2.3.2. Enfin, les sections 2.3.3 et 2.3.4. montrent la caractérisation par EIS du capteur au cours de la modification de surface et la performance analytique du capteur développé pour la détection de MUC1.

2. Label free MUC1 aptasensor based on electrodeposition of gold nanoparticles on screen printed electrodes

2.1. Introduction

Despite the research advances made in the field, cancer still remains a main cause of death worldwide. Detection of tumor markers is important for the clinical diagnosis and evaluation of treatment for patients with certain tumor-associated diseases [181]. In cancer processes, during the growth of the tumor, the cells can release specific proteins into the circulation system. Their levels in serum can be correlated with the stages of tumors. Thus, these proteins can serve as tumor markers for screening and clinical diagnosis of cancer. Due to the disadvantages of convetional methods (e.g. radiation immunological assays, time-resolved fluorescence, chemiluminescence), there is a requirement for the urgent development of new methods for the detection of tumor marker in the serum of patients with low-cost, high speed and real-time control in large-scale disease screening[182]. Immunosensors combine the high sensitivity of sensors with the high specificity of immunoreactions, many immunoassays being developed for the detection of tumor markers[183-188].

MUC1 is a transmembrane glycoprotein expressed by most 'wet' epithelia, such as bladder, breast, gastric, pancreas and ovary[189]. In case of cancer processes MUC1 is overexpressed and shed into blood circulation, where it can be measured by various immunoassays, therefore serving as tumor marker[190].

Aptamers have been widely used as sensing element for the development of sensors used in early cancer diagnosis[191]. Aptamers are synthetic nucleic acids ligands (DNA or RNA) which are artificially synthesized and selected from combinatorial libraries of synthetic nucleic acids through SELEX, to have specificity and affinity for various molecules, including cancer biomarkers.

Aptamer based detection methods are attractive due to their high sensitivity, selectivity to the target molecule and good stability in complex environments. A number of aptasensors for small molecules, proteins, and even cells have been developed[192-193] and used for the construction of biosensing devices[194-196]. Recently, based on the discovery of DNA aptamers targeting MUC1, a few aptamer-based sensors have been developed to detect MUC1-overexpressed breast cancer cells with detection limits between 30 and 10^7 cancer cells/mL[197-199]. An electrochemical sensor for MUC1

was developed using ferrocene carboxylic-doped silica nanoparticles as an immobilization support, with a detection limit of 0.64 U/mL [200].

The key issues with any electrochemical aptamer-based biosensor include the enhancement of aptamer immobilization amount, maintenance of target accessibility and the demonstration of useful detection signals[201]. AuNPs are excellent candidates for bioconjugation, owing to the fact that they are biocompatible and bind readily to a range of biomolecules. The immobilization of the nanoparticles on the electrode increases the surface area and promotes the adsorption capability of the electrode.

Hence, we have developed a very simple impedimetric aptasensor based on a MUC1-binding aptamer immobilized on graphite screen printed electrodes (SPE) modified with AuNPs. The loosely packed aptamers are self-assembled onto gold surface. In impedance measurements, an increase in charge transfer resistance is observed after immobilization of proteins to the sensor surface. Several parameters that could affect the sensor performance were optimized.

2.2. Experimental

2.2.1. Chemicals and instrumentation

MUC1 recombinant protein was provided by Novus Biological. Aptamer 5´-GCAGTTGATCCTTTGGATACCCTGGTTTTTTTTTTTTTTT-3´-SH was purchased from AlphaDNA (Canada). Sodium dihydrogen phosphate, disodium hydrogen phosphate, potassium ferrocyanide ($K_4[Fe(CN)_6]$), potassium ferricyanide ($K_3[Fe(CN)_6]$), sulfuric acid, thioacetic acid, ethylenediaminetetraacetic acid (EDTA) and Tris (hydroxymethyl) aminomethane (TRIS) were obtained from Merck. Bovine serum albumin (BSA), polyoxyethylene sorbitan monolaureate (Tween 20), magnesium chloride, and chloroauric acid were purchased from Sigma–Aldrich. All solutions were prepared using MilliQ water. The following buffers were used: phosphate buffered saline (PBS), pH=7.4 (buffer A), TRIS 10mM, NaCl 100mM, KCl 100 mM, MgCl2 5mM, pH=7.2 (buffer B).

The electrodes used in the experiments were purchased from Dropsens (Spain). We used graphite SPEs with graphite working electrode (4 mm in diameter), graphite counter electrode and a silver pseudo-reference electrode. Electrochemical measurements were performed with AUTOLAB PGSTAT 30 (EcoChemie, Netherlands) with GPES and FRA2 software 4.9.

Cyclic voltammetry was employed for the electrodeposition of AuNPs on SPE in the range of potential between -0.20 and 1.20 V, with a scan rate of 100 mV/s, in the range potential between -0.60 and 0.00 V, with a scan rate of 100 mV/s.

EIS measurements were carried out in the presence of 10 mM $[Fe(CN)_6]^{3/4-}$ in PBS (pH 7.4). The impedance was measured in a frequency range from 100 mHz to 100 kHz at a dc potential of +0.13 V, the formal potential of the $[Fe(CN)_6]^{3/4-}$ redox probe. The data is represented in Nyquist plots (Z'' vs. Z', Z'' = imaginary impedance and Z' = real impedance).

The microscopic images were obtained with a WITEC Alpha 300 System.

All measurements were carried out at room temperature (25ºC).

2.2.2. Preparation of AuNPs modified SPE

In order to construct the aptasensor, the surface of the graphite working electrode was firstly modified with AuNPs.

AuNPs were electrodeposited by CV using a solution of $HAuCl_4$ 0.6 mM in H_2SO_4 0.5M and cycling the potential between -0.2 and 1.2 V, with a scan rate of 100 mV/s, for 15 cycles.

2.2.3. Immobilization of the aptamer and interaction with the protein

For the immobilization of the aptamer on the electrodeposited AuNPs 10 µL of 5 µM aptamer solution was placed on the working electrode and incubated for 30 min. The electrode was then rinsed with distilled water to remove the unbound aptamer, followed by an incubation step with 10 µL of MUC1 solution in buffer B for 60 min.

Electrochemical impedance measurements on modified electrodes with aptamers and MUC1 protein were then performed in PBS in the presence of 10mM $[Fe(CN)_6]^{-3/-4}$ (1:1 mixture) as a redox probe. The concentration of MUC1 protein was quantified by the change of electron transfer resistance.

2.3. Results and discussion

2.3.1. Principle of electrochemical aptamer-based biosensor

Fig. 15 illustrates the principle of the detection of MUC1 by the aptasensor, based on its specific recognition by thiolated aptamers immobilized on AuNPs-modified SPEs. The fabrication of the sensor involves two steps: an electrochemical deposition step and an immobilization step. The surface of graphite SPEs was firstly modified with electrodeposited AuNPs (a). Subsequently, the thiolated aptamer probe was immobilized on the AuNPs modified SPE electrode (b). The aptamer modified AuNPs-graphite SPE was then incubated with various concentrations of MUC1 solution in buffer B for 60 minutes to form the affinity complex (c). Unbound MUC1 protein was then removed by rinsing with buffer. At last, MUC1 proteins were recognized due to the specific interaction between MUC1 and its aptamer, using EIS in 10mM $[Fe(CN)_6]^{-3/-4}$ in buffer A (d).

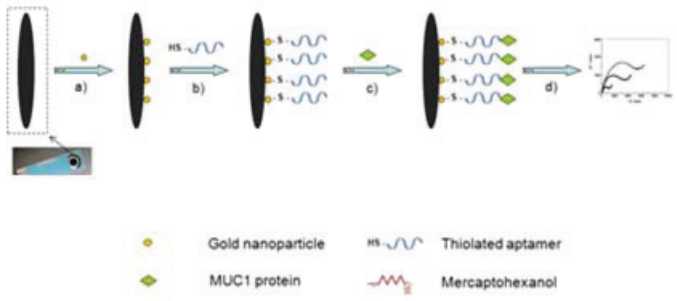

Fig. 15. Steps in the development of the aptasensor for detection of MUC1 by EIS on AuNPs-graphite SPE: (a) electrodeposition of AuNPs, (b) immobilization of thiolated aptamer, (c) affinity reaction with MUC1, (d) EIS measurements.

2.3.2. Optimization of experimental parameters

Several experimental parameters, such as concentration and incubation time with aptamer and incubation time with protein, were optimized in order to find the best conditions for the assay.

The proper immobilization of the aptamer at the surface of transducers is a key step in the fabrication of aptasensors. The immobilization method should ensure a good coverage maintaing also an appropiate density and good orientation of the aptamers. For this, different concentrations of aptamer solution and different incubation times were investigated. The concentration of aptamer was fixed to 1 μM, and the reaction time with the aptamer was varied between 5 and 60 minutes. As the incubation time increased from 5 to 30 minutes, the charge transfer resistance increased as well. The further increase in the incubation time to 60 minutes did not result in a significantly increased signal thus an incubation time of 30 min was considered optimal (Fig 16A). Different concentrations of aptamer (10 nM, 100 nM, 1 μM, 5 μM and 10 μM) were then investigated. An increase in the charge transfer resistance was observed up to 5 μM when the signal tends to level off, indicating a saturation of the AuNPs-modified electrode surface with thiolated aptamers. 5 μM was thus chosen for further experiments (Fig 16B).

The incubation time with the target protein was further optimized. A solution of MUC1 10 ng/mL was added onto aptamer-modified electrodes and left to incubate for 15, 30, 60 and 90 minutes. The charge transfer resistance increases up to 60 min. A relatively small increase in the current was observed when the time was further increased to 90 minutes, therefore an incubation time with the antigen of 60 minutes was considered to be sufficient for the complete formation of the affinity complex (Fig 16C).

In order to check if the sensitivity of the sensor can be improved by using a blocking agent after the aptamer immobilization step, BSA and thioacetic acid were investigated to reduce the nonspecific adsorbtion of the protein on the electrode surface. BSA adsorbs on the electrode surface preventing the adsorbtion of MUC1 protein, whereas thioacetic acid, as a thiolic compound, binds to the free sites of the AuNPs that are not covered with aptamer. For this purpose, after the immobilization of the aptamer on the AuNPs, the modified electrode was rinsed with buffer A and incubated for 30 min with 10 μl either 1% BSA solution or 0.1% and 1% thioacetic solution in buffer A, followed by the incubation step with the protein as previously described. The experiments were carried out for 0 (blank) and 10 ng/mL MUC1 solution and the efficiency of the blocking step was evaluated by comparing the signal to blank ratio ($R_{ct\ 10\ ng/mL}$ / $R_{ct\ blank}$) in all three cases. The resulted signal to blank ratios were 1.02, 0.94 and 1.12 for 1%, BSA, 1% thioacetic acid and 0.1% thioacetic acid, respectively, respect to 2.87 obtained when no blocking agent was used. No improvement was observed in the sensor performance when blocking agents were used, moreover the use of the above mentioned blocking agents seemed to affect the

binding of the antigen to the aptamer, presumably to the alteration of the flexibility and the configuration of the aptamer for further binding of the protein.

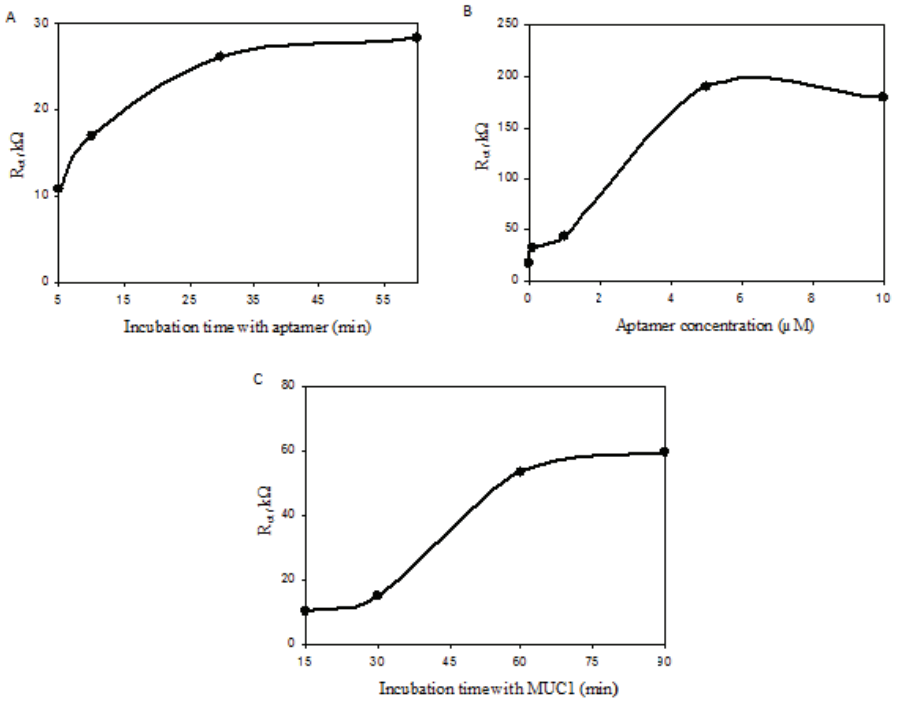

Fig. 16. Optimization of experimental parameters: (A) incubation time with aptamer (5, 10, 30, 60 min), (B) concentration of aptamer (10 nM, 100 nM, 1 μM, 5 μM, 10 μM) and (C) incubation time with antigen (10, 30, 60, 90 min)

2.3.3. Characterization of AuNPs-graphite SPE-based aptasensor by EIS

The graphite SPEs were modified with AuNPs as immobilization platform for the thiolated aptamers and the features of surface-modified aptamer biosensor were investigated by electrochemical impedance spectroscopy (EIS) using 10mM $[Fe(CN)_6]^{-3/-4}$ in buffer A as a redox probe. The results are presented in Fig. 17. The impedance spectra presents a semicircle portion and a linear portion. The semicircle portion at higher frequencies represents the electron-transfer-limited process. The linear portion at lower frequencies represents the diffusion-limited process. The semicircle diameter equals the electron-transfer resistance. Compared to bare graphite electrode (b), a significant decrease in the charge transfer resistance can be observed after

electrodeposition of AuNPs (a), due to the promotion of the electron transfer. The electron transfer resistance increases after the immobilization of aptamers on the AuNPs modified surface (c) as a consequence of the electrostatic repulsion between $[Fe(CN)_6]^{-3/-4}$ anions and the negatively charged aptamers, which suggests that thiolated aptamers have been successfully immobilized on electrodes and obstructed the electron-transfer. A further increase in the resistance occurred after incubation with MUC1 protein, due to the interaction of aptamer with MUC1 protein, a large protein with a molecular weight of 250-1000 kDa, bringing a steric hindrance effect on the electron transfer of $[Fe(CN)_6]^{-3/-4}$ through electrode, resulting in reduced electron transfer speed (d).

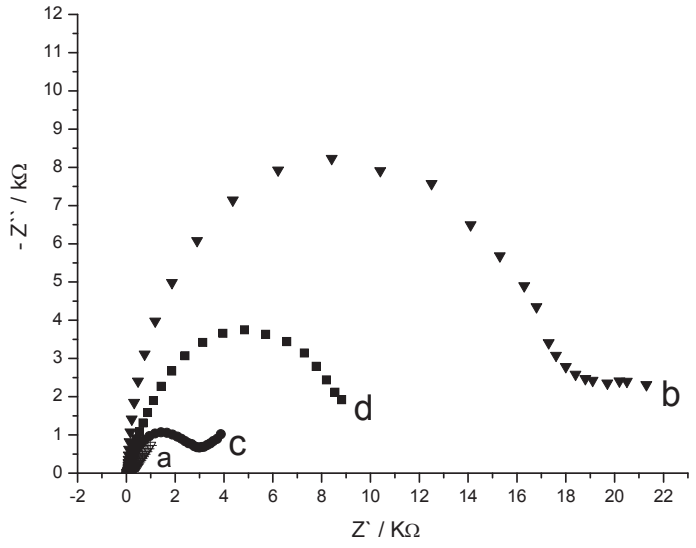

Fig. 17. Nyquist plots of EIS data performed in 10mM $[Fe(CN)_6]^{-3/-4}$ solution for: (a) graphite SPE/AuNPs (b) bare graphite SPE, (c) graphite SPE/AuNPs/Aptamer, (d) graphite SPE/AuNPs/Aptamer/MUC1 protein (5 ng/mL)

To further confirm the electrodeposition of AuNPs on the SPE surface microscopy was employed. The microscopy images show a random distribution of the gold particles on the electrode surface, as well as pores and holes (Fig. 18). The results are in good agreement with the SEM images reported by Ravalli *et al* [157].

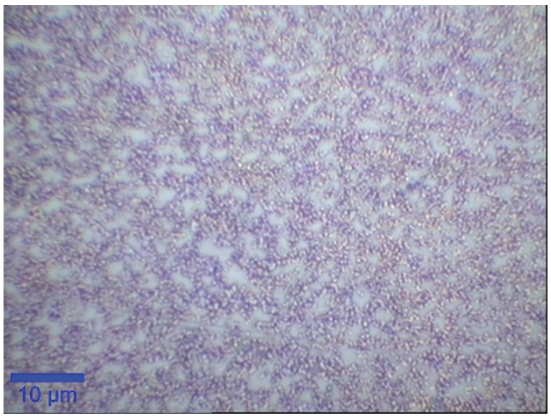

Fig. 18. Microscopy image of AuNPs electrodeposited on the electrode surface from 0.6 mM $HAuCl_4$ solution in 0.5 M H_2SO_4; CV parameters: potential range -0.2 to 1.2 V, 15 cycles, 100 mV/s

2.3.4. Quantitative detection of MUC1 protein

To quantitatively assess the detection limit and response range of the graphite SPE/AuNPs-based MUC1 aptasensor, we studied impedance responses with different MUC1 protein concentrations (2.5–15 ng/mL). The relative change in R_{ct} has been chosen as signaling parameter, as shown in Fig. 19. As the concentration of the MUC1 protein increases, the resultant electron transfer resistance was enhanced. A linear response was obtained in the range of 2.5-15 ng/mL ($y=0.545x+7.801$, $R^2 = 0.968$). The limit of detection was 3.6 ng/mL, calculated as 3.3 times the standard deviation of the blank / slope (n = 3). The dose-response curve is shown as an inset.

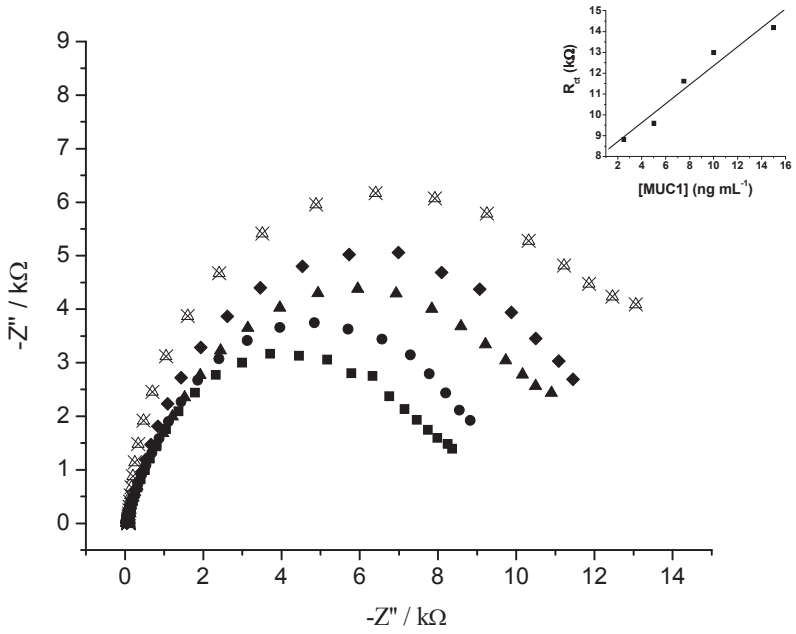

Fig. 19. Change of the electron-transfer resistances (R_{ct}) at the modified AuNPs/GSP electrodes upon the analysis of different concentration of MUC1 protein. R_{ct} data are extracted from the corresponding Nyquist diagrams. Inset: dose-response curve for different concentrations of MUC1 protein.

2.4. Conclusion

In summary, we have introduced a simple and sensitive strategy for the electrochemical detection of human MUC1 protein using aptamer and gold nanoparticles.

Loosely packed aptamers specific for MUC1 antigen were self-assembled onto the surface of graphite screen printed electrodes modified with AuNPs by electrochemical deposition. The interaction between aptamer and MUC1 protein was investigated by electrochemical impedance spectroscopy technique through the change in the charge transfer resistance. An increase of the charge transfer resistance was observed after immobilization of aptamers and proteins to the sensor surface.

The results demonstrate that the electrochemical method using aptamer probe is simple and convenient, and allows quantitative detection of human MUC1 protein.

The calibration curve for the determination of MUC1 protein was obtained under optimized conditions. The estimated limit of detection of the MUC1 protein was 3.6 ng/mL in the linear range of 2.5-15 ng/mL.

Chapitre 3

Contexte

L'objectif de ce chapitre a été de développer des capteurs électrochimiques à empreintes moléculaires pour la détection de drogues, de polluants de l'environnement et de contaminants alimentaires. Nous avons cherché à développer un protocole générique qui pourrait être appliqué à une large gamme de molécules, y compris des composés non électroactifs, en utilisant comme médiateur redox le couple hexacyanoferrite / hexacyanoferrate.

Plusieurs études sont présentées ici, pour le développement de capteurs électrochimiques à base de MIP pour la détection sensible et sélective de différents analytes cibles. Le TNT, la gemcitabine, la tétracycline, l'estradiol et le glyphosate ont été étudiés comme des molécules modèles, sur la base de la technologie à empreintes moléculaires dans les films conducteurs déposés sur des électrodes d'or à l'aide d'une monocouche intermédiaire de *p*-aminothiophénole (PATP) et AuNPs fonctionnalisées avec PATP. Tout d'abord, une monocouche d'auto-assemblage de PATP est formée sur la surface de l'électrode d'or par des liaisons Au-S. Ensuite, le film MIP a été déposé sur l'électrode par l'électropolymérisation du groupement aniline des PATP greffés sur les électrodes d'or et sur AuNPs. Afin d'obtenir des films imprimés, le processus d'électropolymérisation est réalisé en présence de molécules modèles, l'enlèvement subséquent des molecules modèles laissant des cavités qui servent de sites spécifiques de reconnaissance. Une évaluation du protocole expérimental pour la fabrication et la caractérisation électrochimique des films imprimés est présentée dans la section 2.2. La section 3.3.1 traite de l'électrodéposition des films imprimés et non imprimés (contrôle) à l'aide de la voltammetrie cyclique. Puis, dans les sections 3.3.2. et 3.3.3., on discute la caractérisation des films obtenus et la capacité a reconnaître et a lier les analytes cibles en utilisant la voltamétrie à balayage linéaire. La section 3.3.4 traite de l'optimisation des paramètres expérimentaux impliqués dans la performance du capteur. La performance analytique dans des conditions optimisées et l'applicabilité a l'analyse d'échantillons réels sont, ensuite, présentées dans les sections 3.3.5. et 3.3.6., respectivement. Enfin, des études de reproductibilité, de répétabilité et de stabilité sont présentées dans les sections 3.3.7. et 3.3.8.

3. MIP-based sensors for the detection of various analytes of environmental, biomedical and food safety interest

3.1. Introduction

The molecular imprinting technique is a versatile method for the development of biomimetic sensors. The method consits in the polymerization of functional monomers in the presence of template molecules and the subsequent extraction of the template from the resulting polymer matrix, which generates cavities complementary in shape and size with the template. With the advantages of high affinity and specificity, good mechanical strength, thermal and chemical stability, low cost and ease of preparation, molecularly imprinted polymers (MIPs) have found potential applications in many fields such as chromatography [202,203], immunoassays [204] or biomimetic sensors [205, 206]. The non-covalent approach for imprinting materials is more commonly used, due to the less complicated preparation process and the broad selection of functional monomers and possible target molecules [207]. The binding of the target molecule to the recognition sites in MIPs has been investigated using electrochemical, optical or piezoelectric techniques[209-211]. Electrochemical methods have been widely applied, due to their rapidity, simplicity and low cost. The complex preparation process and the low-rate mass transfer and poor site accessibility associated with the conventional bulk method for the preparation of molecularly imprinted polymers has focused the attention on the electropolymerization technique for the deposition of imprinted films. Electrodeposition of polymers consists in the adsorbtion of an electropolymerized material at the eletrode surface and, dissimilar to bulk polymerization , eliminates the need for rigorous synthesis and film preparation typically required by spin- or solvent-casting techniques [212]. Moreover it has the advantage of ease of control over the film thickness by controlling the electrochemical parameters. The use of conducting polymers leads to increased sensitivity. Different types of polymers have been investigated for the preparation of MIPs such as polypyrrole, aniline or poly(*o*-phenylenediamine).

AuNPs have attracted great attention for the development of sensors, owing to their unique physicochemical attributes [213]. The integration of nanoparticles in MIP materials has the benefit of enhancing the number of accessible complementary cavities, the catalytic activity of the surface and the fast equilibration with the analyte [214]. The performance of sensor can thus be improved. For example, Mustafa *et al* reported on a nanocomposite material consisting of a polyurethane-based MIP and Ag_2S nanoparticles leads to a three times higher response than the response of each

constituent towards the detection of 1-butanol by a quartz crystal microbalance sensor [215].

The versatility of the molecularly imprinted method allows the design of artificial receptors for a broad range of molecules, such as food contaminants, drugs, pollutants etc, which can be integrated in sensors.

The detection of explosives has a significant impact on environmental protection and homeland security. Nitro-aromatic explosives, such as trinitrotoluene (TNT) (Fig. 20A), are used in landmines and for military purposes. They infiltrate in soil and groundwater in war zones and near military facilities and contaminate the environment[216]. These compounds are highly toxic and carcinogenic to living organisms, causing health problems, such as aplastic anemia, toxic hepatitis, hepatomegaly, cataract and skin irritation[204]. The detection of explosives is generally performed by sniffer dogs, which have an excellent sense of smell. However, training these dogs involves high costs and limited use from the point of view of time and coverage. Ion mobility spectrometry is the most used method to detect explosives in airports, but the high cost and size limits its use[218]. Thus, increasing efforts have been focused on the development of low-cost, easy-to-use and portable sensing devices for trace detection of explosives. Various sensors have been reported in recent years for the detection of TNT, based on the fluorescence of different materials quenched by TNT, such as creatinine-functionalized quantum dots[219], graphene quantum dots [220] or functional polymers[221], on surface-enhanced Raman spectroscopy substrates based upon highly ordered gold nanoparticles (AuNPs) [222] or silver nanoparticle/graphene nanosheet composites[223], on surface plasmon resonance[224, 225] or on the redox activity of the nitro groups of TNT in electrochemical sensors[226, 227]. Few MIP-based sensors for the detection of TNT have been reported. Among them, different polymer synthesis approaches coupled with electrochemical, piezoelectric and optical detection techniques have been developed[228,229]. Kutner's group developed thiophene derivatives based-MIP chemosensors for the micromolar detection of various nitroaromatic explosives by chronoamperometry and piezoelectric microgravimetry under flow-injection analysis [230]. In another approach, a triple imprinting technique for the fluorescence detection of TNT has been reported. The combination of colloidal crystal templating, mesophase templating and molecular imprinting resulted in a hierarchically structured trimodal porous silica film that was able to selectively bind TNT [231].

Pharmaceutical industry and drug detection in biological fluids is another potential field of application for MIP-based sensors. Given the rapid growth of cancer research field, the development of new analytical methods for the detection of

antineoplastic drugs is of great interest. Gemcitabine (GMT), 4-amino-1-(2-deoxy-2,2-difluoro-β-D-*erythro* pentofuranosyl) pyrimidin -2(1*H*)-on (Fig. 20B), is a nucleoside analog used for the treatment of various carcinomas, such as non-small cell lung cancer, pancreatic cancer, metastatic breast cancer and advanced recurrent ovarian cancer. Monitoring the concentration of antineoplastic drugs is important for the optimization of therapy and management of side effects. If the dose is too low the effects can be reduced or even lost; if it is too high side effects and toxicity can occur. Thus it is important to quantify GMT in biological samples and pharmaceuticals. Several methods have been reported for the detection of GMT in plasma and serum, such as high performance liquid chromatography (HPLC) [232,233,234], HPLC-tandem mass spectrometry HPLC-MS [235] or liquid chromatography-tandem mass spectrometry, LC-MSMS [236]. However, these methods are time consuming and require expensive instrumentation and complex sample pretreatment. Electrochemical sensors are attractive alternatives to measure antineoplastic drugs. A differential pulse voltammetry method was reported for the detection of GMT in pharmaceutical formulations based on its electrochemical oxidation on gold [237] and carbon electrodes [238]. To our best knowledge there has not been yet reported a MIP-based electrochemical sensor for the detection of GMT.

The use of antimicrobial agents in animal feeds for growth promotion, improved feed efficiency, and control and prevention of disease has been widespread since the early 1950s [239]. However, their abuse can seriously affect human health. Tetracyclines (TCs) are broad-spectrum antibiotics that show activity against Gram-positive and Gram-negative bacteria, including some anaerobes [240]. They have been widely used as a veterinary drug and a feed additive, thus they can be found in food products including meat, milk, honey[241-243]. TCs have been used worldwide in apiculture as prophylactic or therapeutic agents in the prevention and treatment of bacterial diseases such as the American Foulbrood (AFB) and the European Foulbrood (EFB), these diseases being highly infectious and deadly to bee broods [244]. TC (Fig. 20C) residue is a problem that should not be neglected as it is not only a threat to public health but also a hurdle to the international trade of the product. TCs have been successfully detected using several methods. The most popular method for TC determination in honey is high-performance liquid chromatography (HPLC) coupled with ultraviolet (UV) detection; LODs ranging from 5 to 12 ng/g have been obtained [245]. This method can provide simultaneous and precise results, but is expensive and requires complex sample pretreatment and qualified personel. The trend in the analysis of TCs in food is to replace laborious methods by simple test methods. The Tetrasensor Honey test kit is a receptor-based assay using dipsticks for the rapid screening of honey for the presence of tetracyclines, its detection capabilities being between 4 to 7 μg/kg [246]. To the best of our knowledge, electrochemical biosensors have been rarely applied for TC detection on solid electrodes. Zhou *et al* [247] and Chen *et*

al [248] have developed tetracycline aptasensors applied to the determination of TC in spiked milk samples, with LODs of 2.2 ng/mL and 1.0 ng/mL, respectively. Furthermore, an indirect competitive assay-based aptasensor for the detection of tetracycline in honey has been developed by Wang *et al* with a LOD of 9.6 pg/mL. [249]

Another group of food and environment contaminants are estrogens, which are currently widely used to fatten animals. Estrogens, including 17β-estradiol (E_2) (Fig 20 D), play critical roles in mammalian female development, fertility, and behavior, being involved in the growth and maturation of the female reproductive tract, regulation of menstrual cycle and ovule implantation [250]. The presence of E_2 in the environment has raised serious concerns on human health; E_2 is an endocrine disruptor chemical (EDC), which interferes with the normal endocrine function, having side effects on growth, metabolism and reproduction of the organisms, and increasing the incidence of cancer and tumors [251]. It can be present in wastewaters, due to its industrial and agricultural applications, and in animal food products, being used to fatten the animals due to its anabolic effect [252]. Thus there is an urge for the development of sensitive and accurate techniques for the detection of E_2. The commonly used techniques, such as HPLC [253] or GC/MS [254], are time and cost-consuming, thus electrochemical sensors gained interest lately through their simplicity and low cost. Zhang *et al* reported on an electrochemical sensor based on electropolymerized MIP with electrodeposited AuNPs amplification for the detection of E_2 in milk samples that exhibited a detection limit of 1.28 fg/mL [255]. In another approach Yuan's group fabricated a MIP based sensor for E_2 based on the electropolymerization of 6-mercaptonicotinic acid on Pt nanoparticles-modified electrode. The sensor was able to detect concentrations of E_2 as low as 0.16 fM [256].

Glyphosate (Gly) (N-(phosphonomethyl)glycine) (Fig. 20E) is the most frequently used herbicide in the world [257, 258]. The continued use of glyphosate raises the potential for residue accumulation in water and crop commodities. Although glyphosate has been considered as a "toxicologically harmless" compound [259], recent studies suggest that glyphosate-based pesticides affect cell cycle regulation[260]. The maximal permissible level of glyphosate in drinking water is 0.70 mg/L in the United States [261] and 0.1 μg/L in the European Union[262]. Therefore, monitoring of glyphosate in drinking water has become increasingly important. Several chromatographic methods have been developed for the analysis of glyphosate, including gas chromatography (GC)[263-265] and liquid chromatography (HPLC)[266-268]. These methods can have high sensitive and accurate detection results. However, the ionic and water-soluble proprieties of glyphosate make the analysis by HPLC advantageous over GC[269-271]. Moreover, they are not cost-effective. So, it is necessary to establish a fast and convenient method to detect glyphosate. Recently, selective sensors for Glyphosate using molecularly imprinted polymer have been developed. Zhao and co-workers

developed a novel Chemiluminescence-molecular imprinting sensor for glyphosate in foodstuff [272]. An optical sensor for the detection of pesticides (chloropyrifos, diazinon and glyphosate) was also developed by forming MIP onto optical fibers [273].

Several studies have been proposed herein, for the development of electrochemical MIP-sensors for the sensitive and selective detection of various target analytes. TNT, gemcitabine, tetracycline, estradiol and glyphosate have been investigated as template molecules, based on molecularly imprinted technology in conductive films deposited on gold electrodes by means of an intermediate monolayer of *p*-aminothiophenol (PATP) and PATP functionalized-AuNPs. Firstly, a self-assembling monolayer of PATP is formed on the gold electrode surface through Au-S bonds. Then, MIP film was deposited on the electrode via electropolymerization of the aniline moiety in PATP grafted on gold electrodes and on AuNPs. In order to obtain imprinted films, the electropolymerization process was performed in the presence of template molecules, the subsequent removal of the template leaving cavities that serve as specific recognition sites. Combining the advantages of molecular imprinting and electrodeposition with those conferred by AuNPS, the developed sensors exhibited good sensitivity and high selectivity. Several parameters influencing the performance of the sensors have been optimized and the resulted sensing materials have been succesfully applied for the analysis of real samples.

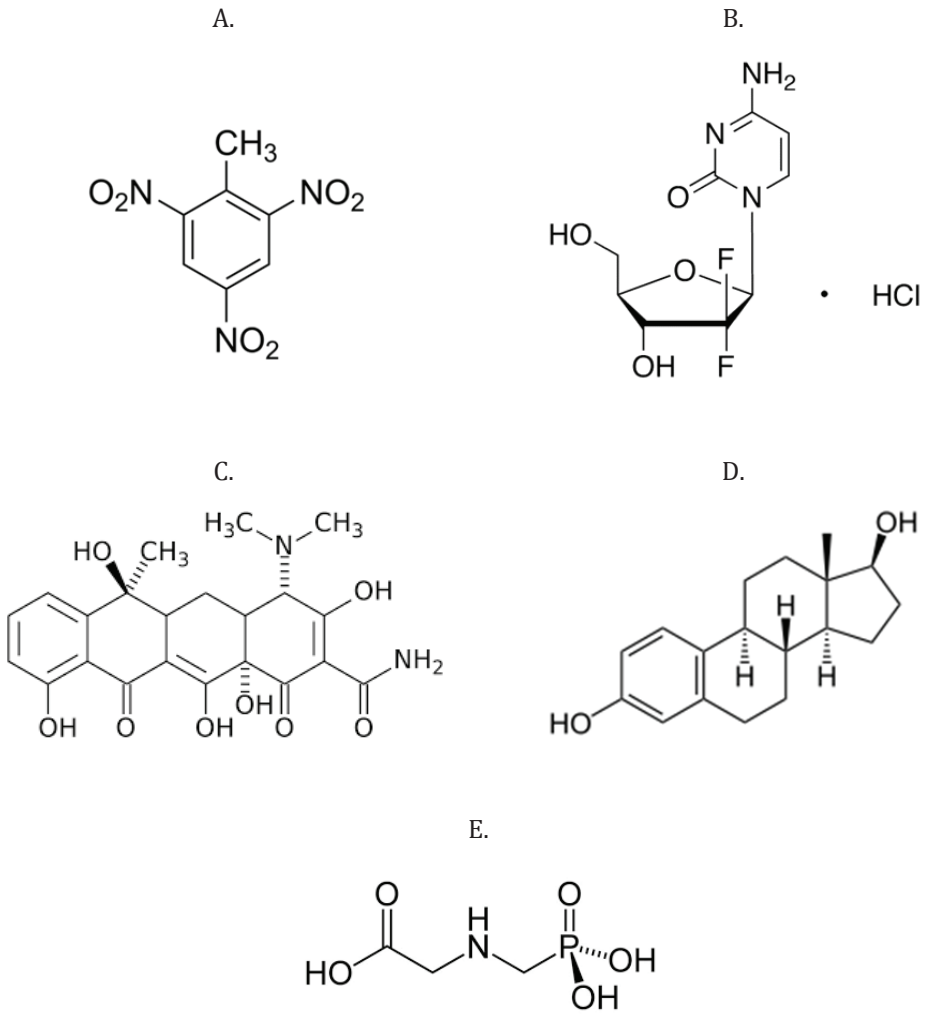

Fig. 20. Chemical structure of template molecules (A) TNT, (B) Gemcitabine, (C) Tetracycline, (D) Estradiol, (E) Glyphosate

3.2. Materials and methods

3.2.1. Chemicals and instrumentation

Trinitrotoluene (TNT), gemcitabine (GMT), tetracicline (TC), estradiol (E2), glyphosate, potassium hexacyanoferrate ($K_4[Fe(CN)_6]$), potassium hexacyanoferrite ($K_3[Fe(CN)_6]$), 2,4-dinitrotoluene (DNT), doxycycline, testosterone,

aminomethylphosphonic acid (AMPA), *p*-aminothiophenol (PATP), tetrachloroauric acid trihydrate($HAuCl_4.3H_2O$), sodium borohydride ($NaBH_4$), bovine serum albumin, acetone, ethanol, methanol and phosphate buffered saline (PBS) tablets, were purchased from Sigma-Aldrich with highest available purity. The gold sols were made up and stored in clean glass vials. All solutions were prepared using Milli-Q water with a resistivity of 18.2 MΩ/cm at 25 °C.

Two honey samples, guaranteed TC-free, were obtained from producers in the region of Taliouine – Morocco. The river samples were collected from Rhone river, Lyon.

The stock solution of TNT and E2 was prepared in acetone, TC in methanol, GMT in double distilled water and Gly in ethanol and stored in refrigerator. The working solutions were prepared daily by dilutions from the stock solution.

Electrochemical measurements were performed using a VOLTALAB-80 PGZ/301 potentiostat-galvanostat (Radiometer Analytical, France), controlled by Voltamaster 4 software. All experiments employed an electrochemical cell containing 5 mL of electrolyte solution, with a gold working electrode (0.17 cm^2), a saturated calomel electrode (SCE) reference electrode and a platinum plate auxiliary electrode (0.54 cm^2). Gold substrates were provided by the RENATECH Platform (LAAS, CNRS Toulouse). They were fabricated using standard silicon technologies.

UV-vis absorption spectra of the AuNPs nanoparticles were recorded at room temperature with a Perkin Elmer Lambda 900 UV/Vis/NIR spectrophotometer between 300 and 800 nm.

3.2.2. Experimental techniques used for fabrication and characterization of the molecularly imprinted sensors

3.2.2.1. Steps in the construction of the MIP sensors

The general protocol for the fabrication of MIP films is illustrated in Fig. 21. Firstly, a monolayer of PATP is self-assembled at the surface of gold electrodes via Au-S bonds between gold and thiol groups of PATP. In the next step, the molecularly imprinted film is deposited on the electrode via electropolymerization in a solution containing PATP-functionalized AuNPs and the template molecule (TNT, GMT, TC, E_2, glyphosate, respectivly). The non-covalent interactions (π-π interactions between the electron-poor TNT and the electron-rich PATP, hydrogen bonds between O atoms in the template and $-NH_2$ groups of PATP etc) promote the embedding of the host

molecules in a three-dimensional polymer-AuNP network. Finally, the template is removed from the complex matrix, forming surface imprinted sites. The presence of AuNPs in the matrix enhace the conductivity (increasing the electron transfer) and the number of imprinted sites, leading to more homogenous distribution of the recognition sites [274].

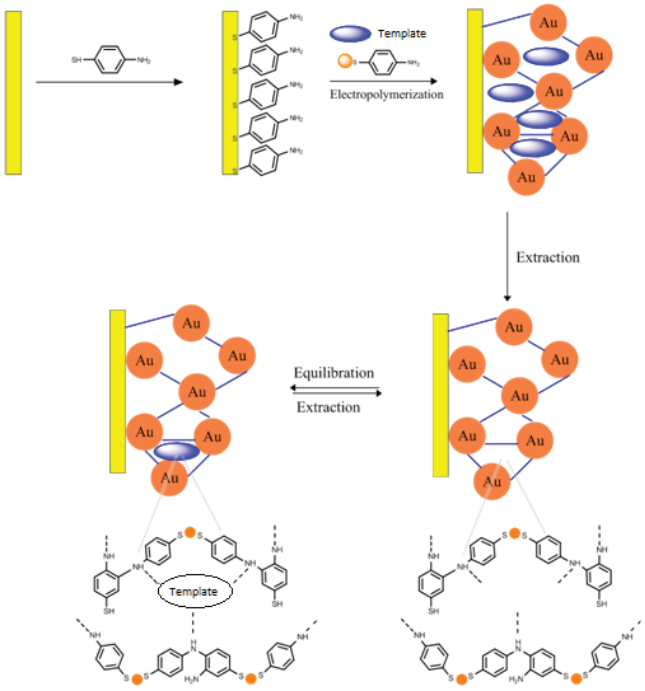

Fig. 21. Protocol for the fabrication of MIP-based sensors

3.2.2.2. Preparation of the functionalized AuNPs

AuNPs functionalized with the monomer (PATP) were used to fabricate sensing films. For this purpose, AuNPs were synthesized according to the procedure described in the literature [275]. For a typical preparation of gold nanoparticles, 31.6 mg (8×10^{-5} mol) of tetrachloroauric(III) acid trihydrate were dissolved in 30 mL of methanol in a round 0.1 L flask equipped with a condenser. A solution of *p*-aminothiophenol (1.6×10^{-4} mol) in 12 mL of a methanol/water (v/v) mixture was added dropwise to the gold salt solution under stirring, which changes its color from yellow to dark brown. After 10 min, 30.4 mg of $NaBH_4$ (8×10^{-4} mol) dissolved in 2.2 mL of water were added dropwise to the mix under vigorous stirring. After 10 min, stirring was stopped and the solution was kept in darkness for 1 hour. The suspension was then filtered through a polymer membrane and washed successively with water and ether. The resulting black powder was dried and stored either as a solid or dispersed in 0.1 N HCl solution. The

UV-vis spectra of gold nanoparticle colloids display a broad surface plasmon band centered around 535 nm. TEM observations presented in Fig. 22 show a mean diameter of around 5 nm with a narrow size distribution.

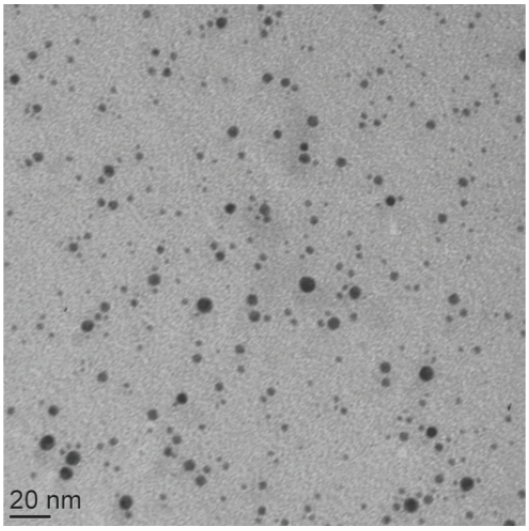

Fig.22. TEM observation of p-aminothiophenol functionalized gold nanoparticles

3.2.2.3. Electrodeposition of molecularly imprinting films onto the gold electrodes

The protocol used for the fabrication of MIP sensors was similar to the procedure reported before by Willer's group [235] with slight changes, which involved reducing the concentration of reagents (functionalized AuNPs from 1 mg/mL to 0.1 mg/mL and template molecule from 1 mg/mL to 0.1 mg/mL) and the use of a redox probe of hexacyanoferrite/hexacyanoferrate (which makes the method applicable to a wider range of molecules, including non-electroactive molecules).

Prior to modification, the surface of gold electrodes was firstly cleaned by rinsing with ethanol, acetone and double distilled water, followed by exposure to UV/ozone and activation with piranha solution for 5 minutes. The gold slides were then immersed in 50 mM PATP ethanolic solution for 24 hours at 4ºC for the formation of SAMs. Afterwards, the electrodes were rinsed with ethanol and double distilled water to remove the physically adsorbed PATP.

Cyclic voltammetry was employed for the electropolymerization of poly-thioaniline AuNP films onto the PATP-modified electrodes. In order to obtain

imprinted films, the electropolymerization was carried out in a solution of 10 mM $[Fe(CN)_6]^{-3/-4}$ in PBS pH 7.2 containing 0.1 mg/mL PATP-functionalized Au NPs and 0.1 mg/mL template solution, by cycling the potential from -0.35 V to +0.80 V vs SCE, at a scan rate of 100 mV/s, for 10 cycles, followed by applying a fixed potential of +0.80 V for 30 min. In the case of estradiol the electropolimerization was carried out from -0.35 to 0.60 V, due to the fact that at 0.60 V the oxidation of estradiol occurs. A control non-imprinted film (NIP) was also prepared in every case, in the same manner, but without any additional gemcitabine. The imprinting was demonstrated by comparison of the selectivity of NIP and MIP towards the binding of the analyte. Regarding the solvent used for the electropolymerization, different organic solvents were added to the electropolymerization solution that would assure the solubility of the template as well as to reduce the surface tension since most MIPs are hydrophobic. Thus, 1 mL acetone was added for TNT and E2 and 1 mL ethanol for TC and Gly (for a total of 5 mL electropolymerization mixture).

The modified electrodes were then washed with extraction solvent for optimum time to remove the imprinted molecules and adsorbates on the surface of the film, trigering the formation of stereo recognition cavities in the MIP film.

3.2.2.4. Electrochemical measurements on MIP and NIP-modified electrodes

Linear sweep voltammetry (LSV) was carried out in 10 mM $[Fe(CN)_6]^{-3/-4}$ in PBS pH 7.2 in the range of potential between +0.80V and -0.35V vs SCE, at a scan rate of 50 mV/s, in order to investigate the release and the uptake process for variable concentrations of analyte solution. Prior to LSV measurements, the electrodes were left in contact for an optimum time with the solution to be analyzed at room temperature, in order to bind the analyte. The films were then rinsed with PBS in order to remove molecules physically adsorbed on the surface of the polymer, and a fixed potential of +800 mV for 5 min was applied. During this step Fe (II) ions were oxidized to Fe (III) and a more stable signal for LSV was obtained.

We analyzed with the prepared imprinted and non-imprinted sensors solutions containing the analytes of interest in various concentrations and based on the results we constructed calibration curves, which allowed us to calculate the detection limit for each sensor. The height of the recorded peak was used as the analytical signal (current density).

3.2.2.5. Surface characterization by atomic force microscopy (AFM)

AFM was used to investigate the surface topography of the electropolymerized films and their rheological response (phase). The AFM measurements were carried out

using an Agilent 5500 AFM (Agilent Technologies, Palo Alto, CA,USA). Silicon tips with a nominal spring constant of 20 Nm^{-1} were used in tapping mode at a frequency of ~300 kHz.

3.2.2.6. Analysis of real samples

After the analysis of the target molecules in buffered solutions, the prepared MIPs were applied for the detection of analytes in complex matrices such as river and tap water, serum, pharmaceutical formulations or honey samples. To evaluate the effect of the matrix on the performance of the sensor, we spiked the samples with different concentrations of analyte. The MIP-sensor was left in contact with the spiked solutions, for the uptake of the analyte and the electrochemical measurements were carried out as described in section 3.2.2.4. The recovery rate was calculated for each sample.

3.3. Results and discussion

3.3.1. Electrochemical preparation of MIP and NIP based sensors

We chose to investigate the formation of the imprinted film through the measurement of its electronic permeability, since it was already shown that the presence of a SAM of thioaminophenol show a small decrease of charge transfer rate of a redox probe such as hexacyanoferrite/hexacyanoferrate [276]. This generic approach would permit to synthesize imprinted films that can be further applicable to a broad range of analytes, including non-electroactive compounds.

Fig. 23 shows the CV curves obtained for the electropolymerization of MIP films, in a solution of PBS containing 0.1 mg/mL PATP-AuNPS, 0.1 mg/mL template, 10 mM $[Fe(CN)_6]^{-3/-4}$. Miscible organic solvents in different proportions were used to ensure the solubility of the template and to reduce the surface tension and minimize hydrophobic interactions, since MIPs are usually hydrophobic[277], as follows: 10% acetone for TNT, 10% methanol for TC, 20% acetone for E2, 20% ethanol for Gly.

The electrochemical polymerization process consists of intermolecular reactions between the aniline moieties of PATP. At the applied potentials the radical anion is formed that initiates the polymerization of PATP. During the electropolymerization process the molecules of templates are embedded in the polymer matrix through non-covalent interactions (hydrogen bonds between $-NH_2$

groups of the polymer and O or N atoms in the structure of template, π-π interactions between the electron-poor template and the electron-rich PATP).

As it can be seen in Fig. 23, the current gradually decreases and the potential shifts to more positive potentials for the oxidation process and more negative for the reduction process, with each scan cycle, due to the continuous formation of polythioanline/AuNP/Template composite films that obstruct the electron transfer from/to the redox probe $[Fe(CN)_6]^{-3/-4}$ towards the surface of the gold electrode. After 10 cycles the current peaks become almost stable. The intensity of the peaks and the decrease of the current density with each cycle are quite different for each template, demonstrating that the presence of the template influences differently the electropolymerization rate, depending on the structure of the template and its interaction with the polymer. For the aromatic compounds (Fig 23 A-D) the electropolymerization rate is higher, while for linear molecules such as Gly (Fig 23 E) the decrease with each polymerization cycle is much lower. The different electropolymerization behaviour might also be explained by the presence of different organic solvents in various proportion in the electropolymerization solution in each case.

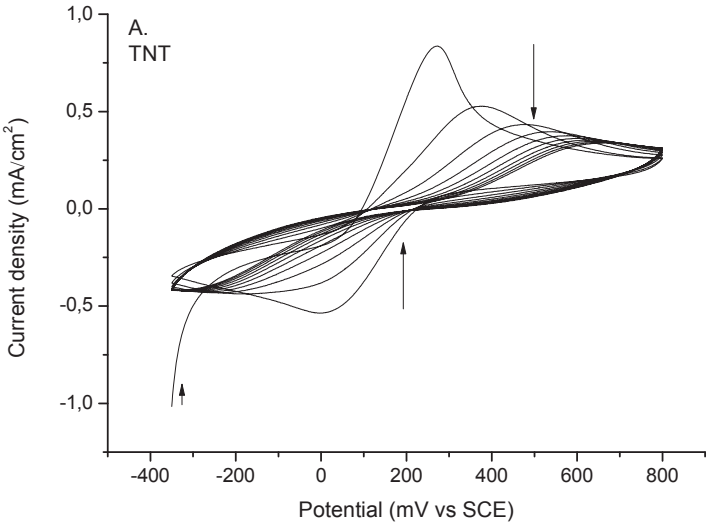

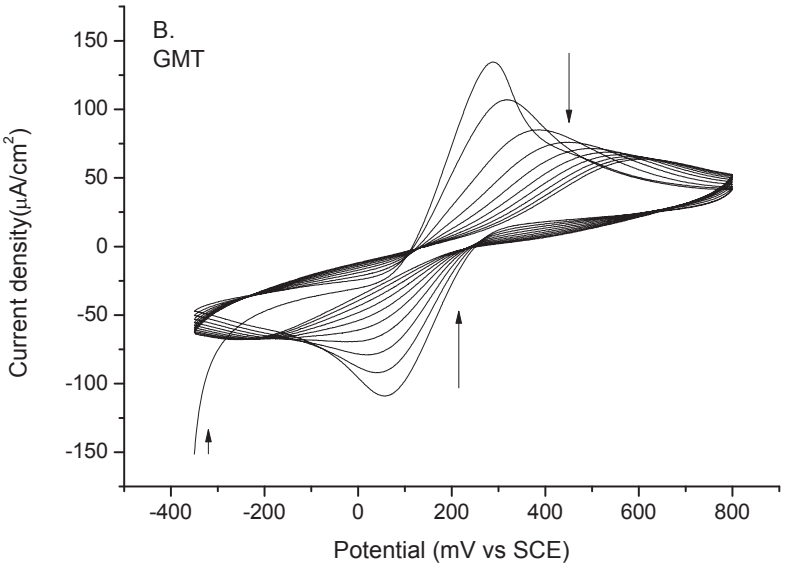
B.
GMT
Current density(μA/cm²)
150
100
50
0
-50
-100
-150
-400
-200
0
200
400
600
800
Potential (mV vs SCE)

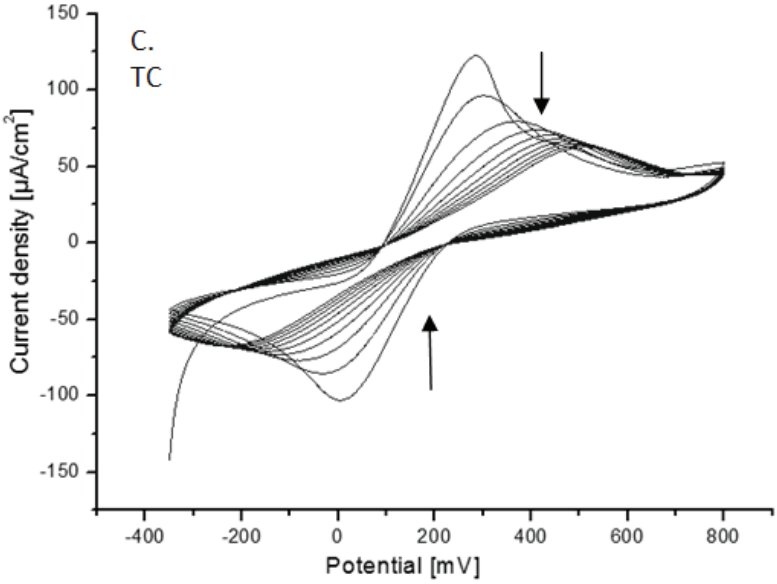
C.
TC
Current density [μA/cm²]
150
100
50
0
-50
-100
-150
-400
-200
0
200
400
600
800
Potential [mV]

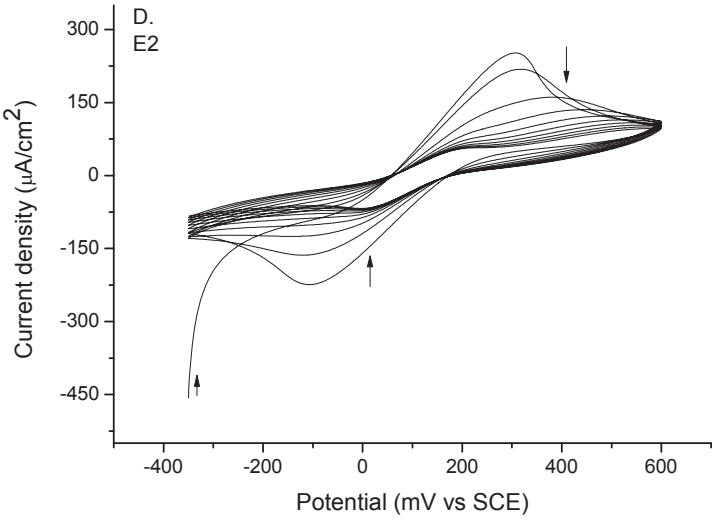

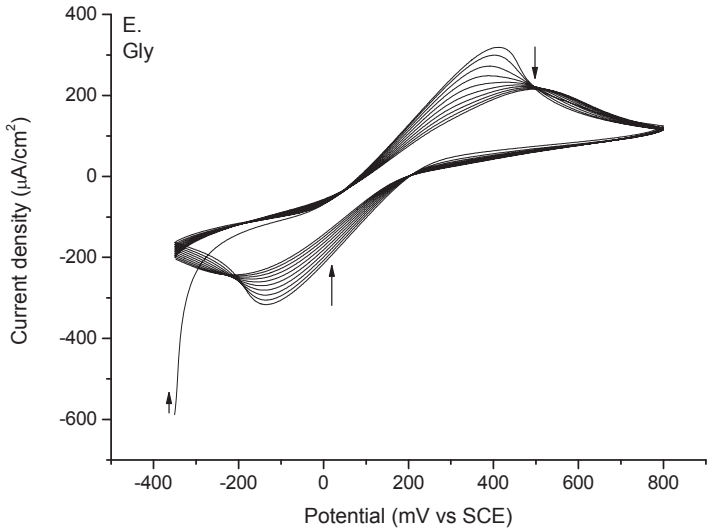

Fig. 23. Monitoring of the electropolymerization of MIP for: (A) TNT, (B) GMT, (C)TC, (D)E2, (E) Gly. CV in 10 mM $[Fe(CN)6]^{3-/4-}$ in PBS pH 7.2 containing 0.1 mg/mL PATP-functionalized Au NPs and 0.1 mg/mL template.

3.3.2. Electrochemical and morphological characterization of MIP and NIP films

After the electropolymerization of MIP and NIP films, their electrochemical behaviour is quite different. Exemplary results are showed for TNT (Fig. 24) and GMT (Fig. 25) .

For the first example (TNT) charge transfer through NIP film is very low, compared to that through MIP. This shows that their morphology should be quite different and that the presence of a template molecule (TNT) could help the charge transfer.

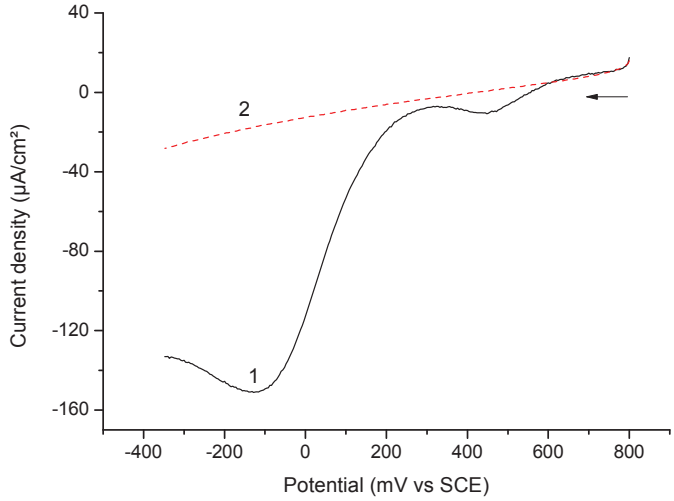

Fig. 24. The MIP (straight line 1) and NIP (dashed line 2) sensors' LSV behavior in the case of TNT, after electropolymerization, in 10 mM $[Fe(CN)6]^{3-/4-}$ in PBS pH 7.2. Potential range: 800 mV to -350 mV. Scan rate 50 mV/s.

Fig. 25 depicts the exemplary electrochemical response of the development of GMT sensors in different steps of the surface modification. For the MIP electrode, a high reduction peak current is obtained after electropolymerization, that is attributed to the presence of template molecules embedded in the polymer matrix, which, through their chemical structure, facilitate the electron transfer of the $[Fe(CN)6]^{-3/-4}$ ion pair at the surface of the electrode. Therefore, after the removal of the template a decrease in the current can be observed. In the contrary, for the NIP electrode, a

compact insulating film is formed in the absence of template molecules, which leads to a dramatically decreased current peak. This indicated that selective cavities, templated by size and shape of gemcitabine were formed in the MIP film.

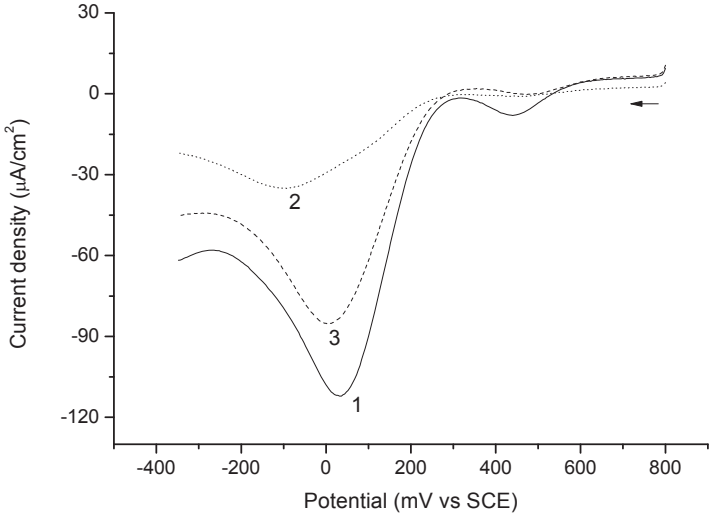

Fig 25. LSV in different steps of the fabrication of imprinted and non-imprinted films fro GMT: after electropolymerization of MIP (straight line 1) and NIP (dot line 2), after extraction of the template from MIP (dash line 3). Potential range: 800 mV to -350 mV. Scan rate 50 mV/s

Fig. 26 shows an example of morphology and phase of the prepared films for the case of TNT, observed by AFM. The obtained images, compared to the bare electrode surface, confirm the electrodeposition of the polymer films onto the electrodes and offer important information about the topography and elastivity modulus of the film surface. The AFM images of the NIP film (c, f) show good coverage of the surface of the electrodes with a homogeneous, compact film. The root mean square (RMS) roughness of the NIP film is found to be 2.2 nm and is very close to that of the bare gold surface (RMS roughness 1.6 nm). For both surfaces, a high homogeneity is observed (close to 4 degrees of phase variation on the observed surface). For the MIP film (b, d) the hybrid polymer film presents a higher RMS roughness of 5.5 nm. A very high phase variation is measured on the observed surface: 24 degrees. This variation is due to the apparent AuNPs, their apparent diameter being around 30 nm, which is larger than that measured with TEM, due to the curvature radii of the silicon tip used. The difference in MIP and NIP morphology is due to the presence of template molecules that totally change the rate of electropolymerization of both films.

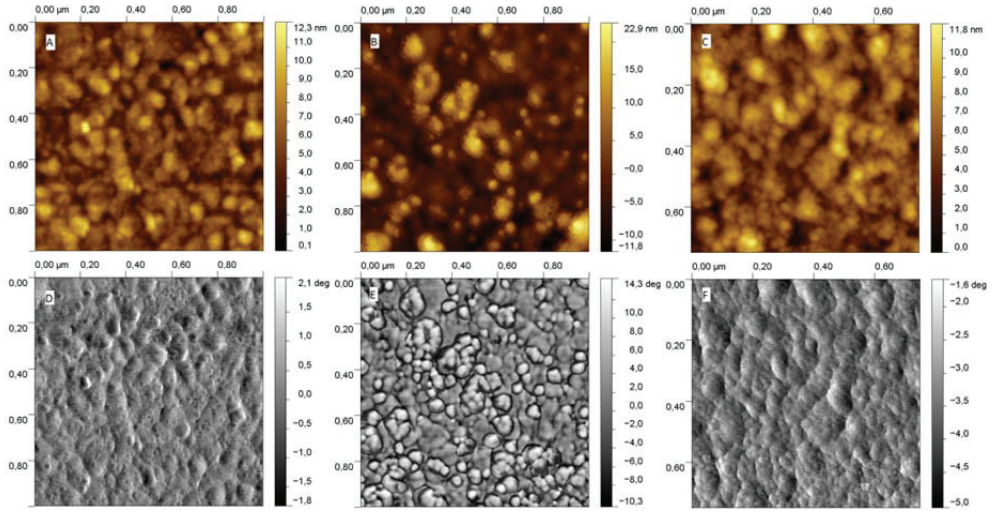

Fig. 26. AFM analysis of bare- (A,D), MIP- (B,E) and NIP- (C,F) electrodes: topography (a, b, c) and phase (d,e, f) 2D images.

3.3.3. Electrochemical behaviour and recognition ability of MIP films towards the target analytes

In order to investigate the uptake process for variable concentrations of template analytes, LSV measurements were employed in a solution of PBS pH 7.2 containing 10 mM $[Fe(CN)_6]^{-3/-4}$. After extraction of template, the prepared MIPs were incubated with solutions of different concentrations of target analytes.

Fig 27A-B illustrates examples of LSV responses of the TNT and E2 imprinted films, respectively, towards the binding of five increasing concentrations of anaytes. Fig 27C-H shows a comparison of LSV responses for imprinted and non-imprinted films towards the binding of various concentrations of TC, GMT and Gly analytes. For MIP films, an increase in the current peak and a shift of the peak potentials to a more positive potential can be observed with the increase of the concentration of analyte, related to the binding of the analyte in the specific cavities. As the concentrations of template molecules in the imprinted film increases, the electron transfer rate increases. The shift of potentials to more positive values shows that the reduction proccess takes place easier when template molecules are embedded in the film. This phenomen can possibly be explained in several ways:

- The rebinding of template molecules in the cavities enables the formation of pathways for the exchange of electrons between the redox mediator and the surface of the electrode, acting as doppants;

- One property of nitroaromatics which may be exploited in detection schemes is their electron accepting capability. Substitution of the electron-withdrawing groups on the aromatic ring lowers the energy of the empty π* orbitals, thereby making these compounds good electron acceptors. Conjugated polymers such as polythioaniline are promising candidates for redox sensing, because they are electron donors [278];

- TC and GMT are also good electron acceptors due to the presence of electron-withdrawing groups, while conjugated polymers such polythioaniline are good electron donors;

- The self-doping of the polythioaniline films in the presence of E2 takes place by oxidation of polythioaniline resulting in formation of cation radicals stabilized by the negative charge on the E2 phenol substituents (weak Bronsted acid, partially deionized in water);

- The presence of glyphosate in the polymeric film increases the electron transfer, due to dopping and swelling effect, the higher concentration of glyphosate in polymer, decreasing polymer resistance and increasing the electron transfer rate [279];

Upon the analysis of NIP films in the same conditions, the current peaks were significantly reduced, due to the fact that after polymerization in the absence of template molecules no cavities were obtained. Therefore NIP failed to recognize the analyte. The current response in the case of NIP is probably due to the adsorption of the analyte on the surface of the polymer.

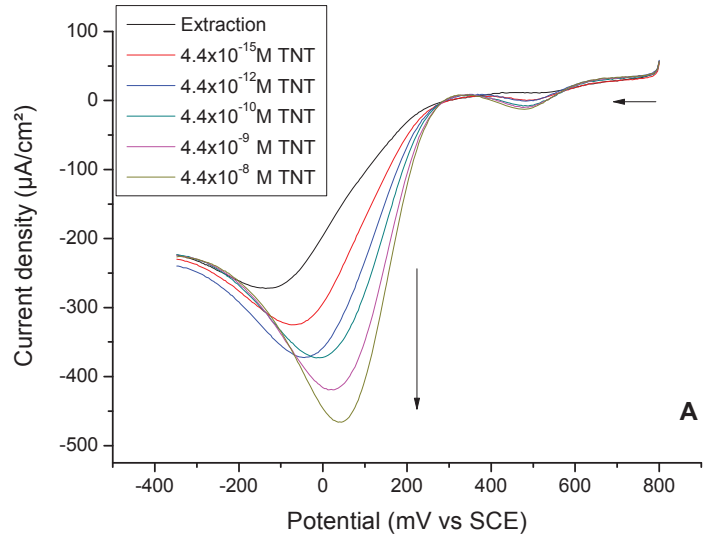
Extraction
4.4x10-15M TNT
4.4x10-12M TNT
4.4x10-10M TNT
4.4x10-9 M TNT
4.4x10-8 M TNT
Current density (μA/cm²)
Potential (mV vs SCE)
A

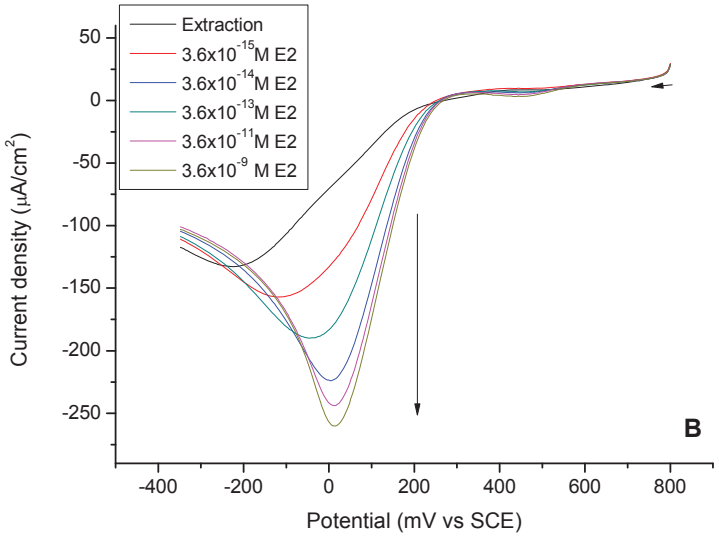
Extraction
3.6x10-15M E2
3.6x10-14M E2
3.6x10-13M E2
3.6x10-11M E2
3.6x10-9 M E2
Current density (μA/cm2)
Potential (mV vs SCE)
B

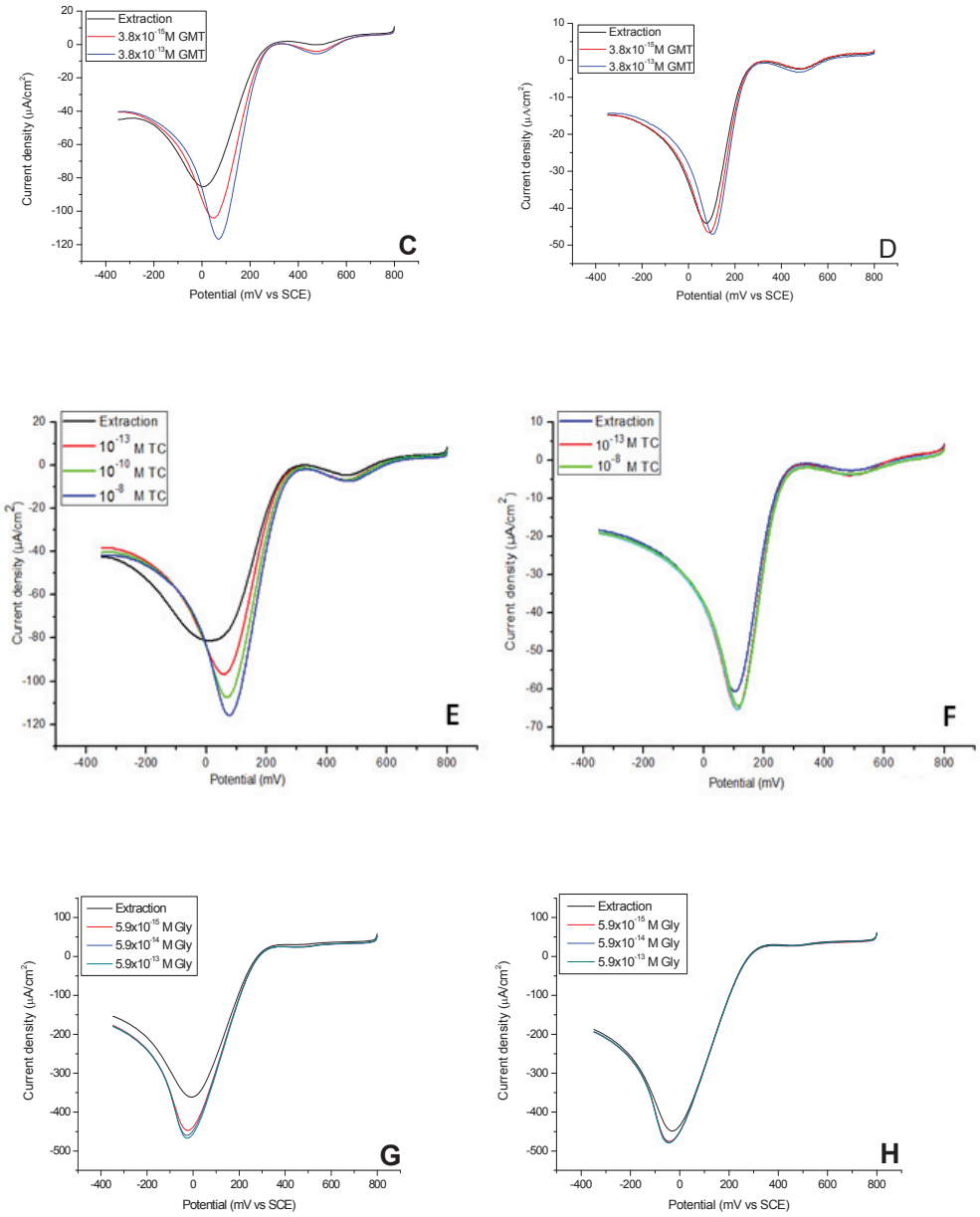

Fig. 27. LSVs after extraction and upon rebinding of various concentrations of template for MIP sensors: A-TNT, B-E2, C-GMT, E-TC, G-Gly) and NIP sensors (D-GMT, F-TC, H-Gly). Potential range: 800 mV to −350 mV vs SCE. Scan rate: 50 mV/s.

3.3.4. Optimization of experimental conditions

3.3.4.1. Optimization of experimental parameters for GMT imprinted sensor

Several parameters, such as composition of the polymerization mixture, pH, extraction and incubation time were optimized for GMT imprintes sensor. Firstly, the effect of different composition of the polymerization mixture was optimized. The concentration of the template was fixed at 0.1 mg/ml, varying just the concentration of AuNPs-monomer. The electropolymerization was thus performed in 10 mM $[Fe(CN)_6]^{-3/-4}$ in PBS pH 7.2 containing a ratio of template:AuNPs-functional monomer of 1:1 and 1:2, respectively, following the protocol described before. After an extraction step, the imprinted film was incubated with different concentrations of gemcitabine in order to investigate the ability of the obtained film to recognize and bind gemcitabine. The best performance of the sensor was obtained for a ratio template:AuNPs-functional monomer of 1:1, the obtained MIP being able to differentiate between increasing concentrations of the analyte (Fig 28).

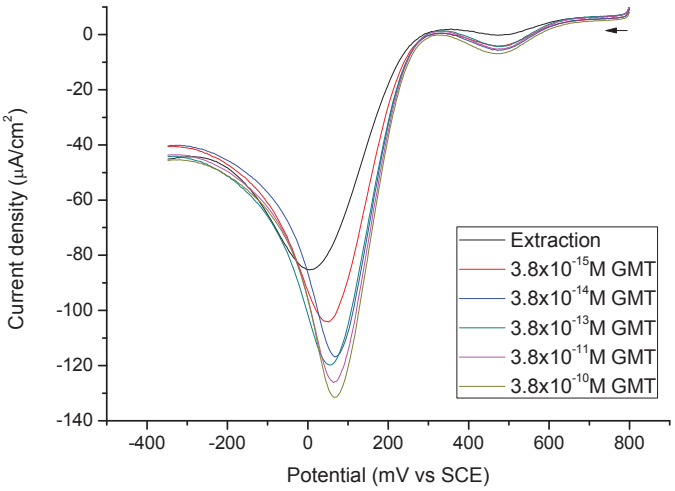

Fig. 28. LSV of MIP obtained with a template:AuNPs-PATP ratio of 1:1 towards different concentrations of gemcitabine

As shown in Fig. 29, for a ratio of 1:2, although a lower signal for extraction was obtained, the resulted film was not able to efficiently differentiate between different concentrations of gemcitabine, therefore a ratio of 1:1 was considered optimum.

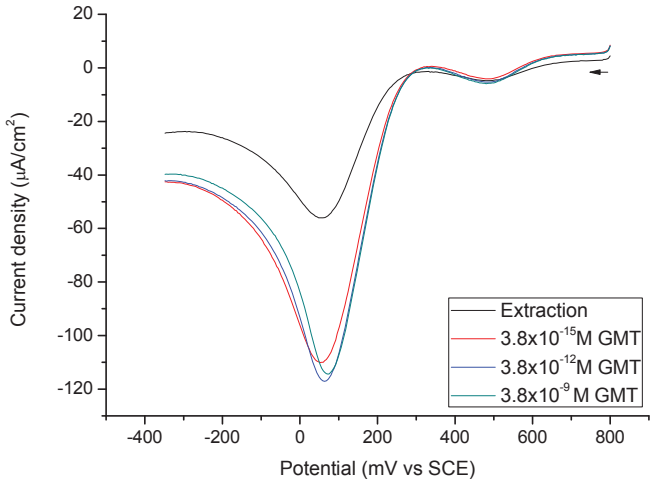

Fig. 29. LSV for MIP obtained with a template: AuNPs-PATP ratio 1:2, towards different concentrations of gemcitabine

Furthermore, for a ratio of 1:1, a template solution 0.1mg/ml was left in contact with the PATP functionalized gold electrode for 2h prior to electropolymerization to promote the assembly of gemcitabine onto the surface of PATP-Au electrode through non-covalent interactions in order to increase the amount of imprited sites [280]. Though, this incubation step lead to poor recognition of gemcitabine (Fig. 30), probably due to the fact that the imprinting sites where formed mostly near the electrode surface making the removal of the template more difficult in this case.

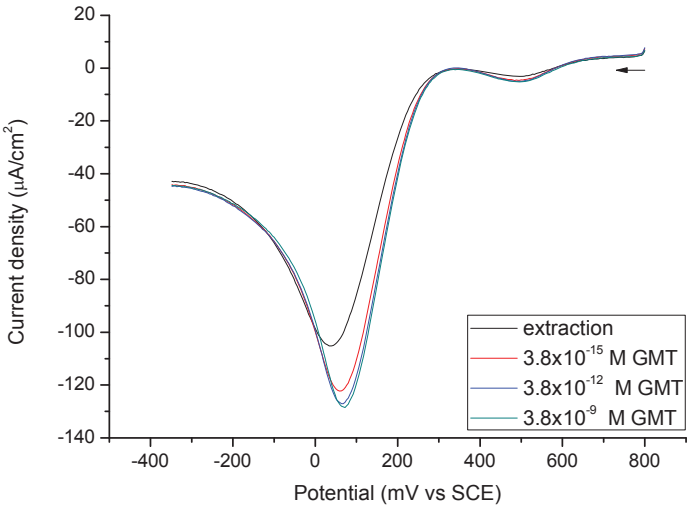

Fig 30. LSV for MIP obtained with an intermediate step of assembly of gemcitabine prior to electropolymerization. Concentration of gemcitabine solution: 0.1 mg/ml; incubation time: 2h; template:monomer ratio 1:1

An important step in obtaining specific recognition cavities is the appropiate extraction of the template molecule from the composite film so that it could rebind GMT. Thus, the pH and extraction time was firstly optimized. The effect of pH on the extraction of GMT was investigated and the modified electrodes were left in contact with washing solutions with various pH (4, 7.2 and 10) for 30 min. Afterwards they were immersed in a solution of GMT 3.8 pM for 30 min and LSV was recorded. The highest increase in the current density respect to the extraction was observed for pH 7.2 (Fig. 31A). Furthermore, the extraction period was optimized, washing the electrodes with PBS pH 7.2 for different times. A decrease of the current was observed from 10 to 30 minutes, due to the removal of GMT molecules which act as electron shuttling units when embedded in the film. After 30 min the response reaches a plateau (Fig. 31B). According to these results pH 7.2 and extraction time 30 min were considered optimum for the removal of GMT from the polymer matrix.

The incubation time is defined as the equilibrium time needed for the uptake of the analyte in the cavities. After extraction for 30 minutes, the electrodes were left in contact with a solution of 3.8 pM GMT for different incubation times. The current density for GMT with respect to extraction increased gradually until 20 min and then remained constant (Fig 31C). Thus, 20 min was selected as incubation time for further experiments.

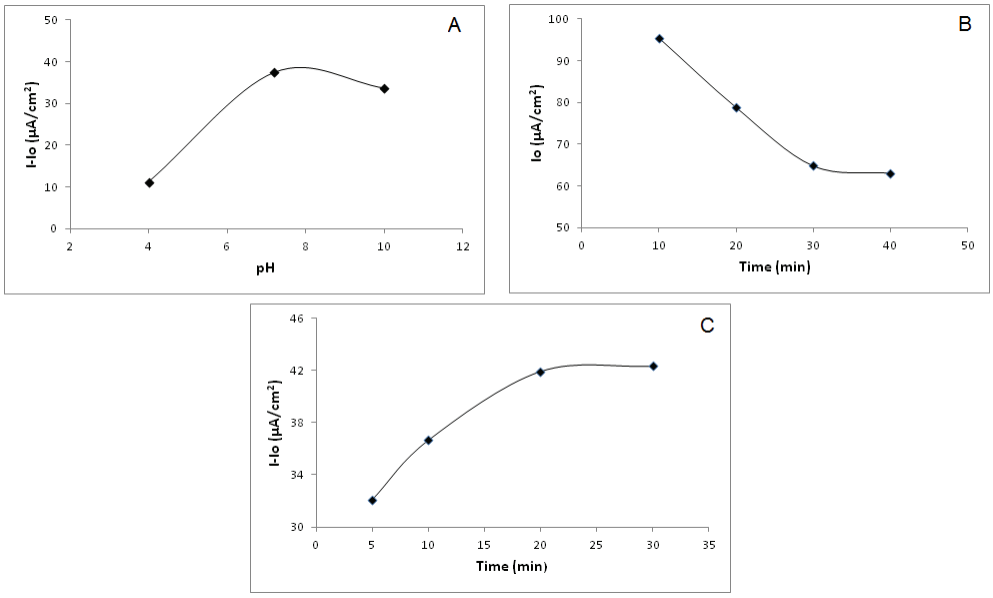

Fig. 31. Optimization of experimental parameters for MIP sensor: pH (A), extraction time (B), incubation time (C).

3.3.4.2. Optimization of experimental parameters for TC imprinted sensor

Several parameters affecting the performance of the TC imprinted sensor, such as, washing conditions and incubation time were investigated. When one parameter was changed, the other parameters were fixed at their optimised values.

In order to get the highest TC recovery, methanol was selected as elution solution since TC is soluble in methanol. A solution of 50 % methanol in PBS was used as washing solution, because after testing this percentage of methanol, the slope of NIP was decreased by a factor 7, compared to that obtained with PBS as washing solution.

The effect of the incubation time with TC from 0 to 60 min was investigated (Fig. 32). The results indicated that the MIP sensor response to TC increased with the increase of the incubation time from 0 to 30 min, and then did not significantly change from 30 to 60 min. In this study, the incubation time of 30 min was chosen.

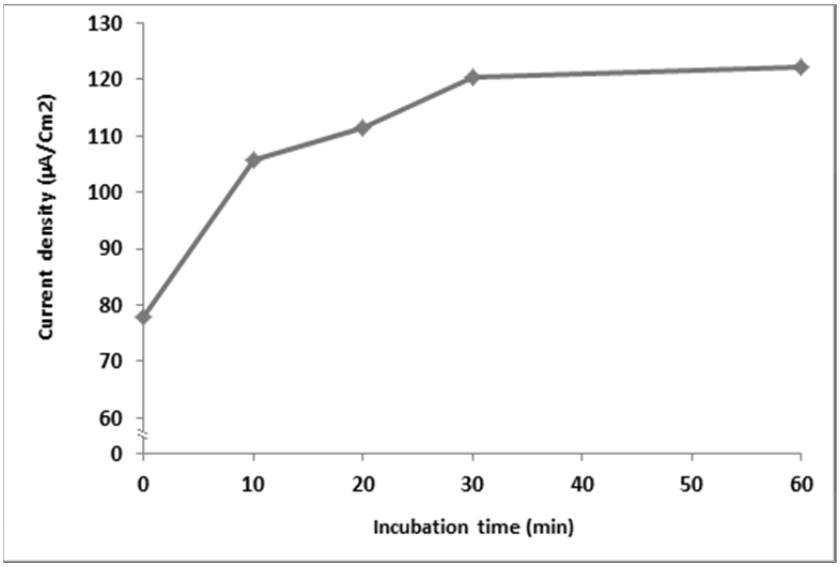

Fig. 32. The effect of the incubation time with tetracyclin on the MIP sensor response

3.3.4.3. Optimization of experimental parameters for Gly imprinted films

The composition of the polymerization mixture for the preparation of Gly was firstly optimized. The electropolymerization was performed in a solution of 10 mM $[Fe(CN)_6]^{3-/4-}$ in PBS pH 7.2 containing various concentrations of functional monomer-AuNPs and template and the results are shown in Table VI. The best performance, in terms of linearity, was obtained when 0.1 mg/ml AuNPs: 0.1 mg/ml template were used, therefore these conditions were used for further experiments.

Table VI. Optimization of the composition of the poymerization mixture

Concentration of template (mg/mL)	Concentration of PATP-AuNPs (mg/mL)	Linearity R^2
0.1	0.2	0.8792
0.5	0.2	0.6107
0.1	0.1	0.9925

To further improve the performance of the sensor, methanol solvent was added to the electropolymerization solution as a porogenic in different amounts and the ratio

between the slope of MIP films and NIP films was evaluated. Methanol solvent was added as a porogenous solvent and to enhance the solubility of the functionalized AuNPs. As showed in Table VII the highest sensitivity was obtained for a PBS solution containing 20% methanol, which displayed the highest slope ratio. Increasing the amount of methanol lead to a lower ratio slope MIP/slope NIP (1.84), decreasing therefore the selectivityof MIP towards glyphosate.

Table VII. Optimization of methanol amount in the electropolymerization solution

Amount of methanol % (v/v)	Slope MIP/Slope NIP
0	2.25
20	3.64
40	1.84

An incubation step with the template molecules prior to electropolymerization is often reported in literature, in order to promote the formation of noncovalent interactions between the monomer and the template [281, 282, 283]. In order to test if introducing this step would result in a better performance of the sensor, we have left the PATP functionalised gold electrode in contact with a solution of glyphosate 0.1 mg/ml for 5 hours. No improvement in the sensitivity (the slope) of MIP sensor was observed in this case, therefore the electropolymerization was carried out directly after functionalization of the electrodes with PATP.

In order to optimize the incubation time MIP and NIP sensors were left in contact with a solution of 59 pM glyphosate for various times and LSV were recorded and compared. The peak current increased substantially with increasing time for the first 10 minutes for both MIP and NIP. A slower increase occured afterwards, reaching a steady state at 45 min, after the adsorbed molecules in the cavities reached saturation (Fig. 33). Although the difference between the peak current of MIP respect to NIP was slightly higher for 30 minutes, when we made a calibration curve in the range of 5.9 fM to 5.9 nM with 30 minutes incubation time, we obtained a lower ratio slope MIP/slope NIP (1.39). Therefore the accumulation time was set to 20 min, when the highest slope was obtained for the calibration curves.

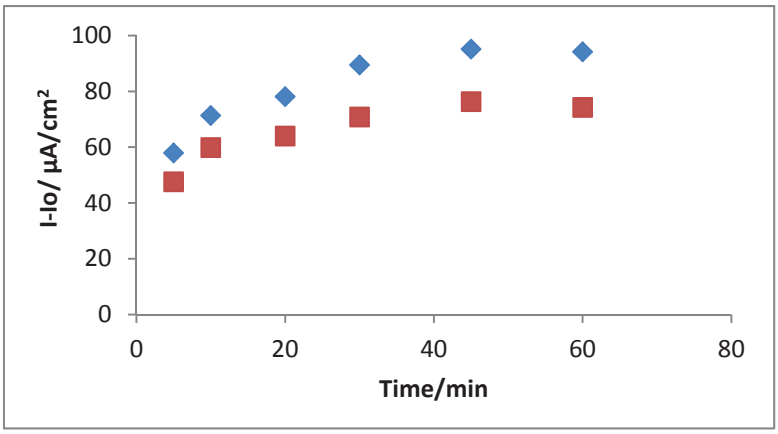

Fig. 33. Optimization of the incubation time with glyphosate; MIP (♦) and NIP (■) films were tested by LSV for a concentration of glyphosate 59 fM.

3.3.5. Analytical performance of the imprinted and non-imprinted polymer

The fabricated sensors were applied for the detection of various concentrations of target analytes in buffered solutions. A linear relationship between the signal-blank/signal ratio ($I-I_0/I_0$) and the logarithmic concentration of the analytes was obtained in each case (Fig. 34). Data points were calculated as the average of three different electrodes The limit of detection was calculated by interpolating the mean current obtained for the blank for three replicates plus three times its standard deviation in the linear equation. Blank is the signal obtained after extraction of the template, upon analysis of a solution containing 10 mM $[Fe(CN)_6]^{-3/-4}$ in PBS pH 7.2 that does not contain any anaylte. A linear range from fM to nM and a low limit of detection in the fM range was obtained for the MIP sensors. The linear equation, linear range and detection limits are presented in table VIII. Compared to MIP the response currents of NIP did not change significantly with the concentrations change, demonstrating the succesful formation of imprintig cavities in MIP films.

Selectivity is an important feature of MIP sensors. The selectivity of the developed sensors was assesed towards the binding of other compounds with similar structures with the templates: 2,4-dinitrotoluene (DNT) for TNT, doxycyline for TC, testosterone for estradiol and AMPA for glyphosate. Solutions of the aboved-metioned compounds were left to incubate with the MIP electrodes, followed by LSV measurements, as previously described. The response of the MIP sensors towards their binding is also illustrated in Fig 33. Low peak currents, similar to NIP, were obtained in this case prooving excelent selectivity of the developed sensors.

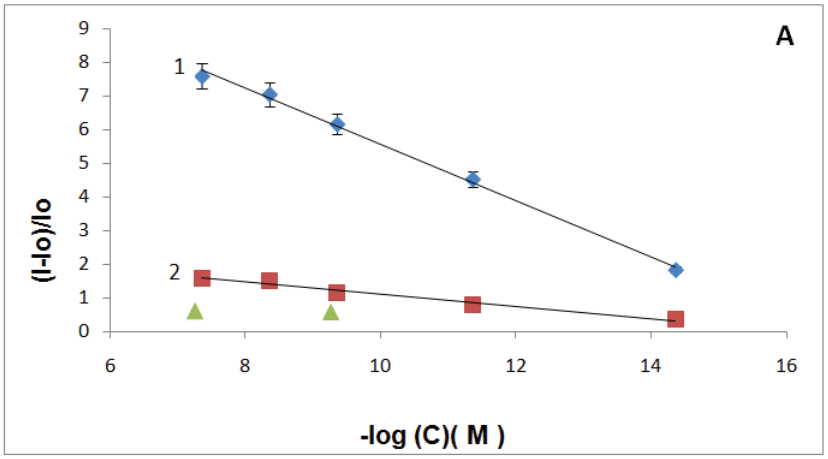
A
1
2
(I-Io)/Io
-log (C)(M)
9
8
7
6
5
4
3
2
1
0
6
8
10
12
14
16

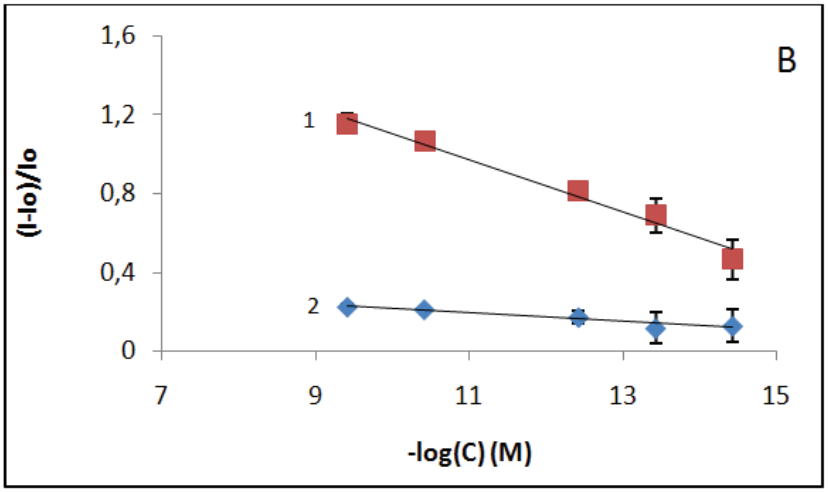
B
1
2
(I-Io)/Io
-log(C) (M)
1,6
1,2
0,8
0,4
0
7
9
11
13
15

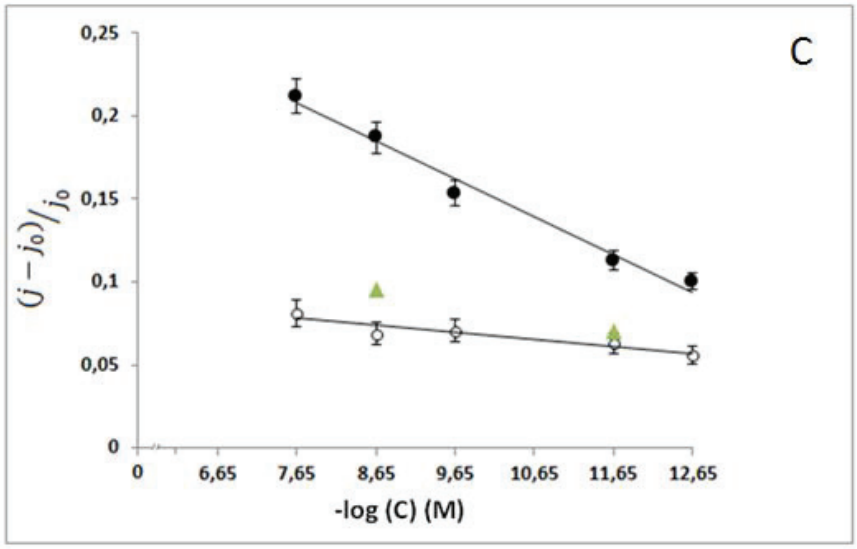
C
0,25
0,2
0,15
0,1
0,05
0
$(j-j_0)/j_0$
0
6,65
7,65
8,65
9,65
10,65
11,65
12,65
-log (C) (M)

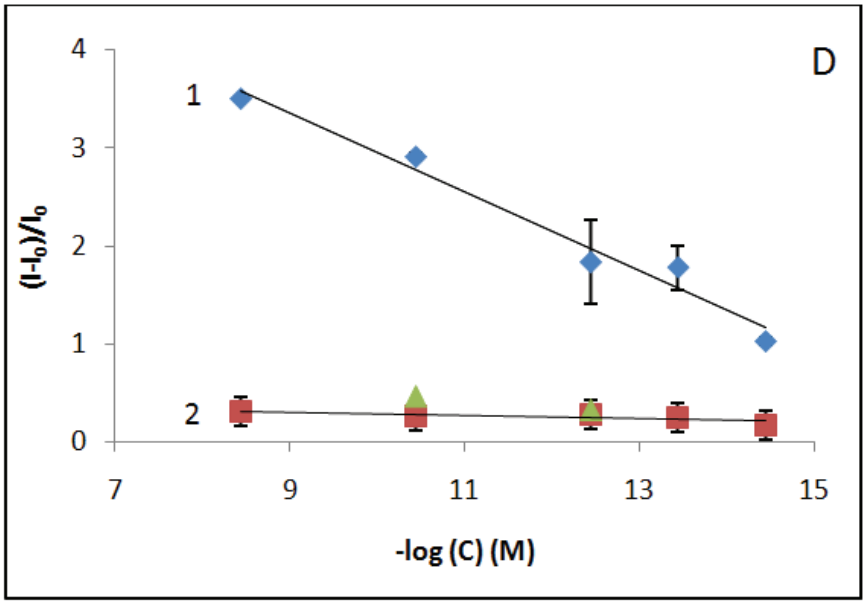
D
4
3
2
1
0
$(I-I_0)/I_0$
1
2
7
9
11
13
15
-log (C) (M)

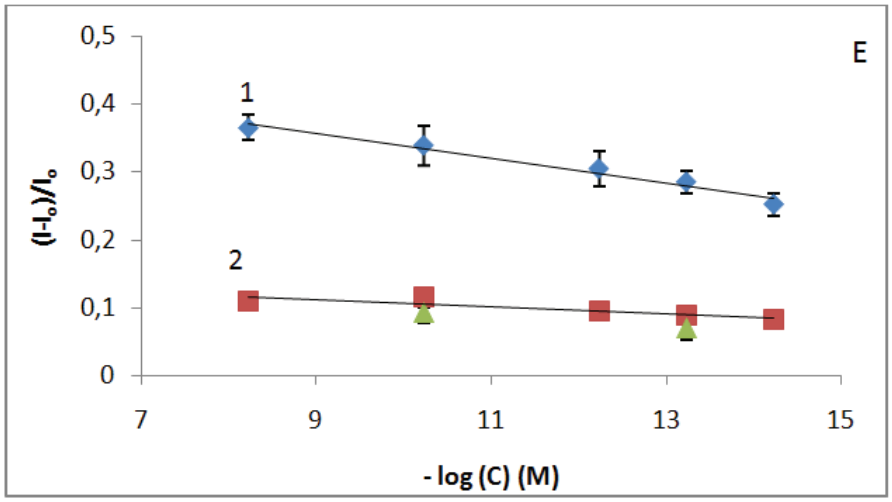

Fig 34. Calibration curves upon analysis of various concentrations of target analytes on MIP-modified sensor (lines 1), NIP-modified sensor (lines 2). Selectivity of MIP sensors upon analysis of different interferents, as metioned in section 3.3.5 (▲)

Table VIII. Analytical performance of MIP sensors

Template	MIP slope	MIP R^2	NIP slope	NIP R^2	Linear range	LOD (fM)	LOQ (fM)
TNT	0.835	0.976	0.182	0.997	4.4 fM-44 nM	0.044	4.4
GMT	0.133	0.980	0.022	0.915	3.8 fM-38 nM	0.003	3.8
TC	0.022	0.982	0.004	0.885	0.2 fM-2.2 nM	0.224	0.2
E2	0.403	0.972	0.016	0.650	3.6 fM-3.6 nM	0.036	3.6
Gly	0.018	0.971	0.005	0.802	5.9 fM-5.9 nM	$5.9x10^{-6}$	5.9

The proposed sensors showed better analytical performances in terms of sensitivities compared to previously reported methods, as shown in Table IX. A wider linear range and a lower LOD is obtained for our sensors, that can be explained by the use of gold nanoparticles that increase the conductivity of the film, as well as the number of imprinted sites and the use of a redox probe.

Table IX. Comparison of different methods reported for the detection of the assayed targets

Analyte	Method	LOD	Linear range	Ref
TNT	MIP sensor based on AuNPs-PATP	200 pM	2.02-629.59 nM	33
	Phone-based portable device based on impedance	70.9 µM	1 µM-1mM	284
	Label free surface enhaced Raman spectroscopy	22.7 nM	0.1 -100 nM	285
	CV on glassy carbon electrode modified with AuNPS/poly (*o*phenylenediamine –aniline film)	2.1 mM	0.25-40 mM	286
GMT	DPV on glassy carbon electrode	0.86 µM	1.05-658.74 µM	287
	DPV on gold electrode	0.05 µM	0.08-13.17 µM	288
	HPLC	20 nM	2-200 µM	289
	HPLC-MS	0.33 nM	0.06 µM – 20.02 mM	290
	LC-MSMS	0.66 nM	6.67 nM – 6.67 µM	291
TC	Colorimetric aptasensor	226 pM	0.3-10 nM	292
	iPhone-based digital image colorimeter	1.03 µM	1.03-20.79 µM	293

	Colorimetric competitive assay based aptasenor	0.2 nM	0.2 nM – 2.07 μM	294
E2	Label-free aptasensor based on vanadium disulfide nanoflowers and AuNPs	1 pM	0.01 - 10 pM	295
	MIP sensor based on AuNPs	4.69 fM	3.67 fM – 0.36 μM	255
	MIP sensor based on PdNPs	0.16 nM	0.3 nM - 0.5 μM	256
Gly	Nanofiber based colorimetric sensor	0.59 μM	0.59 –2956.83 μM	296
	Fluorescence sensor based on DNA/magnetic particles	0.27 nM	1–10000 nM	297
	Prism coupling hollow-core metal-cladded waveguide sensor	1.4 nM	0.0–5.0 nM	298
	AuNPs/MIP electrochemical sensor	2.06 nM	22.95-1037 nM and 3.17-23.30 nM	299
	Luminescent lanthanide MIP sensor	0.59 μM	53.22 nM –590 μM	300

3.3.6. Analyses of real samples

In order to assess the suitability of the developed sensor for the detection of the target analytes in complex matrixes, different samples were analyzed using the protocol previously described. For the environment contaminants TNT, E2 and Gly tap and river water samples were analyzed with the proposed sensors. The samples did not originally contain any analyte, thus they were spiked with the analyte at certain known concentrations.

Serum samples were analyzed in order to check the suitability of MIP films for the detection of GMT in biological fluids, for therapy monitoring. In addition, the GMT imprinted films were also tested for the quantification of GMT in drug formulations. For the analysis of serum samples, comercially available serum was first diluted 1: 100 and filtered through a celulose membrane (Millex-GV, 0.22 μM). The samples were then spiked with various concentrations of GMT and analyzed according to the procedure previously described The results show a strong influence of the matrix on the response of the chemosensor (Fig 35).

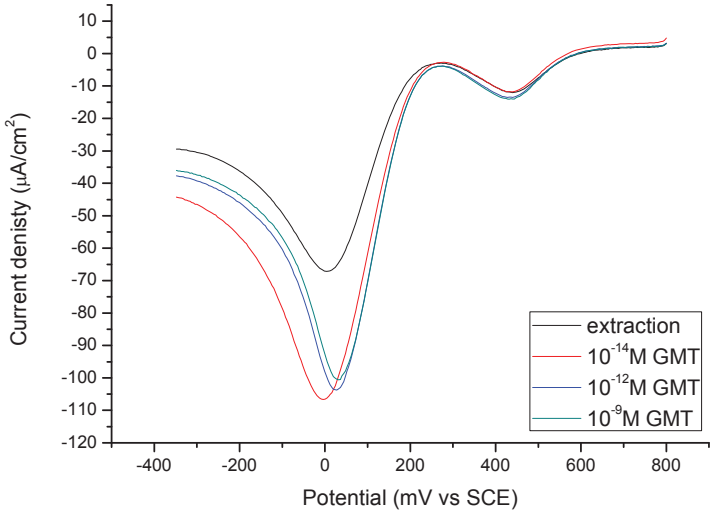

Fig. 35. Analysis of GMT in spiked serum samples; serum dilution with PBS 1:100.

For the detection of GMT in a pharmaceutical formulation, Gemcitabine TEVA 1000 mg, powder for perfusable solution, was assayed with the developed sensor. After reconstitution of the powder in water according to the labelling, the

concentration of GMT in the solution was 38 mg/ml, hence a dilution was made to reach the linear range of the sensor, to 10^{-12} mg/ml GMT. The standard addition method was used, when standard solutions of GMT were added to this solution to reach the concentrations of 10^{-14}, 10^{-12}, 10^{-10} mg/ml. The concentration of GMT found after the analysis with the proposed sensor was 36.89 mg/ml, with an RSD of 1.34%.

Honey samples were analyzed to assess the practical applications of MIP films for the detection of TC in food samples. Honey solutions were prepared as follows: 1 g of honey was added to 1 mL of ethanol and maintained in an ultrasonic bath for 30 min. In order to reduce the matrix effect the samples were then diluted 1/10 (v/v) with PBS and filtered through a 0.8 μm cellulose acetate filter. The samples were then spiked with standard TC solution and measurement were carried out as previously described.

Table X summarizes the results obtained for the application of MIP sensors in real spiked samples. Good recoveries were obtained in all cases, between 96.4% and 106.0%, with good reproducibility (RSD% between 1 and 10), showing that the proposed method is suitable for the analysis of target molecules in complex matrixes, with future perspectives for environmental, biomedical and food safety applications.

Table X. Determination of target analytes by MIP sensors in complex matrices

Analyte	Sample	Added -log (C)/ M	Found -log (C)/ M	Recovery (%)	RSD (n=3)
TNT	Tap water 1	15	15.2	101.3	1
	Tap water 2	12	11.6	96.7	2
	Tap water 3	9	9.2	102.2	2
	River water 1	15	15.0	100.2	10
	River water 2	12	12.0	100.2	3
GMT	Serum 1	14	14.2	101.4	2

	Serum 2	12	11.5	96.4	6
	Serum 3	10	10.2	102.0	3
TC	Honey 1	8.6	8.8	101.8	8
	Honey 2	11.6	12.3	106.0	6
Gly	Tap water 1	13.2	13.6	102.6	4
	Tap water 2	8.2	8.1	98.7	3

3.3.7. Reproducibility and reusability of the imprinted sensor

The fabrication reproducibility was investigated with three different modified electrodes, which were constructed independently with the same procedure. LSV studies were performed on each electrode as previously described towards the binding of one concentration of analyte. The precision of the described procedure was evaluated in terms of RSD%. The obtained results are presented in Table XI. RSD% values were around 6 % indicating a good reproducibility of the fabrication method.

The possibility to reuse the same sensor is an important advantage of MIP-based sensor. To verify the reusability of the GMT imprinted sensor was investigated as an example. For this purpose, several cycles of extraction and incubation with a solution of 3.8 pM GMT were performed on the same electrode. The sensor preserved its response for three cycles with a good reproducibility (RSD 5.5%).

Tabel XI. Reproducibility of the proposed sensors

Analyte	Concentration	RSD % (n=3)
TNT	3.6 pM	6.9
GMT	3.8 pM	6.6
TC	0.2 pM	6.3
E2	36 pM	6.4
Gly	59 fM	6.9

3.3.8. Stability studies

As an example, the stability of the GMT imprinted sensor was examined by measuring the LSV current of 3.8 pM GMT after storing the electrode at 4°C for three days. The sensor retained 61% of the original current if stored in dry state and 105% if kept in PBS. Thus we preferred to prepare a new sensor each time.

3.4. Conclusions

We presented a generic protocol for the development of electrochemical chemosensors based on MIP-based polymer/AuNPs hybrid membrane that can be applied to a broad range of molecules, electroactive and non-electroactive, and for a multisensory platform.

The MIP was prepared on the surface of PATP functionalized gold electrodes by electropolymerization of PATP-functionalized AuNPs in the presence of template molecules. Hexacyanoferrate/hexacyanoferrite was used as redox probe and the permeability of the film towards the redox probe was investigated. This approach allows also the detection of non-electroactive targets.

We applied the proposed method for the detection of several compounds of environmental, biomedical and food safety interest.

The method was firstly applied for the detection of TNT. Compared to the detection of TNT through its own reduction peak [235], the detection through the increase of the electron transfer rate of a redox probe allows the decrease of the LOD by a factor of 10^7. The change of film permeability is due its change of structure in presence of a very low concentration of TNT target molecule compared to that of the amperometric detection of TNT. Furthermore, we reduced the amount of functionalized gold nanoparticles and template, which makes the preparation process presented herein more economical and we assessed the feasibility of the sensor on water sample analysis.

The method was then optimized and applied for the detection of other aromatic compounds - gemcitabine, tetracycline, estradiol - as well as molecules with linear structure – glyphosate.

It is worth mentioning that this is the first time that a MIP sensor for the detection of tetracycline in honey and for gemcitabine in serum and drug formulations is described in the literature.

The easy fabrication and robustness of molecularly imprinted films make them ideal candidates for the development of sensing devices. The optimum conditions for the best performance of the sensors have been optimized, three successive steps

being necessary: extraction (30 min), incubation step (from 20 min to 1 h), washing step (5 min), measurement for less than 1 min. Although the proposed protocol is generic and can be applied for a wide range of molecules, it should be adapted for each target. Some experimental conditions such as incubation and extraction time, extraction solution and porogenic solvent should be optimized each time depending on target analyte, its structure, solubility and interactions with the polymer. The method seems to be more sensitive towards the detection of aromatic compounds respect to aliphatic ones, especially the ones with more electron withdrawing groups, which are electron-poor and can promote better interactions with electron-rich PATP.

The presence of AuNPs in the polymer matrix increases the conductivity of the film, the numer of binding sites and the fast equilibration with the analytes.

The developed sensors showed a wide linear range from fM to nM with low limits of detection and limits of quantification in fM range, lower than that reported for other sensors .

The reproducibility of the fabrication method was also investigated and RSD% values around 6-7% were obtained for the five developed sensors, proving a good sensor-to-sensor reproducibility.

With good sensitivity, selectivity and reproducibility, the hybrid sensors were shown to have the potential to be effective methods for the electrochemical detection of the analytes in complex matrices. The feasibility of their practical applications has been demonstrated in tap and river water, honey, biological fluids and drug formulations proving a great potential for environmental protection, food safety, biomedical and pharmaceutical analysis.

4. General conclusions

The aim of this study was to develop electrochemical affinity sensors based on various recognition receptors with practical applicability in environment protection, food safety and biomedical field.

To develop the sensors we investigated different binding receptors: biological elements, such as antibodies and aptamers, as well as synthetic receptors fabricated using the molecularly imprinted technique. Different nanomaterials were integrated in the developed sensors as immobilization platforms and for the enhancement of the sensitivity.

Different techniques were used to attach biorecognition elements at the surface of the transducers. Nanomaterials, such as magnetic nanoparticles modified with protein G or streptavidin and gold nanoparticles, were used to immobilize antibodies and biotinylated or thiolated aptamers. Molecularly imprinted films were deposited directly at the surface of the transducers via electropolymerization.

One objective of the work herein was the development of disposable immunosensors and aptasensors for the diagnosis of cancer. MUC1 tumor marker was selected as model molecule. A magnetic beads/antibody-based sensor and two aptamer-based sensors based on magnetic beads and gold nanoparticles immobilization platforms, were succesfully developed for the detection of MUC1.

In the first approach antibodies were used to capture the target molecule in a sandwich assay. MUC1 specific antibodies were immobilized on Protein G-magnetic beads. A secondary antibody was added to capture MUC1 target in a sandwich format and a third antibody labelled with AP was used to obtain the DPV signal. Although a high sensitivity was obtained (3.5 ng/mL) the selectivity of the proposed sensor was low when tested in the presence of similar target molecules MUC4 and MUC16. To further increase the specificity, the antibodies were replaced with aptamers, which are able to discriminate between closely related targets. Biotinylated aptamers were linked to streptavidin-magnetic beads to capture MUC1. Secondary biotinylated aptamers were added, which were labelled with streptavidin-AP. The aptasensor exhibited good selectivity and sensitivity (1.4 ng/mL). The feasibility of the aptasensor for clinical use was further demonstrated by the analysis of MUC1 protein in non-pathological and pathological serum samples, offering a promising tool in biomedical applications.

Furthermore, a simple, label free aptasensor was developed for the detection of MUC1. Thiolated aptamers specific for MUC1 were self-assembled on gold nanoparticles electrodeposited on graphite screen-printed electrodes and electrochemical impedance spectroscopy was employed to assess the aptamer-MUC1

interaction. An increase of the charge transfer resistance was observed after immobilization of aptamers and proteins to the sensor surface. A LOD of 3.6 ng/mL was obtained in this case.

A main objective of this work was the development of a generic protocol for the fabrication of molecularly imprinted sensors that can by applied for the detection of environmental pollutants, food contaminants and compounds of biomedical interest.

Sensitive and selective MIP based sensors were fabricated based on electropolymerization of *p*-aminothiophenol functionalized gold nanoparticles on gold electrodes in the presence of various template molecules. Trinitrotoluene, gemcitabine, tetracycline, estradiol and glyphosate were investigated as template molecules.

The electropolymerization was performed by cyclic voltammetry and the performance of the sensors was investigated by linear sweep voltammetry. A solution of hexacyanoferrite/hexacyanoferrate was used as redox mediator, making the method applicable for a broad range of molecules, including non-electroactive ones. The influence of several experimental parameters on the performance of the sensors was investigated and optimized. Although some experimental conditions such as concentrations of monomer and template and the ratio monomer:template were maintained constant, other parameters such as porogenic solvent, incubation and extraction time, extraction solvent had to be optimized for each template, depending on the structure of the template and its interaction with the polymer. Under optimized conditions, wide linear ranges and low detection limits were obtained with the developed MIP-sensors. Selectivity studies were also performed towards the binding of compounds with similar chemical structures and the proposed sensors exhibited good selectivity. Furthermore, the proposed sensor have been successfully applied for the detection of above mentioned target analytes in complex matrices (tap and river water, hney, serum, drug formulations) with good recoveries and high accuracy.

The affinity sensors developed in this work are simple to fabricate, easy to operate, sensitive and selective, with potential practical applications on real samples.

5. Originality of the thesis

The originality of the thesis consists in the development of a generic protocol for the fabrication of molecularly imprinted polymer-based electrochemical sensors applicable to a broad range of molecules, including non-electractive species. The sensitive films were prepared directly on the surface of the electrodes by electropolymerization of *p*-aminothiophenol-functionalized gold nanoparticles in the presence of template molecules. Hexacyanoferrate/hexacyanoferrite was used as redox mediator and the modifications that occur in the structure of the polymer matrix in the presence of small amounts of analytes are investigated. The use of gold nanoparticles ensures high sensitivity and fast equilibration with the analyte. The method is economical, making use of small amounts of reagents, fast and can be applied for the detection of target molecules in complex matrices. Moreover, it is the first time electrochemical molecularly imprinted sensors were applied for the detection of tetracycline in honey and of gemcitabine in drug formulations and serum samples.

Another element of novelty is that, to our knowledge an assay based on aptamer-modified magnetic beads and screen printed microarray for the detection of Mucin 1 tumor biomarker has not been previously reported in the literature. The coupling of aptamers with magnetic beads offers the advantage of the detection of the protein in complex matrices, due to the fact that aptamers as synthetic molecules are more specific and less influenced by the matrix effect and the use of magnetic beads improves the washing steps reducing the matrix effect. The aptasensors was tested on real serum samples from cancer patients, showing great potential for future clinical application in early stage cancer diagnosis.

REFERENCES

1. Eggins B.R, Chemical sensors and biosensors, John Wiley & sons, West Sussex, England, 2002
2. Fouletier J, Fabry P. Chemical and biological microsensors application in liquid media. Wiley, 2013
3. Leech D. Affinity biosensors. Chemical Society Reviews. 1994;23(3):205-213
4. Turner A.P.F. Biosensors: sense and sensibility. Chemical Society Reviews. 2013;42:3184
5. Ronkainen N.J, Halsall H.B, Heineman W.R. Electrochemical biosensors. Chemical Society Reviews. 2010:39;1747-1763
6. Subrahmanyam S, Piletsky S.A, Turner A.P.F. Application of natural receptors in sensors and assays. Analytical chemistry. 2002;74:3942-3951
7. Wang J. Glucose biosensors: 40 years of advances and challenges. Electroanalysis. 2001;13:983-988
8. Uygun Z.O, Uygun Ertugrul H.D. A short footnote: Circuit design for faradaic impedimetric sensors and biosensors. Sensors and Actuators B. 2014;202:448-453
9. Chukkasat K, Kanatharana P, Limbut W, Numnuam A, Thavarungkul P. Ultra trace analysis of small molecule by label-free impedimetric immunosensor using multilayer modified electrode. Biosensors and Bioelectronics. 2011;26(11):4571-4578
10. Ertugrul H.D, Uygun Z.O. Impedimetric biosensors for label-free and enzymless detection, in: Rinken Toonika (Ed.), State of the arts in Biosensors, Intech, Rjeka, 2013, pp. 179-196
11. Ronkainen-Matsuno N.J, Thomas J.H, Halsall H.B, Heineman W.R. Electrochemical immunoassay moving into the fast lane. TrAC Trends in Analytical Chemistry. 2002;21(4):213-226
12. Dedik J, Janovcova M, Dejmkova H, Barek J, Peckova K. Utilization of Unmodified Screen-Printed Carbon Electrodes in Electroanalysis of Organic Compounds (An Overview), Sensing in Electroanalysis, Vol. 6 (K. Kalcher, R. Metelka, I. Švancara, K. Vyt_as; Eds.), pp. 129-138. 2011 University Press Centre, Pardubice, Czech Republic.
13. Zourob M, Recognition receptors in Biosensors, Chapter 2: Surface Sensitization Techniques and Recognition Receptors Immobilization on Biosensors and Microarrays by Vincent Dugas, Abdelhamid Elaissari, and Yves Chevalier, Springer New York 2010, pag 47
14. Gubala V, Harris L.F, Ricco A.J, Tan M.X, Williams D.E. Point of care diagnostic: status and future. Analytical chemistry. 2012;84:487-515.
15. Phuong D.T, Cao X.T. Label-free electrochemical immunosensor based on cerium oxide nanowires for *Vibrio cholerae* O1 detection. Materials Science and Engeneering C, 2016; 58:953-959
16. Zhu Z, Shi L, Feng H, Zhou S. Single domain antibody coated gold nanoparticles as enhancer for *Clostridium difficile* toxin detection by electrochemical impedance immunosensors. Bioelectrochemistry. 2015;101:153-158

17. Rafique S, Bin W, Bhatti A.S. Electrochemical immunosensor for prostate-specific antigens using a label-free second antibody based on silica nanoparticles and polymer brush. Bioelectrochemistry. 2015;101:75-83
18. González-Techera A, Zon M.A, Molina P.G, Fernández H, González-Sapienza G, Arévalo F.H. Development of a highly sensitive noncompetitive electrochemical immunosensor for the detection of atrazine by phage anti-immunocomplex assay. Biosensors and Bioelectronics. 2015;64:650-656
19. Martini E, Merola G, Tomassetti M, Campanella L. Agent orange herbicides, organophosphate and triazinic pesticides analysis in olive oil and industrial oil mill waste effluents using new organic phase immunosensors. Food Chemistry. 2015;169:358-365
20. Zamfir L-G, Geana I, Bourigua S, Rotariu L, Bala C, Errachid A, Jaffrezic-Renault N. Highly sensitive label-free immunosensor for ochratoxin A based on functionalized magnetic nanoparticles and EIS/SPR detection. Sensors and Actuators B: Chemical. 2011;159(1):178-184
21. Karaseva N.A, Ermolaeva T.N. Piezoelectric immunosensors for the detection of individual antibiotics and the total content of penicillin antibiotics in foodstuffs. Talanta. 2014;120:312-317
22. Darwish I.A, Wani T.A, Alanazi A.M, Hamidaddin M.A, Zargar S. Kinetic-exclusion analysis-based immunosensors versus enzyme-linked immunosorbent assays for measurement of cancer markers in biological specimens. Talanta. 2013;111:13–19
23. Luppa P.B, Sokoll L.J, Chan D.V. Immunosensors – principles and applications to clinical chemistry. Clinica Chimica Acta. 2001;314: 1-26
24. Fowler J.M, Wong D.K.Y, Halsall H.B, Heineman W.R, Recent developments in electrochemical immunoassays and immunosensors, Chapter 5 in Electrochemical sensors, biosensors and their biomedical applications, Academic press, 2008, Pages 115–143
25. Zhang X, Ju H, Wang J, Electrochemical Sensors, Biosensors and their Biomedical Applications, Elsevier, 2008, 237-260
26. Bahadir E.B, Sezginturk M.K. Applications of electrochemical immunosensors for early clinical diagnostic. Talanta. 2015;132: 162-174
27. Ghindilis A.L, Atanasov P, Wilkins M, Wilkins E. Immunosensors: electrochemical sensing and other engeneering approaches. Biosensors and Bioelectronics. 1998;13:113-131
28. Qiu J.D, Liang R.P, Wang R, Fan L.X, Chen Y.W, Xia X.H. A label-free amperometric immunosensor based on biocompatible conductive redox chitosan-ferrocene/gold nanoparticles matrix. Biosensors and Bioelectronics. 2009;25:852-857
29. Wang H, Li X, Mao K, Li Y, Du B, Zhang Y, Wei Q. Electrochemical immunosensor for α-fetoprotein detection using feroferric oxide and horseradish peroxidase as signal amplification labels. Analytical Biochemistry. 2014;465:121-126
30. Yin Z, Liu Y, Jiang L-P, Zhu J-J. Electrochemical immunosensor of tumor nectrosis factor α based on alkaline phosphatase functionalized nanospheres. Biosensors and Bioelectronics. 2011;26(5):1890-1894
31. Tang J, Tang D, Li Q, Su B, Qiu B, Chen G. Sensitive electrochemical immunoassay of carcinoembrionic antigen with signal dual-amplification using glucose oxidase and an artificil catalase. Analytica Chimica Acta. 2011;697(1-2):16-22

32. Wang G, Gang X, Zhou X, Zhang G, Huang H, Zhang X, Wang L. Electrochemical immunosensor with graphene/gold nanoparticles platform and ferrocene derivatives label. Talanta. 2013;103:75-80
33. Ho J.A, Chang H.C, Shih N.Y, Wu L.C, Chang Y.F, Chen C.C, Chou C, Diagnostic detection of human lung cancer-associated antigen using a gold nanoparticle-based electrochemical immunosensor. Analytical Chemistry. 2010;82(14):5944-5950
34. Viswanathan S, Rani C, Ho J.A. Electrochemical immunosensor for multiplexed detection of food-borne pathogens using nanocrystal bioconjugates and MWCNT scree-printed electrodes. Talanta. 2012;94:315-319
35. Kyprianou D, Chianella I, Guerreiro A, Piletska E.V, Piletsky S.A. Development of optical immunosensors for detection of proteins in serum. Talanta. 2013;103:260-266
36. Conneely G, Aherne M, Lu H, Guilbault G.G. Electrochemical immunosensors for the detection of 19-nortestosterone and methytestosterone in bovine urine. Sensors and Actuators B: Chemical, 2007;121(1):103-112
37. Vabbina P.K, Kaushik A, Pokhrel N, Bhansali S, Pala N. Electrochemical cortisol immunosensors based on sonochemically synthesized zinc oxide 1D nanorods and 2D nanoflakes. Biosensors and Bioelectronics. 2015;63:124-130
38. Acharya D, Dhar T.K, A novel broad-specific noncompetitive immunoassay and its application in the determination of total aflatoxins. Analytica Chimica Acta. 2008;630(1):82-90
39. Chaocharoen W, Suginta W, Limbut W, Ranok A, Numnuam A, Khunkaewla P, Kanatharana P, Thavarungkul P, Schulte A. Electrochemical detection of the disease marker human chitinase-3-like protein 1 by matching antibody-modified gold electrodes as label-free immunosensors. Bioelectrochemistry. 2015;101:106-113
40. Ihara M, Suzuki T, Kobayashi N, Ueda H. Open-sandwich enzyme immunoassay for one-step noncompetitive detection of corticosteroid 11-deoxycortisol. Analitical Chemistry. 2009;81(20):8298-8304
41. Matharu Z, Bandodkar A.M, Gupta V, Malhotra B.D. Fundamentals and application of ordered molecular assemblies to affinity biosensing. Chemical Society Review. 2012;41:1363-1402
42. Hock B. Antibodies for immunosensors. Analytica Chimica Acta. 1997;347:177-186.
43. Gopinath S.C.B, Tang T-H, Citartan M, Chen Y. Lakshmipriya. Current aspects in immunosensors. Biosensors and Bioelectronics. 2014;57:292-302
44. Tombelli S, Minunni M, Mascini M. Analytical applications of aptamers. Biosensors and Bioelectronics. 2005;20:2424-2434.
45. Nezlin R. Aptamers in immunological research. Immunology letters. 2014;162:252-255.
46. Smuc T, Ahn I.Y, Ulrich H. Nucleic acid aptamers as high affinity ligands in biotechnology and biosensorics. Journal of Pharmaceutical and Biomedical Analysis. 2013;81-82:210-217
47. Ling Z. Wang M-H, Wang J-P, Ye Z-Z. Application of biosensor surface immobilization methods for aptamer. Chinese journal of analytical chemistry. 2011;39(3):432-438
48. Ellington A.D, Szostak J.W. In vitro selection of RNA molecules that bind specific ligands. Nature. 1990;346(6287):818-822
49. Tuerk C, Gold L. Systematic evolution of ligands by exponential enrichment: RNA ligands to bacteriophage T4 DNA polymerase. Science. 1990;249(4968):505-510

50. Ninomiya K, Yamashita T, Kawabata S, Shimizu N. Targeted and ultrasound-triggered drug delivery using liposomes co-modified with cancer cell-targeting aptamers and a thermosensitive polymer. Ultrasonics Sonochemistry. 2014;21(4):1482-1488
51. Sundaram P, Wower J, Byrne M.E. A nanoscale drug delivery carrier using nucleic acid aptamers for extended release of therapeutic. Nanomedicine: Nanotechnology, Biology and Medicine. 2012;8(7):1143-1151
52. Liang H-R, Hu G-Q, Li L, Gao Y-W, Yang S-T, Xia X-Z. Aptamers targeting rabies virus-infected cells inhibit street rabies virus in vivo. International Immunopharmacology. 2014;21(2):432-438
53. Shigdar S, Qiao L, Zhou S-F, Xiang D, Wang T, Li Y, Lim L.Y, Kong L, Li L,Duan W. RNA aptamers targeting cancer stem cell marker CD133. Cancer letters. 2013;330(1):84-95
54. Ding F, Guo S, Xie M, Luo W, Yuan C, Huang W, Zhang X-L, Zhou X. Diagnostic applications of gastric carcinoma cell aptamers in vitro and in vivo. 2015;134:30-36
55. Zelada-Guillén G.A, Blondeau P, Rius F.X, Riu J. Carbon nanotube-based aptasensors for the rapid and ultrasensitive detection of bacteria. Methods., 2013;63(3): 233-238
56. Meini N, Farre C, Chaix C, Kherrat R, Dzyadevych S, Jaffrezic-Renault N. A sensitive and selective thrombin impedimetric aptasensor based on tailored aptamers obtained by solid-phase synthesis. Sensors and Actuators B: Chemical. 2012;166-167: 715-720
57. Xu H, Gorgy K, Gondran C, Le Goff A, Spinelli N, Lopez C, Defrancq E, Cosnier S. Label-free impedimetric thrombin sensor based on poly(pyrrole-nitrilotriacetic acid)-aptamer film. Biosensors and Bioelectronics. 2013;41:90-95
58. Han B, Zhao C, Yin J, Wang. High performance aptamer affinity chromatography for single-step selective extraction and screening of basic protein lyzozyme. Journal of Chromatography B. 2012;903:112-117
59. Zhou Z-M, Feng Z, Zhou J, Fang B-Y, Qi X-X, Ma Z-Y, Liu B, Zhao Y-D, Hu X-B. Capillary electrophoresis-chemiluminescence detection for carcino-embryonic antigen based on aptamer/graphene oxide structure. Biosensors and Bioelectronics. 2015;64:493-498
60. Dick L.W, McGown L.B. Aptamer-enhanced laser desorption/ionization for affinity mass spectrometry. Analitical Chemistry. 2004;76:3037–3041
61. Yoshimoto k, Nishio M, Sugasawa H, Nagasaki Y. Direct Observation of Adsorption-Induced Inactivation of Antibody Fragments Surrounded by Mixed-PEG Layer on a Gold Surface. Journal of American Chemical Society. 2010;132:7982-7989
62. Ou C, Chen S, Yuan R, Chai Y, Zhong X. Layer-by-layer self assembled multilayer films of multi-walled carbon nanotubes and platinum-Prussian blue hybrid nanoparticles for the fabrication of amperomteric immunosensors. Journal of Electroanalytical Chemistry. 2008;624:287-292
63. Wan Y, Su Y, Zhu X, Liu G, Fan C. Development of electrochemical immunosensors towards point of care diagnosis. Biosensors and Bioelectronics. 2013;47:1-11
64. Jin W, Yang G, Shao H, Qin A. A label-free impedimetric immunosensor for detection of 1-aminohydantoin residue in food samples based on sol-gel embedding antibody. Food Control. 2014;39:185-191
65. Frederix F, Bonroy K, Laureyn W, Reekmans G, Campitelli A, Dehaen W, Maes G, Enhanced performance of an affinity biosensor interface based on mixed self-assembled monolayers of thiols on gold. Langmuir. 2003;19, 4351-4357

66. Holford T.R.J, Davis F, Higson S.P.J, Recent trends in antibody based sensors. Biosensors and Bioelectronics. 2012;34:12-24
67. Mukundan H, Anderson A.S, Grace W.K, Grace K.M, Hartman N, Martinez J.S, Swanson B.I. Waveguide-based biosensors for pathogen detection. Sensors. 2009;9:5783-5809
68. cancer.gov
69. www.ons.gov.uk
70. Ferlay J, Steliarova-Foucher E, Lortet-Tieulent J, Rosso S, Coebergh JWW, Comber H, Forman D, Bray F. Cancer incidence and mortality patterns in Europe: Estimates for 40 countries in 2012. European Journal of cancer 2013;49:1374-1403
71. Atkinson A. J, Colburn W. A, DeGruttola V. G, DeMets D. L, Downing G.J, Hoth D.F, Oates J. A, Peck C.C, Schooley R.T, Spilker, B.A *et al*. Biomarkers and Surrogate Endpoints: Preferred Definitions and Conceptual Framework. Clinical Pharmacological Therapy. 2001;69:89 -95.
72. Kappusamy P, Govindan N, Yussof M, Ichwan S. Proteins are potent biomarkers to detect colon cancer progression. Saudi Journal of Biological Sciences. 2014, *In press*
73. Rusling JF, Sotzing G, Papadimitrakopoulosa F. Designing nanomaterial-enhanced electrochemical immunosensors for cancer biomarker proteins. Bioelectrochemistry. 2009;76(1-2):189-194
74. Florea A, Cristea C, Sandulescu R. MUC1 marker for the detection of ovarian cancer. Farmacia. 2014;62(1):1-13
75. Jang H.D, Kim S.K, Chang H, Choi J-W. 3D label-free prostate specific antigen (PSA) immunosensor based on graphene-gold composites. Biosensors and Bioelectronics. 2015;63:546-551
76. Moon J-M, Kim Y.H, Cho Y. A nanowire-based label-free immunosensor: Direct incorporation of PSA antibody in electropolymerized polypyrrole. Biosensors and Bioelectronics. 2014;57:157-161
77. Panini N.V, Messina G.A, Salinas E, Fernandez H, Raba J. Integrated microfluidic systems with an immunosensor modified with carbon nanotubes for detection of PSA in human serum samples. Biosensors and Bioelectronics. 2008;23(7):1145-1151
78. Kavosi B, Salimi A, Hallaj R, Amani K. A highly sensitive prostate-specific antigen immunosensor based on gold nanoparticles/PAMAM dendrimer loaded MWCNTS/chitosan/ionic liquid nanocomposite. Biosensors and Bioelectronics. 2014;52:20-28
79. Ren X, Wang H, Wu D, Fan D, Zhang Y, Du B, Wei Q. Ultrasensitive immunoassay for CA125 detection using acid site compound as signal and enhancer. Talanta. 2015;144:535-541
80. Wang S, Ge L, Yan M, Yu J, Song X, Ge S, Hunag J. 3D microfluidic origami electrochemiluminescence immunodevice for sensitive point-of-care testing of carcinoma antigen 125. Sensors and Actuators B. 2013;176:1-8.
81. Wang X, Chu C, Shen L, Deng W, Yan M, Ge S, Yu J, Song X. An ultrasensitive electrochemical immunosensor based on the catalytical activity of MoS_2-Au composite using Ag nanospheres as labels. Sensors and Actuators B:Chemical. 2015;206:30-36.
82. Feng D, Li L, Fang X, Han X, Zhang Y. Dual signal amplification of horseradish peroxidase functionalized nanocomposite as trace label for the electrochemical detection of carcinoembryonic antigen. Electrochimica Acta. 2014;127:334-341.

83. Peng H-P, Hu Y, Liu A-L, Chen W, Lin X-H, Yu X-B. Label-free electrochemical immunosensor based on multi-functional gold nanoparticles-polydopamine-thionine-graphene oxide nanocomposites film for determination of alpha-fetoprotein. Journal of Electroanalytical Chemistry. 2014;712:89-95
84. Zhang H, Liu L, Fu X, Zhu Z. Microfluidic beads-based immunosensor for sensitive detection of cancer biomarker proteins using multienzyme-nanoparticle amplification and quantum dots labels. Biosensors and Bioelectronics. 2013;42:23-30.
85. Yang F, Yang Z, Zhuo Y, Chai Y, Yuan R. Ultrasensitive electrochemical immunosensor for carbohydrate antigen 19-9 using Au/porous graphene nanocomposites as platform and Au@Pd core/shell bimetallic functionalized graphene nanocomposites as signal enhancers. Biosensors and Bioelectronics. 2015;66:356-362.
86. Weng S, Chen M, Zhao C, Liu A, Lin L, Liu Q, Lin J, Lin X. Label-free electrochemical immunosensor based on $K_3[Fe(CN)_6]$ as signal for facile and sensitive determination of tumor necrosis factor-alpha. Sensors and Actuators B: Chemical. 2013;184:1-7
87. Wang Y, Zhang Y, Su Y, Li F, Ma H, Li H, Du B, Wei Q. Ultrasensitive non-mediator electrochemical immunosensors using Au/Ag/Au core/double shell nanoparticles as enzyme-mimetic labels.Talanta. 2014;124:60-66
88. Wang J, El-Bahrawy MA. Expression profile of mucins in ovarian mucinous tumors: distinguishing primary ovarian from metastatic tumors. International Journal of Gynecolycal Pathology. 2014;33(2):166-75.
89. Garbar C, Mascaux C, Curé H, Bensussan A. Muc1/Cd227 immunohistochemistry in routine practice is a useful biomarker in breast cancers. Journal of Immunoassay Immunochemistry. 2013;34(3):232-45.
90. Li J, Hu YM, Du YJ, Zhu LR, Qian H, Wu Y, Shi WL. Expressions of MUC1 and vascular endothelial growth factor mRNA in blood are biomarkers for predicting efficacy of gefitinib treatment in non-small cell lung cancer. BMC Cancer. 2014 Nov 19;14:848.
91. Remmers N, Anderson JM, Linde EM, DiMaio DJ, Lazenby AJ, Wandall HH, Mandel U, Clausen H, Yu F, Hollingsworth MA. Aberrant expression of mucin core proteins and o-linked glycans associated with progression of pancreatic cancer. Clinical Cancer Research. 2013;19(8):1981-93.
92. Bozkaya G, Korhan P, Cokaklı M, Erdal E, Sağol O, Karademir S, Korch C, Atabey N. Cooperative interaction of MUC1 with the HGF/c-Met pathway during hepatocarcinogenesis. Molecular Cancer. 2012 Sep 11;11:64.
93. Saeland E, Belo AI, Mongera S, van Die I, Meijer GA, van Kooyk Y. Differential glycosylation of MUC1 and CEACAM5 between normal mucosa and tumour tissue of colon cancer patients. International Journal of Cancer. 2012;131(1):117-28.
94. Nath S, Mukherjee P. MUC1: a multifaceted oncoprotein with a key role in cancer progression. Trends in molecular medicine. 2014;20(6):332-342
95.. Zhao J, He X, Bo B, Liu X, Yin Y, Li G. *et al,* A "signal-on" electrochemical aptasensor for simultaneous detection of two tumor markers. Biosensors and Bioelectronics. 2012;34(1): 249-252
96.. Altintas Z, Kallempudi S, Sezerman U, Gurbuz Y. A novel magnetic particle-modified electrochemical sensor for immunosensor applications. Sensors and Actuators B, 2012;174: 187– 194

97. Li H, He J, Li S, Turner A. Electrochemical immunosensor with *N*-doped graphene-modified electrode for label-free detection of the breast cancer biomarker CA 15-3. Biosensors and Bioelectronics. 2013;43:25–29
98. Zhu X, Yang J, Liu M, Wu Y, Shen Y, Li G. Sensitive detection of human breast cancer cells based on aptamer–cell–aptamer sandwich architecture. Analytica Chimica Acta, 2013;764: 59-63
99. Ma F, Ho C, Cheng AKH, Yu HZ. Immobilization of redox-labeled hairpin DNA aptamers on gold: Electrochemical quantitation of epithelial tumor marker mucin 1. Electrochimica Acta. 2013;110:139-145
100. Hong C, Yuan R, Chai Y, Zhuo Y, Ferrocenyl-doped silica nanoparticles as an immobilized affinity support for electrochemical immunoassay of cancer antigen 15-3, Anal Chim Acta, 2009;633:244–249
101. Taleat Z, Cristea C, Marrazza G, Mazloum-Ardakani M, Săndulescu R. Electrochemical immunoassay based on aptamer–protein interaction and functionalized polymer for cancer biomarker detection. Journal of Electroanalytical Chemistry. 2014;717–718: 119-124
102. Chen X, Zhang Q, Chunhua Q, Hao N, Xu L, Cheng Y. Electrochemical aptasensor for mucin 1 based on dual signal amplification of poly(*o*-phenylenediamine) carrier and functionalized carbon nanotubes tracing tag. Biosensors and Bioelectronics. 2015;64:485-492.
103. Yin T, Qin W. Applications of nanomaterials in potentiometric sensors. TrAC Trends in Analytical Chemistry. 2013;51:79-86.
104. Rocha-Santos T.A.P. Sensors and biosensors based on magnetic nanoparticles. Trends in Analytical Chemistry. 2014;62:28–36
105. Bayramoglu G, Ozalp V.C, Arica M. Magnetic Polymeric Beads Functionalized with Different Mixed-Mode Ligands for Reversible Immobilization of Trypsin. Industrial and Engineering Chemistry Research. 2014;53:132−140
106. Philippova O, Barabanova A, Molchanov V, Khokhlov. Magnetic polymer beads: Recent trends and developments in syntheric design and applications. European Polymer Journal. 2011;47:542–559
107. Palecek E, Fojta M. Magnetic beads as versatile tools for electrochemical DNA and protein biosensing. Talanta. 2007;74:276–290
108. Khan M.S, Vishakante G.D, Siddaramaiah H. Gold nanoparticles: a paradigm shift in biomedical applications. Advances in Colloid and Interface Science. 2013;199-200:44-58
109. Saha K, Agasti S.S, Kim C, Li X, Rotello V.M. Gold nanoparticles in chemical and biological sensing. Chemical Reviews. 2012;112: 2739-2779
110. Turkevich J, Stevenson P.C, Hillier J. A study of the nucleation and growth processes in the synthesis of colloidal gold. Discussions of the Faraday Society. 1951;11:55
111. Brust M, Walker M, Bethell D, Schiffrin D.J, Whyman R. Synthesis of thiol-derivatised gold nanoparticles in a two-phase liquid–liquid system. Journal of the Chemical Society, Chemical Communications. 1994;7 801-802
112. Yu D, Zeng Y, Qi Y, Zhou T, Shi G. A novel electrochemical sensor for determination of dopamine based on AuNPs@SiO_2 core-shell imprinted composite. Biosensors and Bioelectronics. 2012;38(1):270-277

113. Hu Y, Li L, Guo L. The sandwich-type aptasensor based on gold nanoparticles/DNA/magnetic beads for detection of cancer biomarker protein AGR2. Sensors and Actuators B: Chemical. 2015;209:846-852
114. Yadav S.K, Agrawal B, Goyal R.N. AuNPs-poly-DAN modified pyrolytic graphite sensor for the determination of Cefpodoxime Proxetil in biological fluids. Talanta. 2013;108:30-37
115. Li G, Liu L, Qi X, Guo Y, Sun W, Li X. Development of a sensitive electrochemical DNA sensor by 4-aminothiophenol self-assembled on electrodeposited nanogold electrode coupled with Au nanoparticles labeled reporter ssDNA. Electrochimica Acta.2012;63:312-317
116. Singh J, Khanra P, Kuila T, Srivastava M, Das A.K, Kim N.H, Jung B.J, Kim D.Y, Lee S.H, Lee D.W, Kim D.G, Lee J.H. Preparation of sulfonated poly(ether–ether–ketone) functionalized ternary graphene/AuNPs/chitosan nanocomposite for efficient glucose biosensor. Process Biochemistry.2013;48(11):1724-1735
117. Guo S, Wang E. Synthesis and electrochemical applications of gold nanoparticles. Analytica Chmica Acta. 2007;598:181-192
118. Wulff G, Sahran A. The use of polymers with enzyme-analogous structures for the resolution of racemates. Angewandte Chemie International Edition. 1972;11(4):341.
119. Arshady R, Mosbach K. Synthesis of substrate-selective polymers by host-guest polymerization. Macromolecular Chemistry And Physics. 1981;182(2):687-692.
120. Komiyama M, Takeuchi T, Mukawa T, Asanuma H. Molecular imprinting from fundamentals to applications. Wiley-VCH Verlag GmbH & Co. KgaA, 2003, 9-19
121. Shen X, Xu C, Ye L. Molecularly imprinted polymers for clean water: analysis and purification. Industrial and Engineering Chemistry Research. 2013;52 (39): 13890–13899
122. Piletsky S, Turner A. Molecular imprinting of polymers. Landes Biosciences. 2006. Chapter 6. A new generation of chemical sensors based on MIPs pp 64-74
123. Haupt K, Mosbach K. Molecularly imprinted polymers and their use in biomimetic sensors. Chemical Reviews. 2000;100:2495-2504
124. Schirhagl R. Bioapplications for molecularly imprinted polymers. Analytical Chemistry. 2014;86:250-261
125. Da Silva H, Pacheco J.G, Magalhaes J, Viswanathan S, Delerue-Matos C. MIP-graphene-modified glassy carbon electrode for the determination of trimethoprim. Biosensors and Bioelectronics. 2014;52(15):56-61
126. Wang S, Ge L, Li L, Yan M, Ge S, Yu J. Molecularly imprinted polymer grafted paper-based multi-disk micro-disk plate for chemiluminescence detection of pesticide. Biosensors and Bioelectronics. 2013;50(15):262-268
127. Yu J.C.C, Lai E.P.C. Interaction of ochratoxin A with molecularly imprinted polypyrrole film on surface plasmon resonance sensor. Reactive and Functional Polymers. 2005;63(3):171-176
128. Pradhan S, Boopathi M, Kumar O, Baghel A, Pandey P, Mahato T.H, Singh B, Vijayaraghavan R. Molecularly imprinted nanopatterns for the recognition of biological warfare agent ricin. Biosensors and Bioelectronics. 2009;25(3):592-598
129. Sharma P.S, Iskierko Z, Pietrzyk-Le A, D'Souza F, Kutner W. Bioinspired intelligent molecularly imprinted polymer for chemosensing: a minireview. Electrochemistry communications. 2015;50:81-87

130. Ansell R.J. Molecularly imprinted polymers in pseudoimmunoassay. Journal of Chromatography B. 2004;804:151-165
131. Liu P, Zhang X, Xu W, Guo C, Wang S. Electrochemical sensor for the determination of brucine in human serum based on molecularly imprinted poly-*o*-phenylenediamine/SWNTs composite film. Sensors and Actuators B: Chemical. 2012;*163(1*):*84-89*
132. Xue C, Wang X, Zhu W, Han Q, Zhu C, Hong J, Zhou X, Jiang H. Electrochemical serotonin sensing interface based on double-layered membrane of reduced graphene oxide/polyaniline nanocomposites and molecularly imprinted polymers embedded with gold nanoparticles. Sensors and Actuators B: Chemical. 2014;196: 57-63
133. Hrichi H, Louhaichi M.R, Monser L, Adhoum N. Gliclazide voltammetric sensor based on electropolymerized molecularly imprinted polypyrrole film onto glassy carbon electrode. Sensors and Actuators B: Chemical. 2014;204:42-49
134. Shin M.J, Hong W.H. Sensing capability of molecularly imprinted self-assembled monolayer. Biochemical Engineering Journal. 2011;54(1):57-61
135. Khadro B, Sanglar C, Bonhomme A, Errachid A, Jaffrezic-Renault N. Molecularly imprinted polymers (MIP) based electrochemical sensor for detection of urea and creatinine. Procedia Engeneering. 2010;5:371-374
136. Mazzotta E, Picca R.A, Malitesta C, Piletsky S.A, Piletska E.V. Development of a sensor prepared by entrapment of MIP particles in electrosythesised polymer films for electrochemical detection of ephedrine. Biosensors and Bioelectronics. 2008;23(7):1152-1156
137. Ji J, Zhou Z, Zhao X, Sun J, Sun X. Electrochemical sensor based on molecularly imprinted film at Au nanoparticles-carbon nanotubes modified electrode for the determination of cholesterol. Biosensors and Bioelectronics.2015;66:590-595
138. Zhong M, Teng Y, Pang S, Yan L, Kan X. Pyrrole-phenylboronic acid: A novel monomer for dopamine recognition and detection based on imprinted electrochemical sensor. Biosensors and Bioelectronics. 2015;64(15):212:218
139. Zhang X, Peng Y, Bai J, Ning B, Sun S, Hong X, Liu Y, Liu Y, Gao Z. A novel electrochemical sensor based on electropolymerized molecularly imprinted polymer and gold nanomaterials amplification for estradiol detection. Sensors and Actuators B: Chemical. 2014;200:69-75
140. Luo J, Fan C, Wang X, Liu R, Liu X. A novel electrochemical sensor for paracetamol based on molecularly imrpinted polymerics micelles. Sensors and Actuators B: Chemical. 2013;188:909-916
141. Zhang j, Niu Y, Li S, Luo R, Wang C. A molecularly imprinted electrochemical sensor based on sol-gel technology and multiwalled carbon nanotubes-Nafion functional layer for determination of 2-nonylphenol in environmental samples. Sensors and actuators B: Chemical. 2014;193:844-850
142. Yang G, Zhao F. Electrochemical sensor for chloramphenicol based on novel multiwalled carbon nanotubes@molecularly imprinted polymer. Biosensors and Bioelectronics. 2015;64:416-422
143. Rezaei B, Boroujeni M.K, Ensafi A.A. A novel electrochemical nanocomposite imprinted sensor for the determination of lorazepam based on modified polypyrrole@sol-gel@gold nanoparticles/pencil graphite electrode. Electrochimica Acta 2014;123:332-339
144. Bakas I, Hayat A, Piletsky S, Piletska E, Chehimi M.M, Noguer T, Rouillon R. Electrochemical impedimetric sensor based on molecularly imprinted polymers/sol-gel

chemistry for methidathion organophosphorus insecticide recognition. Talanta. 2014;130:294-298
145. Chen J, Huang H, Zeng Y, Tang H, Li L. A novel composite of molecularly imprinted polymer-coated PdNPs for electrochemical sensing norepinephrine. Biosensors and Bioelectronics.2015;65:366-374.
146. Chikkaveeraiah BV, Bhirde AA, Morgan NY, Eden HS, Chen X. Electrochemical immunosensors for detection of cancer protein biomarkers. ACS Nano 2012;6:6546-6561.
147. Pérez-López B, Merkoçi A. Nanomaterials based biosensors for food analysis applications. Trends in Food Science & Technology 2011;22:625-639.
148. Zhang WY, Asiri AM, Liu DL, Du D, Lin YH. Nanomaterial-based biosensors for environmental and biological monitoring of organophosphorus pesticides and nerve agents. Trac-Trends in Analitical Chemistry. 2014;54:1-10.
149. Diaconu I, Cristea C, Harceaga V, Marrazza G, Berindan-Neagoe I, Sandulescu R. Electrochemical immunosensors in breast and ovarian cancer. Clinica Chimica Acta 2013;425:128-138.
150. Ricci F, Adornetto G, Palleschi G. A review of experimental aspects of electrochemical immunosensors. Electrochimica Acta 2012;84:74-83.
151. Gopinath SC, Tang TH, Citartan M, Chen Y, Lakshmipriya T. Current aspects in immunosensors. Biosensors and Bioelectronics. 2014;57:292-302.
152. Makaraviciute A, Ramanaviciene A. Site-directed antibody immobilization techniques for immunosensors. Biosensors and Bioelectronics. 2013;50:460-471.
153. Taleat Z, Cristea C, Marrazza G, Mazloum-Ardakani M, Săndulescu R. Electrochemical immunoassay based on aptamer–protein interaction and functionalized polymer for cancer biomarker detection. Journal of Electroanalytical Chemistry 2014;717-718:119-124.
154. Mascini M, Palchetti I, Tombelli S. Nucleic acid and peptide aptamers: fundamentals and bioanalytical aspects. Angewandte Chemie Int Ed Engl. 2012;51:1316-1332.
155. Hayat A, Barthelmebs L, Marty JL. Enzyme-linked immunosensor based on super paramagnetic nanobeads for easy and rapid detection of okadaic acid. Analica Chimica Acta. 2011;690:248-252.
156. Laschi S, Palchetti I, Marrazza G, Mascini M. Enzyme-amplified electrochemical hybridization assay based on PNA, LNA and DNA probe-modified micro-magnetic beads. Bioelectrochemistry. 2009;76:214-220.
157. Ravalli A, dos Santos GP, Ferroni M, Faglia G, Yamanaka H, Marrazza G. New label free CA125 detection based on gold nanostructured screen-printed electrode. Sensors and Actuators B-Chemistry. 2013;179:194-200.
158. Ambrosi A, Castaneda MT, Killard AJ, Smyth MR, Alegret S, Merkoci A. Double-codified gold nanolabels for enhanced immunoanalysis. Analitical Chemistry. 2007;79:5232-5240.
159. Taleat Z, Ravalli A, Mazloum-Ardakani M, Marrazza G. CA 125 Immunosensor Based on Poly-Anthranilic Acid Modified Screen-Printed Electrodes. Electroanalysis. 2013;25:269-277.
160. Al-Khafaji QAM, Harris M, Tombelli S, et al. An Electrochemical Immunoassay for HER2 Detection. Electroanalysis. 2012;24:735-742.
161. Eguílaz M, Moreno-Guzmán M, Campuzano S, González-Cortés A, Yáñez-Sedeño P, Pingarrón JM. An electrochemical immunosensor for testosterone using functionalized magnetic beads and screen-printed carbon electrodes. Biosensors and Bioelectronics. 2010;26:517-522.

162. Moreno-Guzman M, Gonzalez-Cortes A, Yanez-Sedeno P, Pingarron JM. A disposable electrochemical immunosensor for prolactin involving affinity reaction on streptavidin-functionalized magnetic particles. Analitica Chimica Acta. 2011;692:125-130.
163. Chikkaveeraiah BV, Mani V, Patel V, Gutkind JS, Rusling JF. A disposable electrochemical immunosensor for prolactin involving affinity reaction on streptavidin-functionalized magnetic particles. Biosensors and Bioelectronics. 2011;26:4477-4483.
164. Erdem A, Congur G, Eksin E. Multi channel screen printed array of electrodes for enzyme-linked voltammetric detection of MicroRNAs. Sensors and Actuators B-Chemistry. 2013;188:1089-1095.
165. Giallo MLD, Ariksoysal DO, Marrazza G, Mascini M, Ozsoz M. Disposable Electrochemical Enzyme-Amplified Genosensor for Salmonella Bacteria Detection. Analytical Letters 2005;38:2509-2523.
166. Laschi S, Miranda-Castro R, Gonzalez-Fernandez E, et al. A new gravity-driven microfluidic-based electrochemical assay coupled to magnetic beads for nucleic acid detection. Electrophoresis. 2010;31:3727-3736.
167. Meric B, Kerman K, Marrazza G, Palchetti I, Mascini M, Ozsoz M. Disposable genosensor, a new tool for the detection of NOS-terminator, a genetic element present in GMOs. Food Control. 2004;15:621-626.
168. Zani A, Laschi S, Mascini M, Marrazza G. A New Electrochemical Multiplexed Assay for PSA Cancer Marker Detection. Electroanalysis. 2011;23:91-99.
169. Lau SK, Weiss LM, Chu PG. Differential expression of MUC1, MUC2, and MUC5AC in carcinomas of various sites: an immunohistochemical study. American Journal of Clinical Pathology. 2004;122:61-69.
170. Vlad AM, Diaconu I, Gantt KR. MUC1 in endometriosis and ovarian cancer. Immunology Research. 2006;36:229-236.
171. Mukhopadhyay P, Chakraborty S, Ponnusamy MP, Lakshmanan I, Jain M, Batra SK. Mucins in the pathogenesis of breast cancer: implications in diagnosis, prognosis and therapy. Biochimica et Biophysica Acta. 2011;1815:224-240.
172. Kaira K, Nakagawa K, Ohde Y, et al. Depolarized MUC1 expression is closely associated with hypoxic markers and poor outcome in resected non-small cell lung cancer. International Journal of Surgical Pathology. 2012;20:223-232.
173. Wen W, Hu R, Bao T, Zhang X, Wang S. An insertion approach electrochemical aptasensor for mucin 1 detection based on exonuclease-assisted target recycling. Biosensors and Bioelectronics. 2015;71:13-17.
174. Winter JM, Tang LH, Klimstra DS, et al. A novel survival-based tissue microarray of pancreatic cancer validates MUC1 and mesothelin as biomarkers. PLoS ONE. 2012;7:e40157.
175. Ferreira CS, Matthews CS, Missailidis S. DNA aptamers that bind to MUC1 tumour marker: design and characterization of MUC1-binding single-stranded DNA aptamers. Tumour Biology. 2006;27:289-301.
176. Hu R, Wen W, Wang Q, et al. Novel electrochemical aptamer biosensor based on an enzyme–gold nanoparticle dual label for the ultrasensitive detection of epithelial tumour marker MUC1. Biosensors and Bioelectronics. 2014;53:384-389.
177. Cheng AKH, Su HP, Wang A, Yu HZ. Aptamer-Based Detection of Epithelial Tumor Marker Mucin 1 with Quantum Dot-Based Fluorescence Readout. Analytical Chemistry. 2009;81:6130-6139.

178. Centi S, Tombelli S, Minunni M, Mascini M. Aptamer-based detection of plasma proteins by an electrochemical assay coupled to magnetic beads. Analytical Chemistry. 2007;79:1466-1473.
179. Corfield AP. Mucins: A biologically relevant glycan barrier in mucosal protection. Biochimica et Biophysica Acta. 2014.
180. Polanski M, Anderson NL. A list of candidate cancer biomarkers for targeted proteomics. Biomarkers Insights. 2007;1:1-48.
181. Dharmaraj N, Chapela PJ, Morgado M, et al. Expression of the transmembrane mucins, MUC1, MUC4 and MUC16, in normal endometrium and in endometriosis. Human Reproduction. 2014;29:1730-1738.
182. Wu J, Fu ZH, Yan F, Ju H. Biomedical and clinical applications of immunoassays and immunosensors for tumor markers.Trends in Analitical Chemistry, 2007;26:679-688.
183. Chen H, Jiang C, Yu C, Zhang S, Liu B, Kong J. Protein chips and nanomaterials for application in tumor marker immunoassays. Biosensors and Bioelectronics. 2009;24:3399-3411.
184. Rasooly A, Jacobson J. Development of biosensors for cancer clinical testing. Biosensors and Bioelectronics. 2006;21:1851-1858.
185. Wu J, Yan YT, Yan F, Ju HX. Electric field-driven strategy for multiplexed detection of protein biomarkers using a disposable reagentless electrochemical immunosensor array. Analytical Chemistry. 2008;80:6072–6077.
186. Lin JH, Ju HX. Electrochemical and chemiluminescent immunosensors for tumor markers. Biosensensors and Bioelectronics. 2005;20:1461-1470.
187. Rong Q, Feng F, Ma Z. Metal ions doped chitosan–poly(acrylic acid) nanospheres: Synthesis and their application in simultaneously electrochemical detection of four markers of pancreatic cancer. Biosensors and Bioelectronics, 2016;15:148-154
188. Kellner C, Botero ML, Latta D, Drese K, Fragoso A, O'Sullivan CK. Automated microsystem for electrochemical detection of cancer markers. Electrophoresis. 2011:32;926-930.
189. Thuerlemann C, Haeberli A, Alberio L. Monitoring thrombin generation by electrochemistry: development of an amperometric biosensor screening test for plasma and whole blood. Clinical Chemistry. 2009;55:505-512.
190. Graves R, Hilgers J, Fritsche H, Hayes D, Robertson JFR. MUC-1 mucin assays for monitoring therapy in metastatic *breast* cancer. The Breast. 1998;7:181-186.
191. Kjällman THM, Peng H, Soeller C, Travas-Sejdic J. Effect of Probe Density and Hybridization Temperature on the Response of an Electrochemical Hairpin-DNA Sensor. Analytical Chemistry. 2008;80:9460-9466.
192. Soontornworajit B, Wang Y. Nucleic acid aptamers for clinical diagnosis: cell detection and molecular imaging. Analytical Bioanalytical Chemistry. 2011;399:1591-1599.
193. Song SP, Wang LH, Li J, Zhao JL, Fan CH. Aptamer-based biosensors. Trends in Analytical Chemistry. 2008;27:108-117.
194. Degefa TH, Hwang S, Kwon D, Park JH, Kwak J. Electrochemical Aptamer-Based Biosensors: Recent Advances and Perspectives. Electrochimica Acta. 2009;54: 6788-6791.
195. Yan XL, Cao ZJ, Lau CW, Lu JZ. DNA aptamer folding on magnetic beads for sequential detection of adenosine and cocaine by substrate-resolved chemiluminescence technology. Analyst. 2010;135:2400-2407.

196. Zheng J, Cheng GF, He PG, Fang YZ. An aptamer-based assay for thrombin via structure switch based on gold nanoparticles and magnetic nanoparticles. Talanta 80 (2010) 1868-1872.
197. Rowe AA, Miller EA, Plaxco KW. Reagentless Measurement of Aminoglycoside Antibiotics in Blood Serum via an Electrochemical, Ribonucleic Acid Aptamer-Based Biosensor. Analytical Chemistry. 2010;82:7090-7095.
198. Li T, Fan Q, Liu T, Zhu X, Zhao J, Li G. Detection of breast cancer cells specially and accurately by an electrochemical method. Biosensensors and Bioelectronics. 2010;25:2686-2689.
199. Wei W, Li DF, Pan XH, Liu SQ. Electrochemiluminescent detection of mucin 1 protein and MCF-7 cancer cells based on the resonance energy transfer. Analyst. 2012;137:2101-2106.
200. Zhu X, Yang J, Liu M, Wu Y, Shen Z, Li G. Sensitive detection of human breast cancer cells based on aptamer-cell-aptamer sandwich architecture. Analytica Chimica Acta. 2013;764:59-63.
201. Hong C, Yuan R, Chai Y, Zhuo Y. Ferrocenyl-doped silica nanoparticles as an immobilized affinity support for electrochemical immunoassay of cancer antigen 15-3. Analytica Chimica Acta. 2009;633:244.
202. Yu J, Wang S, Zhao G, Wang B, Ding L, Zhang X, Xie J, Xie F. Determination of urinary aromatic amines in smokers and nonsmokers using a MIPs-SPE coupled with LC–MS/MS method. Journal of Chromatography B. 2014;958:130-135
203. Gonçalves Santos M, Vilela Vitor R, Lopes Andrade F, Martins I, Costa Figueiredo E. Molecularly imprinted solid phase extraction of urinary diethyl thiophosphate and diethyl dithiophosphate and their analysis by gas chromatography–mass spectrometry. Journal of Chromatography B. 2010;909:70-76.
204. Piletsky SA, Piletska EV, Bossi A, Karim K, Lowe P, Turner APF. Substitution of antibodies and receptors with molecularly imprinted polymers in enzyme-linked and fluorescent assays. Biosensors and Bioelectronics. 2001;16:701-707.
205. Peeters M, Troost FJ, Van Grinsven B, Horemans F, Alenus J, *et al*. MIP-based biomimetic sensor for the electronic detection of serotonin in human blood plasma. Sensors and Actuators B-Chemical. 2012; 171–172:602-610.
206. Alizadeh T, Ganjali MR, Zare M, Norouzi P. Development of a voltammetric sensor based on a molecularly imprinted polymer (MIP) for caffeine measurement. Electrochimica Acta. 2010;55:1568-1574.
207. Zhang H, Ye L, Mosbach K. Non-covalent molecular imprinting with emphasis on its application in separation and drug development. Journal of Molecular Recognition. 2006;19:248–259.
208. Suriyanarayanan S, Cywinski PJ, Moro AJ, Mohr GJ, Kutner W. Chemosensors Based on Molecularly Imprinted Polymers. Topics in Current Chemistry. 2012;325:165-265.
209. Tokonami S, Shiigi H, Nagaoka T. Review: Micro- and nanosized molecularly imprinted polymers for high-throughput analytical applications. Analytica Chimica Acta. 2009;641:7-13.
210. Yano K, Karube I. Molecularly imprinted polymers for biosensor applications. TrAC-Trends in Analytical Chemistry. 1999;18:199–204.

211. Schirhagl R. Bioapplications for Molecularly Imprinted Polymers. Analytical Chemistry. 2014;86:250-261.
212. Apodaca DC, Pernites RB, Ponnapati RR, Del Mundo FR, Advincula RC. Electropolymerized Molecularly Imprinted Polymer Films of a Bis-Terthiophene Dendron: Folic Acid Quartz Crystal Microbalance Sensing. ACS Applied Materials Interfaces. 2011:3(2);191–203.
213. Saha K, Agasti SS, Kim C, Li X, Rotello VM. Gold nanoparticles in chemical and biological sensing. Chemical Reviews. 2012;112:2739-2779.
214. Lv YY, Xu W, Lin FW, Wu J, Xu ZK. Electrospun nanofibers of porphyrinated polyimide for the ultra-sensitive detection of trace TNT. Sensors and Actuators B-Chemical. 2013;184:205-211.
215. Mustafa G, Lieberzeit PA. Molecularly imprinted polymer–Ag_2S nanoparticle composites for sensing volatile organics. RCS Advances. 2014;4:12723-12728.
216. Pesavento M, D'Agostino G, Alberti G, Biesuz R, Merli D. Voltammetric platform for detection of 2,4,6-trinitrotoluene based on a molecularly imprinted polymer. Analytical Bioanalytical Chemistry. 2013;405:3559-3570.
217. Letzel S, Göen T, Bader M, Angerer J, Kraus T. Exposure to nitroaromatic explosives and health effects during disposal of military waste. Occupational and Environmental Medicine. 2003;60:483-488
218. Blue R, Vobecka Z, Skabara PJ, Uttamchandani D. The development of sensors for volatile nitro-containing compounds as models for explosive detection. Sensors and Actuators B:Chemical. 2013;176:534-542
219. C. Carrillo-Carrión C, B.M. Simonet BM, M. Valcárcel M. Determination of TNT explosive based on its selective interaction with creatinine-capped CdSe/ZnS quantum dots. Analytica Chimica Acta. 2013;792:93-100
220. Fan L, Hu Y, Wang X, Zhang L, Li F, *et al*. Fluorescence resonance energy transfer quenching at the surface of graphene quantum dots for ultrasensitive detection of TNT. Talanta. 2012;101:192–197.
221. Lu YY, Xu W, Lin FW, Wu J, Xu ZK. Electrospun nanofibers of porphyrinated polyimide for the ultra-sensitive detection of trace TNT. Sensors and Actuators B-Chemical 2013;184:205-211.
222. Liu X, Zhao L, Shen H, Xu H, Lu L. Ordered gold nanoparticle arrays as surface-enhanced Raman spectroscopy substrates for label-free detection of nitroexplosives. Talanta. 2011;83:1023-1029.
223. Liu M, Chen W. Graphene nanosheets-supported Ag nanoparticles for ultrasensitive detection of TNT by surface-enhanced Raman spectroscopy. Biosensors and Bioelectronics. 2013;46:68–73.
224. Singh P, Onodera T, Mizuta Y, Matsumoto K, Miura N, Toko K. Dendrimer modified biochip for detection of 2,4,6 trinitrotoluene on SPR immunosensor: Fabrication and advantages. Sensors and Actuators B-Chemical. 2009;137:403-409
225. Kawaguchi T, Ravi Shankaran D, Kim SJ, Vengatajalabathy Gobi K, Matsumoto K, *et al*. Fabrication of a novel immunosensor using functionalized self-assembled monolayer for trace level detection of TNT by surface plasmon resonance. Talanta. 72 (2007) 554-560

226. Garcia Breijo E, Olguin Pinatti C, Masot Peris R, Alcañiz Fillol M, Martínez-Máñez R, Soto Camino J. TNT detection using a voltammetric electronic tongue based on neural networks. Sensors and Actuators A. 2013;192:1-8.
227. De Sanoit J, Vanhove E, Mailley P, Bergonzo P. Electrochemical diamond sensors for TNT detection in water. Electrochimica Acta. 2009;54:5688-5693.
228. Sharma PS, D'Souza F, Kutner W. Molecular imprinting for selective chemical sensing of hazardous compounds and drugs of abuse. Trends in Analytical Chemistry. 2012;34:59-77.
229. Sharma PS, D'Souza F, Kutner W. Molecular imprinting for selective sensing of some biohazardous compounds, Chap 4 in: Portable chemical sensors - weapons against bioterrorism, Nikolelis, D. (Ed.), Springer, Berlin, 2012, pp. 63-94.
230. Huynh TP, Sosnowska M, Sobczak JW, Nesterov VN, F. D'Souza, Kutner W. Simultaneous Chronoamperometry and Piezoelectric Microgravimetry Determination of Nitroaromatic Explosives Using Molecularly Imprinted Thiophene Polymers. Analytical Chemistry. 2013;85:8361-8368
231. Zhu W, Tao S, Tao C, Li W, Lin C *et al*. Hierarchically Imprinted Porous Films for Rapid and Selective Detection of Explosives. Langmuir. 2011;27:8451–8457
232. Lanz C, Früh M, Thormann W, Cerny T, Lauterburg BH. Rapid determination of gemcitabine in plasma and serum using reversed-phase HPLC. Journal of Separation Science. 2007;30(12):1811-20.
233. Wang LZ, Goh BC, Lee NH, Noordhuis P, Peters GJ. An expedient assay for determination of gemcitabine and its metabolite in human plasma using isocratic ion-pair reversed-phase high-performance liquid chromatography. Theraputic Drug Monitoring. 2003; 25(5):552-7.
234. Kirstein MN, Hassan I, Guire DE, Weller DR, Dagit JW, Fisher JE. Remmel RP, High-performance liquid chromatographic method for the determination of gemcitabine and 2′,2′-difluorodeoxyuridine in plasma and tissue culture media. Journal of Chromatography B. 2006;835(1-2): 136–142
235. Marangon E, Sala F, Caffo O, Galligioni E, D'Incalci M, Zucchetti M. Simultaneous determination of gemcitabine and its main metabolite, dFdU, in plasma of patients with advanced non-small-cell lung cancer by high-performance liquid chromatography-tandem mass spectrometry. Journal of Mass Spectrometry. 2008;43(2):216-223.
236. Wang LZ, Yong WP, Soo RA, Lee SC, Soong R, Lee HS, Goh BC. Rapid Determination of Gemcitabin e and Its Metabolite in Human Plasma by LC-MSMS through Micro Protein Precipitation with Minimum Matrix Effect. Journal of Pharmaceutical Science & Research. 2009;1(3):23-32
237. Naik KM, Nandibewoor ST. Electro-oxidation and determination of gemcitabine hydrochloride, an anticancer drug at gold electrode. Journal of Industrial and Engineering Chemistry. 2013;19:1933–1938
238. Kalanur SS, Katrahalli U, Seetharamappa J. Electrochemical studies and spectroscopic investigations on the interaction of an anticancer drug with DNA and their analytical applications. Journal of Electroanaytical Chemistry. 2009;636:93–100.
239. Lee C, Langlois BE, Dawson KA. Detection of tetracycline resistance determinants in pig isolates from three herds with different histories of antimicrobial agent exposure. Applied and Environmental Microbiology. 1993;59(5):1467–1472.
240. Goodman GA, Goodman LS, Rall TW, Murad F. The Pharmacological Basis of Therapeutics, seventh ed., Mac-Millan, New York,1985.

241. Cinquina AL, Longo F, Anastasi G, Giannetti L, Cozzani R. Validation of a high-performance liquid chromatography method for the determination of oxytetracycline, tetracycline, chlortetracycline and doxycycline in bovine milk and muscle. Journal of Chromatography A. 2003;987:227-233.
242. Furusawa N. Spiramycin, Oxytetracycline and sulphamonomethoxine conents of eggs and egg-forming tissues of laying hens. Zentralbl Veterinarmed A. 1999;46:599–603.
243. De Wasch K, Brabander HD, Hoof JV, Backer J. Detection of residues of tetracycline antibiotics in pork and chicken meat: correlation between results of screening and confirmatory tests. Analyst. 1998;123:2737–2741.
244. Martel AC, Zeggane S, Drajnudel P, Faucon JP, Aubert M. Tetracycline residues in honey after hive treatment. Food Additives Contaminants. 2006;23:265–273.
245. Li J, Chen L, Wang X, Jin H, Ding L, Zhang K *et al*. Determination of tetracyclines residues in honey by on-line solid-phase extraction high-performance liquid chromatography. Talanta. 2008;75:1245–1252.
246. Reybroeck W, Ooghe S, De Brabander H, Daeseleire E Validation of the tetrasensor honey test kit for the screening of tetracyclines in honey. Journal of agricultural and food chemistry. 2007;55:8359–8366.
247. Zhou L, Li DJ, Gai L, Wang JP, Li YB. Electrochemical aptasensor for the detection of tetracycline with multi-walled carbon nanotubes amplification. Sensors and Actuators B: Chemical. 2012;162:201–208.
248. Chen D, Yao D, Xie C, Liu D. Development of an aptasensor for electrochemical detection of tetracycline. Food Control. 2014;42:109–115
249. Wang S, Yong W, Liu J, Zhang L, Chen Q, Dong Y. Development *of an* indirect competitive assay-based aptasensor for highly sensitive detection of tetracycline residues in honey. Biosensors and Bioelectronics. 2014;57:192–198.
250. DeCantazaro D. Sex steroids as pheromones in mammals: the exceptional role of estradiol. Hormones and Behaviour. 2015;68:103-116.
251. Fan L, Zhao G, Shi H, Liu M. A simple and label-free aptasensor based on nickel hexacyanoferrate nanoparticles as signal probe for highly sensitive detection of 17β-estradiol. Biosensors and Bioelectronics. 2015;68:303-309.
252. Huang KJ, Liu YJ, Zhang JZ, Cao JT, Liu YM. Aptamer/Au nanoparticles/cobalt sulfide nanosheets biosensor for 17β-estradiol detection using a guanine-rich complementary DNA sequence for signal amplification. Biosensors and Bioelectronics. 2015;67:184-191.
253. Shi Y, Peng DD, Shi CH, Zhang X, Xie YT, Lu B. Selective determination of trace 17β-estradiol in dairy and meat samples by molecularly imprinted solid-phase extraction and HPLC. Food Chemistry. 2011;126:1916-1925.
254. Tsakalof AK, Gkagtzis DC, Koukoulis GN, Hadjichristodoulou CS. Development of GC–MS/MS method with programmable temperature vaporization large volume injection for monitoring of 17β-estradiol and 2-methoxyestradiol in plasma. Analytica Chimica Acta. 2012;709:73-80.
255. Zhang X, Peng Y, Bai J, Ning B, Sun S, Hong X, Liu Y, Liu Y, Gao Z. A novel electrochemical sensor based on electropolymerized molecularly imprinted polymer and gold nanomaterials amplification for estradiol detection. Sensors and Actuators B-Chemical. 2014;200:69-75.

256. Yuan L, Zhang J, Zhou P, Chen J, Wang R, Wen T, Li Y, Zhou X, Jiang H. Electrochemical sensor based on molecularly imprinted membranes at platinum nanoparticles-modified electrode for determination of 17β-estradiol. Biosensors and Bioelectronics. 2011;29:29-33.
257. Sirinathsinghji E. USDA Scientist Reveals All. Glyphosate Hazards to Crops, Soils, Animals and Consumers. Science in Society. 2012;53:36-39
258. Hu JY, Chen CL, Li JZ. A simple method for the determination of glyphosate residues in soil by capillary gas chromatography with nitrogen phosphorus. Journal of Analitical Chemistry. 2008;63:371-375.
259. Williams GM, Kroes R, Munro IC. Safety evaluation and risk assessment of the herbicide Roundup and its active ingredient, glyphosate, for humans. Regulatory Toxicology and Pharmacology. 2000;31:117.
260. Marc J, Mulner-Lorillon O, Bellé R. Glyphosate-based pesticides affect cell cycle regulation. Biology of The Cell. 2004;96:245-249.
261. Guo J, Zhang Y, Luo Y, Shen F, Sun C. Efficient fluorescence resonance energy transfer between oppositely charged CdTe quantum dots and gold nanoparticles for turn-on fluorescence detection of glyphosate. Talanta. 2014;125:385-392.
262. Rubio F, Veldhuis LJ, Clegg BS, Fleeker JR, Hall JC. Comparison of a Direct ELISA and an HPLC Method for Glyphosate Determinations in Water. Journal of Agricultural and Food Chemistry.2002;51:691-696.
263. Hori Y, Fujisawa M, Shimada K, Hirose Y. Determination of the Herbicide Glyphosate and its Metabolite in Biological Specimens by Gas chromatography-mass Spectrometry. A Case of Poisoning by Roundup® Herbicide. Journal of Analytical Toxicology. 2003;27:162-166.
264. Motojyuku M, Saito T, Akieda K, Otsuka H, Yamamoto I, Inokuchi S. Determination of glyphosate, glyphosate metabolites, and glufosinate in human serum by gas chromatography–mass spectrometry. Journal of Chromatography B. 2008;875:509-514.
265. Tadeo JL, Sánchez-Brunete C, Pérez RA, Fernández MD. Analysis of herbicide residues in cereals, fruits and vegetables. Journal of Chromatography A 200;882:175-191.
266. Hidalgo C, Rios C, Hidalgo M, Salvadó V, Sancho JV, Hernández F. Improved coupled-column liquid chromatographic method for the determination of glyphosate and aminomethylphosphonic acid residues in environmental waters. Journal of Chromatography A. 2004;1035:153-157.
267. Vreeken RJ, Speksnijder P, Bobeldijk-Pastorova I, Noij THM. Selective analysis of the herbicides glyphosate and aminomethylphosphonic acid in water by on-line solid-phase extraction–high-performance liquid chromatography–electrospray ionization mass spectrometry. Journal of Chromatography A. 1998;794:187-199.
268. De Llasera MPG, Gómez-Almaraz L, Vera-Avila LE, Peña-Alvarez A. Matrix solid-phase dispersion extraction and determination by high-performance liquid chromatography with fluorescence detection of residues of glyphosate and aminomethylphosphonic acid in tomato fruit. Journal of Chromatography A. 2005;1093:139-146.
269. Stalikas CD, Pilidis GA, Karayannis MI. An integrated gas chromatographic method towards the simultaneous determination of phosphoric and amino acid group containing pesticides. Chromatographia. 2000;51:741-746.
270. Jayasumana C, Gunatilake S, Senanayake P. Glyphosate, Hard Water and Nephrotoxic Metals: Are They the Culprits Behind the Epidemic of Chronic Kidney Disease of Unknown

Etiology in Sri Lanka?. International Journal of Environmental Research and Public Health. 2014;11:2125-2147.
271. Madhun YA, Young JL, Freed VH. Binding of Herbicides by Water-soluble Organic Materials from Soil1. Journal of Environment Quality.1986:15;64-68.
272. Zhao P, Yan M, Zhang C, Peng R, Ma D, Yu J. Determination of glyphosate in foodstuff by one novel chemiluminescence-molecular imprinting sensor. Spectrochimica Acta Part A: Molecular and Biomolecular Spectroscopy. 2011;78:1482-1486.
273. Sassolas B.P.-S.a.J.M. A. Biosensors for Pesticide Detection: New Trends. American Journal of Analytical Chemistry. 2012;3:210-232.
274. Pramanik S, Zheng C, Zhang X, Emge TJ, Li J. New microporous metal-organic framework demonstrating unique selectivity for the detection of high explosives and aromatic compounds. Journal of American Chemical Society. 2011;133:4153-4155.
275. Debouttière PJ, Roux S, Vocanson F, Billotey C, Beuf O *et al*. Design of Gold Nanoparticles for Magnetic Resonance Imaging. Advanced Functional Materials. 2006;16:2330-2339.
276. Cho SH, Kim D, Park SM. Electrochemistry of conductive polymers 41. Effects os felf-assembeled monolayers of aminothiophenols on polyaniline films. Electrochimica Acta. 2008;53:3820-3827
277. Ansell RJ. Molecularly imprinted polymers in pseudoimmunoassay, Journal of Chromatography B. 2004;804:151-165.
278. Toal SJ, Trogler WC. Polymer sensors for nitroaromatic explosives detection. Journal of Materials Chemistry. 2006;16:2871-2883
279. Alizadeh T. Application of electrochemical impedance spectroscopy and conventional rebinding experiments for the investigation of recognition characteristic of bulky and nano-sized imprinted polymers. Materials Chemistry and Physics 2012;135:1012-1023.
280. Wang Z, Li H, Chen J, Xue Z, Wu B, Lu X. Acetylsalicilic acid electrochemical sensor based on PATP-AuNPs modified molecularly imprinted polymer film. Talanta. 2011;85:1672-1679.
281. Zhang X, Peng Y, Bai J, Ning B, Sun, *et al*. A novel electrochemical sensor based on electropolymerized molecularly imprinted polymer and gold nanomaterials amplification for estradiol detection Sensors and Actuators B: Chemical. 2014;200:69-75.
282. Xie C, Li H, Li S, Wu J, Zhang Z. Surface Molecular Self-Assembly for Organophosphate Pesticide Imprinting in Electropolymerized Poly(p-aminothiophenol) Membranes on a Gold Nanoparticle Modified Glassy Carbon Electrode, Analytical Chemistry. 2009;82:241-249.
283. Wang Q, Ji J, Jiang D, Wang Y, Zhang Y, Sun X. An electrochemical sensor based on molecularly imprinted membranes on a P-ATP-AuNP modified electrode for the determination of acrylamide. Analytical Methods. 2014;6:6452-6458.
284. Zhang D, Jiang J, Chen J, Zhang Q, Lu Y, Yao Y, Li S, Liu GL, Liu Q. Smartphone-based portable biosensing system using impedance measurement with printed electrodes for 2,4,6-trinitrotoluene (TNT) detection. Biosensors and Bioelectronics. 2015;70:81-88.
285. Jamil AKM, Izake EL, Sivanesan A, Fredericks PM. Rapid detection of TNT in aqueous media by selective label free surface enhanced Raman spectroscopy. Talanta. 2015;134:732-738.
286. Sağlam Ş, Üzer A, Tekdemir Y, Erçağ E, Apak R. Electrochemical sensor for nitroaromatic type energetic materials using gold nanoparticles/poly(*o*-phenylenediamine–aniline) film modified glassy carbon electrode. Talanta. 2015;139:181-188.

287. Kalanur SS, Katrahalli U, Seetharamappa J. Electrochemical studies and spectroscopic investigations on the interaction of an anticancer drug with DNA and their analytical applications. Journal of Electroanalytical Chemistry. 2009;636:93–100279
288. Naik KM, Nandibewoor ST. Electro-oxidation and determination of gemcitabine hydrochloride, an anticancer drug at gold electrode. Journal of Industrial and Engineering Chemistry. 2013;19:1933–1938
289. Kirstein MN, Hassan I, Guire DE, Weller DR, Dagit JW, Fisher JE. Remmel RP, High-performance liquid chromatographic method for the determination of gemcitabine and 2′,2′-difluorodeoxyuridine in plasma and tissue culture media. Journal of Chromatography B. 2006;835(1-2): 136–142
290. Marangon E, Sala F, Caffo O, Galligioni E, D'Incalci M, Zucchetti M. Simultaneous determination of gemcitabine and its main metabolite, dFdU, in plasma of patients with advanced non-small-cell lung cancer by high-performance liquid chromatography-tandem mass spectrometry. Journal of Mass Spectrometry. 2008;43(2):216-223.
291. Wang LZ, Yong WP, Soo RA, Lee SC, Soong R, Lee HS, Goh BC. Rapid determination of gemcitabine and its metabolite in human plasma by LC-MSMS through micro protein precipitation with minimum matrix effect. Journal of Pharmaceutical Science & Research. 2009;1(3):23-32
292. Ramezani M, Danesh NM, Lavaee P, Abnous K, Taghdisi SM. A novel colorimetric triple-helix molecular switch aptasensor for ultrasensitive detection of tetracycline. Biosensors and Bioelectronics. 2015;70:181-187.
293. Masaway P, Harfield A, Namwong A. An iPhone-based digital image colorimeter for detecting tetracycline in milk. Food Chemistry. 2015;184:23-29.
294. Wang S, Liu J, Yong W, Chen Q, Zhang L, Dong Y, Su H, Tan T. A direct competitive assay-based aptasensor for sensitive determination of tetracycline residue in Honey. Talanta. 2015;131:562-569.
295. Huang KJ, Liu YJ, Shi GW, Yang XR, Liu YM. Label-free aptamer sensor for 17β-estradiol based on vanadium disulfide nanoflowers and Au nanoparticles. Sensors and Actuators B: Chemical. 2014;201:579-585.
296. De Almeida LKS, Chigome S, Torto N, Frost CL, Pletschke BI. A novel colorimetric sensor strip for the detection of glyphosate in water. Sensors and Actuators B: Chemical. 2015;206:357-363.
297. Lee HU, Jung DU, Lee JH, Song YS, Park C, Kim SW. Detection of glyphosate by quantitative analysis of fluorescence and single DNA using DNA-labeled fluorescent magnetic core–shell nanoparticles. Sensors and Actuators B: Chemical. 2013;177:879-886.
298. Dai H, Sang M, Wang Y, Du R, Yuan W *et al*. Determination of trace glyphosate in water with a prism coupling optical waveguide configuration, Sensors and Actuators A: Physical. 2014;218:88-93.
299. Prasad BB, Jauhari D, Tiwari MP. Doubly imprinted polymer nanofilm-modified electrochemical sensor for ultra-trace simultaneous analysis of glyphosate and glufosinate. Biosensors and Bioelectronics. 2014;59:81-88.
300. Jenkins AL, Yin R, Jensen JL. Molecularly imprinted polymer sensors for pesticide and insecticide detection in water, Analyst. 2001;126:798-802.